

# **AB diblock copolymers via RAFT-mediated miniemulsion polymerization**

-  
by  
Nathalie Bailly

Thesis presented in partial fulfillment of the requirements for the degree of  
Master of Science (Polymer Science)

at the  
University of Stellenbosch



Promoter: Prof. R.D. Sanderson  
Co-promoter: Dr M.P. Tonge

Stellenbosch  
December 2008

## **Declaration**

By submitting this thesis electronically, I declare that the entirety of the work contained therein is my own, original work, that I am the owner of the copyright thereof (unless to the extent explicitly otherwise stated) and that I have not previously in its entirety or in part submitted it for obtaining any qualification.

Date: 20 August 2008

Copyright © 2008 Stellenbosch University

All rights reserved

## Abstract

The Reversible addition fragmentation chain transfer (RAFT) technique is a robust and versatile technique that enables the synthesis of polymers of controlled molecular weight and polydispersity. The application of the RAFT technique in heterogeneous aqueous media has attracted great interest in academics and industry due to it being more environmentally friendly, besides its other advantages. To date, the synthesis of well-defined high molecular weight polymers via the RAFT process under industrially relevant conditions still remains a challenge for polymer chemists.

The study addresses the application of the RAFT process in heterogeneous media, namely in miniemulsion polymerization, for the synthesis of AB diblock copolymers of *n*-butyl methacrylate and styrene.

AB diblock copolymers of high molecular weight were successfully prepared via a two-step method. In the first step, a dithiobenzoate monofunctional RAFT agent was used in bulk polymerization with the first monomer, *n*-butyl methacrylate. After the polymerization, the majority of the polymer chains contained the thiocarbonyl-thio RAFT agent functionality, which makes the chains potentially active for chain extension. The polymeric RAFT agent (also referred to as the starting block) obtained in the first step was chain extended in the second step, in miniemulsion, upon further addition of fresh initiator and the second monomer, styrene.

The effects of the initiator/RAFT agent concentration ratio on the miniemulsion systems were investigated. The miniemulsion systems used for the high molecular weight AB diblock copolymers exhibited living features despite the high polydispersity indices. Kinetic results showed an increase in the rate of polymerization throughout the polymerization. Size exclusion chromatography (SEC) results indicated significant broadening in the molecular weight distributions and a steep increase in the polydispersity during the polymerization. It was concluded that the broad molecular weight distributions and steep increase in the polydispersity was not only related to the initiator concentration but possibly due to other factors such as inhomogeneity in the

mini-emulsion system and a transition in the kinetic behavior during the polymerization. Secondary particle formation emerged from kinetic data and transmission electron microscopy (TEM) results, but this was not supported by the SEC results.

The effect of the use of a water-soluble initiator on the mini-emulsion system was also investigated. Results indicated a similar behavioral pattern as observed in the AIBN-initiated systems, and not much improvement in terms of the molecular weight distributions and polydispersity was seen.

The effect of the molecular weight of the diblock copolymers on the mini-emulsion system was investigated. Poly(*n*-butyl methacrylate)-*b*-poly(styrene) diblock copolymers of lower molecular weight were synthesized via the two-step process. Kinetic results indicated a similar behavioral trend as to that of the high molecular weight diblock copolymers synthesized, however SEC chromatograms showed narrower molecular weight distributions and low polydispersity indices.

## Opsomming

Die addisie fragmentasie ketting oordrag proses (*eng* reversible addition fragmentation chain transfer (RAFT)) is 'n kragtige en veelsydige tegniek wat die navorsers toelaat om polimere van gekontroleerde molekulêre massa en polidispersiteit te beheer. Die aanwending van die RAFT-tegniek in heterogene water-gebaseerde media het alreeds baie groot belangstelling tussen die akademiese en industriële navorsers gewek omrede dit omgewingsvriendelik is en ook baie ander voordele kan inhou. Die sintese van gedefinieerde hoë molekulêre massa polimere via die RAFT-proses onder kondisies wat van belang is vir die industrie, bly nogsteeds 'n uitdaging vir polimeer-chemici.

Hierdie studie behels die aanwending van die RAFT-proses in heterogene media, naamlik mini-emulsiepolimerisasie vir die sintese van AB diblokkopolimere van *n*-butielmetakrilaat en stireen.

AB diblokkopolimere van hoë molekulêre massa is suksesvol via 'n tweestap metode berei. In die eerste stap is 'n RAFT-verbinding in 'n massapolimerisasie met die eerste monomeer, *n*-butielmetakrilaat. Na polimerisasie bevat meeste van die kettings die RAFT-verbinding funksionaliteit wat dit potensieel aktief vir ketting-verlenging maak. Die polimeriese RAFT-verbinding (ook na verwys as die begin-blok) wat in die eerste stap verkry is, is ketting-verleng in die tweede stap in mini-emulsie na verdere byvoeging van vars afsetter en die tweede monomeer, stireen.

Die effek van die verhouding van die afsetter/RAFT-verbindingkonsentrasie op die mini-emulsiesisteen ondersoek. Die mini-emulsie sisteme van hoë molekulêre massa vertoon lewendige eienskappe ten spyte van die hoë polidispersiteit. Kinetiese resultate het 'n toename in die tempo van polimerisasie getoon. Grootte-uitsluitingsvloeistofchromatografie het duidelike verbredings in die molekulêre massa verspreidingsdistribusies en 'n stewige toename in polidispersiteit getoon. Die afleiding hieruit dat hierdie stewige toename nie verband hou met die konsentrasie van die afsetter nie, maar heel moontlik ook as gevolg van ander faktore in die mini-emulsie sisteem soos 'n verandering in die kinetiese gedrag gedurende die polimerisasie. Transmissie

elektronmikroskopie (TEM) resultate het getoon dat sekondêre partikel vorming plaasgevind het maar is nie ondersteun deur die resultate van grootte-uitsluitingsvloeistofchromatografie nie.

Die effek van die verandering in die tiepe afsetter (wateroplosbaar en wateronoplosbaar) is ook ondersoek en beskryf. Resultate het 'n soortgelyk gedragspatroon getoon soos waargeneem soos in die sisteme waar AIBN afsetter gebruik is, getoon. Daar is nie 'n groot verskil in terme van die molekulêre massa verspreiding en polidispersiteit opgemerk nie.

Die effek van molekulêre massa van die diblokkopolimere op die mini-emulsiesisteme is ook ondersoek. Poly(*n*-butielmetakrilaat)-*b*-poli(stireen) diblokkopolimere van laer molekulêre massa is via die twee-stapmetode berei. Kinetiese resultate het 'n soortgelyke gedragspatroon as die blokkopolimere van hoë molekulêre massa getoon, maar grootte-uitsluitingsvloeistofchromatografie resultate het 'n nouer molekulêre massa verspreiding en laer polidispersiteit getoon.

## **Acknowledgements**

Firstly, I would like to thank the Department of Chemistry and Polymer Science for the financial support provided for the research presented in this thesis.

The following individuals must be acknowledged

- My promoter, Professor Sanderson for the opportunity to study at the Institute of Polymer Science. Thank you for your support, motivation and encouragement throughout my MSc study.
- My supervisor, Dr M. Tonge for your guidance, your patience, your time and sharing of your knowledge. This was very much appreciated.
- Dr Mohammed Jaffer for TEM analyses and Gareth Bayley for the analysis of my endless GPC samples.
- All my colleagues in the lab, Dr Patrice Hartmann, Vernon, Austin, Adine, Ineke, Yolande, Pauline, Lee-Sa, Walid, Nagi, Hussein - thank you for all your support, encouragement and enjoyable times together.
- The theoretical laser physicist, Francesca Mountfort, thank you for your friendship, advice and help during difficult times.
- To the most important people in my life, my family, thank you for your unconditional love and support during this time.

***“Per ardua ad astra”***

**(Anon)**

Through adversity to reach the stars

---

## **Table of contents**

List of abbreviations .....	v
List of symbols.....	vi
List of schemes .....	viii
List of tables.....	x
List of figures.....	xii

---

### **Chapter 1: Introduction and objectives**

1.1 Introduction.....	2
1.2 Free radical polymerization .....	2
1.3 Controlled free radical polymerization .....	2
1.4 Objectives of the study.....	4
1.5 Thesis layout .....	6
1.6 References.....	8

---

### **Chapter 2: Theoretical background**

2.1 Introduction.....	10
2.1.2 Chain reaction steps .....	12
2.2 Homogeneous and heterogeneous free radical polymerization .....	18
2.2.1 Homogeneous systems.....	18
2.2.2 Heterogeneous systems.....	18
2.3 Miniemulsion Polymerization.....	21
2.3.1 History.....	21
2.3.2 Miniemulsion preparation .....	21
2.3.3 Particle nucleation in emulsion and miniemulsion systems .....	23
2.3.4 Mechanism and kinetics of nucleation in emulsion and miniemulsion systems.....	24
2.3.4.1 Emulsion systems.....	24
2.3.4.2 Phase transfer events in emulsion polymerization.....	27
2.3.5 Miniemulsion systems .....	30
2.3.6 Particle stability in miniemulsion systems.....	31
2.4 Controlled free radical polymerization .....	34



2.4.1 History and developments.....	33
2.4.2 Mechanisms .....	36
2.5 Reversible addition fragmentation chain transfer (RAFT) .....	39
2.5.1 General structure of a RAFT agent.....	39
2.5.2 RAFT mechanism .....	41
2.5.3 Controlled free radical polymerization in heterogeneous aqueous media .....	44
2.5.4 RAFT in heterogeneous aqueous systems .....	45
2.5.5 Stability of RAFT agent in heterogeneous aqueous media.....	45
2.6 The use of free radical and controlled free radical polymerizations in block copolymer synthesis.....	47
2.6.1 The RAFT process and block copolymers.....	48
2.7 References.....	52

---

### **Chapter 3: Synthesis and characterization of RAFT agents and diblock copolymers**

3.1 Introduction.....	58
3.2 RAFT agent synthesis .....	60
3.2.1 Background .....	61
3.2.2 Materials .....	61
3.2.3 Experimental procedure .....	62
3.2.3.1 Synthesis of dithiobenzoic acid .....	62
3.2.3.2 Synthesis of bis(thiobenzoyl) disulfide.....	62
3.2.3.3 Synthesis of 2-cyanoisoprop-2-yl dithiobenzoate (CIDB) .....	63
3.2.3.4 Characterization of RAFT agent.....	63
3.3 Block copolymer synthesis .....	64
3.3.1 Step I: Preparation of the initial block (polymeric RAFT agent) via RAFT/ bulk Polymerization .....	66
3.3.1.1 Experimental procedure .....	66
3.3.2 Step II: Preparation of diblock copolymers via RAFT/Miniemulsion Polymerization .....	67
3.4 Analytical techniques used for the characterization of block copolymers .....	69
3.4.1 Size exclusion chromatography (SEC) .....	69
3.4.2 Dynamic light scattering (DLS).....	70

3.4.3 Transmission electron microscopy (TEM) .....	70
3.5 References.....	71

---

**Chapter 4: Results and Discussion**

4.1 Introduction.....	73
4.2 Poly( <i>n</i> -butyl methacrylate) and poly(styrene) blocks (polymeric RAFT agents) via RAFT-mediated bulk polymerizations.....	74
4.2.1 Results.....	74
4.3 Chain extension via RAFT-mediated miniemulsion polymerization .....	75
4.3.1 Chain extension of initial poly( <i>n</i> -butyl methacrylate) block with <i>n</i> -butyl methacrylate and initial poly(styrene) block with styrene in miniemulsion.....	76
4.3.2 Results.....	76
4.3.3 Dynamic light scattering .....	80
4.3.4 Conclusions.....	81
4.4 Chain extension of initial poly ( <i>n</i> -butyl methacrylate) block with styrene in miniemulsion.....	82
4.4.1 Results.....	82
4.4.2 Dynamic light scattering .....	85
4.4.3 Transmission electron microscopy .....	87
4.4.4 Discussion .....	88
4.4.5 Conclusions.....	92
4.5 The influence of the different initiator/RAFT agent molar ratios on the RAFT-mediated miniemulsion system.....	93
4.5.1 Results.....	93
4.5.2 Dynamic light scattering .....	104
4.5.3 Transmission electron microscopy .....	105
4.5.4 Conclusions.....	107
4.6 Oil-soluble versus water-soluble initiators in RAFT-mediated miniemulsion systems.....	107
4.6.1 Chain extension of initial poly( <i>n</i> -butyl methacrylate) block with styrene using water-soluble KPS initiator.....	108
4.6.2 Results.....	109

4.6.3 Dynamic light scattering .....	113
4.6.4 Transmission electron microscopy .....	113
4.6.5 Conclusions.....	114
4.6.6 Overall conclusions.....	115
4.7 Chain extension of initial poly( <i>n</i> -butyl methacrylate) block of lower molecular weight with styrene in miniemulsion.....	116
4.7.1 Results.....	117
4.7.2 Dynamic light scattering .....	121
4.7.3 Transmission electron microscopy .....	122
4.7.4 Conclusions.....	123
4.7.5 Overall conclusions.....	124
4.8 References.....	126
<hr/>	
<b>Chapter 5: Conclusions and recommendations</b>	
5.1 Conclusions.....	128
5.2 Recommendations for future work .....	131
<hr/>	
Appendix A: 2-cyanoisoprop-2-yl dithiobenzoate (CIDB) .....	133
Appendix B: Mathematical model for the miniemulsion system .....	135
Appendix C: Statistical analysis of TEM.....	136

## List of abbreviations

ATRP	Atom transfer radical polymerization
AIBN	Azobisisobutyronitrile
<i>n</i> -BMA	<i>n</i> -butyl methacrylate
CIDB	cyano-2-isoprop-2-yl dithiobenzoate
CLRP	Controlled living radical polymerization
DDI	Distilled deionized water
DLS	Dynamic light scattering
DMSO	Dimethyl sulfoxide
ESMS	Electron spray mass spectroscopy
FRP	Free radical polymerization
GPC	Gel-permeation chromatography
HD	Hexadecane
KOH	Potassium hydroxide
KPS	Potassium persulfate
NMP	Nitroxide mediated polymerization
NMR	Nuclear magnetic resonance
PBMA	Poly( <i>n</i> -butyl methacrylate)
PDI	Polydispersity index
PSt	Polystyrene
RAFT	Reversible addition fragmentation transfer
RI	Refractive index
SEC	Size exclusion chromatography
SFRP	Stable free radical polymerization
SLS	Sodium lauryl sulfate
UV	Ultraviolet
TEM	Transmission electron microscopy
THF	Tetrahydrofuran

## List of Symbols

$C_t$	rate of chain transfer
$C_w$	concentration of monomer in aqueous phase
$C_p$	particle phase monomer concentration
$D_w$	diffusivity of monomeric radicals in the aqueous phase
$FW_{RAFT}$	molecular weight of RAFT agent
$FW_M$	molecular weight of monomer
$j_{crit}$	length of $j$ mer
$k_{add}$	addition rate coefficient
$k_{t, aq}$	termination rate coefficient in the aqueous phase
$k_{p, aq}$	propagation rate coefficient in the aqueous phase
$k_{dM}$	rate coefficient for a single molecule desorbing
$k_d$	termination by coupling rate coefficient
$k_p$	propagation rate coefficient
$k_{tc}$	termination by coupling rate coefficient
$k_{td}$	termination by disproportionation rate coefficient
$k_t$	rate coefficient of termination
$[M]_0$	initial monomer concentration
$[M]$	concentration of monomer
$\overline{M}_n$	number average molar mass
$N_A$	Avagadro's number
$N_c$	number of particles
$\overline{n}$	average number of radicals per particle
$n$	number of moles
$[P^*]$	concentration of the propagating radical
$[I]_0$	initial concentration of initiator
$[I]$	initiator concentration
$[RAFT]_0$	initial RAFT agent concentration
$R_p$	rate of polymerization

$V_i$	molar volume of the monomer
$f$	radical efficiency
$r$	radius of the droplet
$t$	time
$T$	temperature
$\rho$	rate coefficient of radical entry
$x$	fractional conversion
$z$	length of zmer

## List of Schemes

Scheme 1.1: Technique for reversible termination.

Scheme 2.1: Decomposition of an initiator.

Scheme 2.2: Addition of a primary radical to monomer.

Scheme 2.3: Propagation of propagating radicals by monomer addition.

Scheme 2.4: Two radical termination mechanisms: combination and disproportionation.

Scheme 2.5: The chain transfer process with styrene.

Scheme 2.6: Controlled free radical polymerization via deactivation/activation process.

Scheme 2.7: Controlled free radical polymerization via degenerative transfer.

Scheme 2.8: General structure of RAFT agent.

Scheme 2.9: The RAFT mechanism.

Scheme 2.10: Intermediate structure formed during AB block copolymerization.

Scheme 3.1: Formation of Grignard reagent.

Scheme 3.2: Formation of dithiobenzoic acid.

Scheme 3.3: Formation of bis(thiobenzoyl) disulfide.

Scheme 3.4: Synthesis of 2-cyanoisoprop-2-yl dithiobenzoate.

Scheme 3.5: Block copolymer formation via a monofunctional RAFT agent.

Scheme 3.6: Representation of the two step reaction procedure for the synthesis of AB diblock copolymers.



## List of Tables

Table 3.1: Bulk polymerization reaction composition for the synthesis of initial blocks (polymeric RAFT agents).

Table 3.2: Block copolymer miniemulsion compositions.

Table 4.1: Initial poly(*n*-butyl methacrylate) and poly(styrene) blocks (polymeric RAFT agents synthesized by bulk polymerization at 80 °C for 70 minutes, initiated by AIBN).

Table 4.2: Characteristics of the polymer formed in the final latices obtained for the chain extension reactions in RAFT-mediated miniemulsion polymerization at 75 °C for 2 hours.

Table 4.3: DLS results for the chain extension of initial poly(*n*-butyl methacrylate) with *n*-butyl methacrylate (reaction 1), and the chain extension of initial poly(styrene) with styrene (reaction 2) in RAFT-mediated miniemulsion polymerization.

Table 4.4: Characteristics of poly(*n*-butyl methacrylate)-*b*-poly(styrene) diblock copolymer formed in RAFT-mediated miniemulsion polymerization at 75 °C for 2 hours, initiated by AIBN.

Table 4.5: DLS results for the poly(*n*-butyl methacrylate)-*b*-poly(styrene) diblock copolymer latex in RAFT-mediated miniemulsion, at 75 °C, initiated by AIBN.

Table 4.6: Characteristics of the polymer formed in the final latices obtained for the chain extension reactions in RAFT-mediated miniemulsion polymerization at 75 °C for 2 hours.

Table 4.7: DLS results for the poly(*n*-butyl methacrylate)-*b*-poly(styrene) diblock copolymers in RAFT-mediated miniemulsion, at 75 °C, initiated by AIBN.

Table 4.8: Characteristics of the polymer formed in the final latices obtained for the chain extension reactions in RAFT-mediated miniemulsion polymerization at 75 °C for 2 hours.

Table 4.9: DLS results for the poly(*n*-butyl methacrylate)-*b*-poly(styrene) diblock copolymer in RAFT-mediated miniemulsion, at 75 °C, initiated by KPS.

Table 4.10: Characteristics of the polymer formed in the final latices obtained for the chain extension reactions in RAFT-mediated miniemulsion polymerization at 75 °C for 3 hours, initiated by AIBN.

Table 4.11: DLS results for the poly(*n*-butyl methacrylate)-*b*-poly(styrene) diblock copolymer in RAFT-mediated miniemulsion polymerization at 75 °C for 3 hours, initiated by AIBN.

## List of Figures

Figure 2.1: Formation of a miniemulsion.

Figure 2.2: The three intervals in emulsion polymerization.

Figure 2.3: Miniemulsion polymerization showing the final latex particles.

Figure 4.1: Normalized SEC chromatogram for the chain extension of initial poly(*n*-butyl methacrylate) block with *n*-butyl methacrylate in RAFT-mediated miniemulsion polymerization at 75 °C for 2 hours, initiated by AIBN, using PBMA-RAFT agent batch 2.

Figure 4.2: UV and RI overlay of the final sample of the chain extension of initial poly(*n*-butyl methacrylate) block with *n*-butyl methacrylate in RAFT-mediated miniemulsion polymerization at 75 °C for 2 hours, initiated by AIBN.

Figure 4.3: Normalized SEC chromatogram of the chain extension of an initial poly(styrene) block with styrene in RAFT-mediated miniemulsion polymerization at 75 °C for 1 hour, initiated by AIBN.

Figure 4.4: UV and RI overlay of the chain extension of an initial poly(styrene) block with styrene in RAFT-mediated miniemulsion polymerization at 75 °C for 1 hour, initiated by AIBN.

Figure 4.5: Evolution of  $\overline{M}_n$  and PDI for poly(*n*-butyl methacrylate)-*b*-poly(styrene) in RAFT-mediated miniemulsion polymerization at 75 °C for 2 hours, initiated by AIBN, using PBMA-RAFT agent batch 1.

Figure 4.6: (A) Normalized SEC chromatograms for the chain extension of initial poly(*n*-butyl methacrylate) block with styrene in RAFT-mediated miniemulsion at 75 °C, initiated by AIBN, using-PBMA-RAFT agent batch 1. (B) Evolution of molar mass distribution with conversion for poly(*n*-butyl methacrylate)-*b*-poly(styrene) in RAFT-mediated miniemulsion at 75 °C initiated by AIBN, using PBMA-RAFT batch 1.

Figure 4.7: DLS size distribution graph of the final poly (*n*-butyl methacrylate)-*b*-poly(styrene) diblock copolymer latex in RAFT-mediated miniemulsion, at 75 °C, initiated by AIBN.

Figure 4.8: TEM image (A) Before polymerization; (B) After polymerization of the poly(*n*-butyl methacrylate)-*b*-poly(styrene) diblock copolymer prepared by RAFT-mediated miniemulsion polymerization at 75 °C for 2 hours, initiated by AIBN.

Figure 4.9: (A) Monomer conversion versus reaction time for the synthesis of poly(*n*-butyl methacrylate)-*b*-poly(styrene) in RAFT-mediated miniemulsion at 75 °C for 2 hours, initiated by AIBN, using PBMA-RAFT batch 2. Reaction 4, [AIBN]/[RAFT agent] = 1:2, Reaction 5, [AIBN]/[RAFT agent] = 1:10, Reaction 6, [AIBN]/[RAFT agent] = 1:20.

(B) Semilogarithmic plot of monomer conversion versus reaction time for the synthesis of poly(*n*-butyl methacrylate)-*b*-poly(styrene) in RAFT-mediated miniemulsion 75 °C for 2 hours, initiated by AIBN, using PBMA-RAFT batch 2. Reaction 4, [AIBN]/[RAFT agent] = 1:2, Reaction 5, [AIBN]/[RAFT agent] = 1:10, Reaction 6, [AIBN]/[RAFT agent] = 1:20.

Figure 4.10: Evolution of  $\overline{M}_n$  and PDI for poly(*n*-butyl methacrylate)-*b*-poly(styrene) in RAFT-mediated miniemulsion polymerization at 75 °C for 2 hours using PBMA-RAFT agent batch 2: (A) Reaction 4, [AIBN]/[RAFT agent] = 1:2 (B) Reaction 5, [AIBN]/[RAFT agent] = 1:10 (C) Reaction 6, [AIBN]/[RAFT agent] = 1:20.

Figure 4.11: Normalized SEC chromatograms for the chain extension of the initial PBMA block with styrene in RAFT-mediated miniemulsion polymerization at 75 °C for 2 hours, initiated by AIBN using PBMA-RAFT batch 2 (A) Reaction 4, [AIBN]/[RAFT agent] = 1:2 (B) Reaction 5, [AIBN]/[RAFT agent] = 1:10 (C) Reaction 6, [AIBN]/[RAFT agent] = 1:20.

Figure 4.12: DRI signal scaled for conversion for poly(*n*-butyl methacrylate)-*b*-poly(styrene) diblock copolymer in RAFT-mediated miniemulsion polymerization at 75 °C for 2 hours, initiated by AIBN (A) reaction 4 [AIBN]/[RAFT agent] = 1:2 (B) reaction 5 [AIBN]/[RAFT agent] = 1:10.

Figure 4.13: TEM images of poly(*n*-butyl methacrylate)-*b*-poly(styrene) latices prepared by RAFT-mediated miniemulsion polymerization at 75 °C for 2 hours, initiated by AIBN. (A) Reaction 4, [AIBN]/[RAFT agent] = 1:2 (B) Reaction 5, [AIBN]/[RAFT agent] = 1:10 (C) Reaction 6, [AIBN]/[RAFT agent] = 1:20.

Figure 4.14: Chemical structure of the oil-soluble initiator AIBN (2,2'-azobis(isobutyronitrile)) and the water-soluble initiator KPS (potassium peroxydisulfate).

Figure 4.15: (A) Monomer conversion versus reaction time for the synthesis of poly(*n*-butyl methacrylate)-*b*-poly(styrene) in miniemulsion polymerization at 75 °C for 2 hours, initiated by KPS. (B) Semilogarithmic plot of monomer conversion versus reaction time for the synthesis of poly(*n*-butyl methacrylate)-*b*-poly(styrene) in miniemulsion polymerization at 75 °C for 2 hours, initiated by KPS.

Figure 4.16: Evolution of  $\overline{M}_n$  and PDI for poly(*n*-butyl methacrylate)-*b*-poly(styrene) diblock copolymer in RAFT-mediated miniemulsion polymerization, at 75 °C for 2 hours, initiated by KPS.

Figure 4.17: (A) Normalized SEC chromatogram for poly(*n*-butyl methacrylate)-*b*-poly(styrene) in RAFT-mediated miniemulsion, at 75 °C, initiated by KPS.

(B) DRI signal scaled for conversion for poly(*n*-butyl methacrylate)-*b*-poly(styrene) in RAFT-mediated miniemulsion, at 75 °C, initiated by KPS.

Figure 4.18: TEM image of poly(*n*-butyl methacrylate)-*b*-poly(styrene) latex prepared by RAFT-mediated miniemulsion polymerization, initiated by KPS.

Figure 4.19: (A) Monomer conversion versus reaction time for the synthesis of poly(*n*-butyl methacrylate)-*b*-poly(styrene) in RAFT-mediated miniemulsion polymerization at 75 °C for 3 hours, initiated by AIBN. (B) Semilogarithmic plot of monomer conversion versus reaction time for the synthesis of poly(*n*-butyl methacrylate)-*b*-poly(styrene) in RAFT-mediated miniemulsion polymerization at 75 °C for 3 hours, initiated by AIBN.

Figure 4.20: Evolution of  $\overline{M}_n$  and PDI for poly(*n*-butyl methacrylate)-*b*-poly(styrene) in RAFT-mediated miniemulsion polymerization at 75 °C for 3 hours, initiated by AIBN, using PBMA-RAFT agent batch 5.

Figure 4.21: (A) Normalized SEC chromatograms for the chain extension of the initial PBMA block with styrene in RAFT-mediated miniemulsion polymerization at 75 °C initiated by AIBN, using PBMA-RAFT agent batch 5. (B) DRI signal scaled for conversion for poly(*n*-butyl methacrylate)-*b*-poly(styrene) in RAFT-mediated miniemulsion, at 75 °C, initiated by AIBN.

Figure 4.22: UV and RI overlay for the chain extension of initial poly(*n*-butyl methacrylate) block with styrene in miniemulsion at 75 °C initiated by AIBN, using PBMA-RAFT agent batch 5. The initial PBMA block is also included (bold line).

Figure 4.23: DLS size distribution graph for poly(*n*-butyl methacrylate)-*b*-poly(styrene) diblock copolymer in RAFT-mediated miniemulsion polymerization at 75 °C for 3 hours, initiated by AIBN.

Figure 4.24: TEM image of poly(*n*-butyl methacrylate)-*b*-poly(styrene) latex prepared by RAFT-mediated miniemulsion polymerization at 75 °C for 3 hours, initiated by AIBN. (A) before polymerization (B) after polymerization.

*Chapter One*  
*Introduction and objectives*



### **1.1 Introduction**

In industry, there is an increasing demand for the synthesis of novel materials with specific properties that can be used for specific applications. Since the properties of polymers are dependent on both their chemical composition and microstructure, a major focus in polymer science is on the methods that enable the precise control of the composition and the macromolecular structure of polymeric materials.<sup>1,2</sup>

The focus in this research study is specifically on the use of a controlled free radical technique, namely RAFT (Reversible addition fragmentation chain transfer) for the synthesis of well-defined AB diblock copolymers in heterogeneous aqueous media, using existing monomers.

### **1.2 Free radical polymerization**

In the mid-1930s free radical polymerization was recognized and, ever since, much research has been directed towards discovering and understanding more about the use of chain reactions for the synthesis of useful materials. Free radical polymerization is a chain growth process, and is one of the oldest and most widely used techniques for the synthesis of polymers. Free radical polymerization has several attractive features in that it is less sensitive to impurities, unlike other techniques such as anionic polymerization; it is compatible with a wide range of monomers<sup>3</sup>; it can be conducted in a range of reaction conditions, and it can be conducted in homogeneous and heterogeneous media. All these advantages make this technique one of the most popular in industry for producing commercial polymers. However, it does suffer from several drawbacks: it is difficult to control the molecular weight, difficult to synthesize polymers of low polydispersity and chemical homogeneity, difficult to introduce defined end groups, and to synthesize well-defined diblock, triblock and multiblock copolymers. Conventional free radical polymerization is therefore limited in designing high performance materials with specific properties.<sup>4</sup>

### **1.3 Controlled free radical polymerization**

The synthesis of well-defined polymers with controlled structural parameters was first carried out by Szwarc in 1956 using anionic polymerization.<sup>5</sup> However, this technique

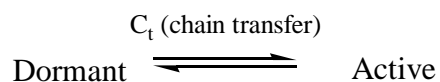
## *Chapter One Introduction and Objectives*

---

requires stringent conditions, is limited to a number of monomers, and is an expensive process that results in expensive final products which are all unfavorable in commercial production. In 1982 the first steps towards controlled radical polymerization were taken by Otsu and coworkers.<sup>5</sup>

After the mid-1980s, other approaches were investigated in the development of controlled radical polymerization. In 1998 Rizzardo and coworkers reported on the RAFT process that offers polymers of narrow polydispersity and predetermined molecular weight.<sup>6</sup> The RAFT process is a robust technique that is compatible with a broad range of monomers and reaction conditions, and it is capable of controlling polymerization in both homogeneous and heterogeneous media.

The process of controlled radical polymerization involves the addition of a specific compound to a conventional free radical polymerization reaction. An equilibrium is established between the propagating active and dormant species with fast exchange between the species. This is illustrated in Scheme 1.1.



Scheme 1.1: Technique for reversible termination.

ATRP (Atom transfer radical polymerization), NMP (Nitroxide mediated polymerization) and RAFT are examples of controlled techniques and, although the mechanisms differ, the principle of controlling radical polymerization is the same.

With the advent of controlled radical polymerization, polymers of tailor-made molecular weight and polydispersity are achievable. Polymers of controlled architecture such as diblock, triblock, star-shaped and branched structures have been prepared.<sup>7</sup> Since controlled radical polymerization combines the versatility of free radical polymerization with the control of anionic polymerization, it is presently, at research level, one of the most common methods used for the synthesis of block copolymers. The development in controlled free radical polymerization has opened a new avenue to the synthesis of block copolymers under less stringent conditions than those necessary for ionic polymerization.

There are several routes that exist for the synthesis of block copolymers via the RAFT process. The most studied route is the use of monofunctional RAFT agent. Other routes involve the use of difunctional RAFT agents and trithiocarbonates, multifunctional low molecular weight RAFT agents and multifunctional macromolecular RAFT agents.<sup>8-10</sup>

Most of the research published in the academic literature is based on the use of controlled radical polymerization in homogeneous aqueous media. Aqueous phase polymerization is of great interest in industry due to the fact that the reaction mixture is water based (no volatile compounds present), which makes it environmentally friendly; the final product is in latex form and can therefore be easily processed; and the heat dissipation in heterogeneous aqueous systems is more efficient than in solvent or bulk systems.<sup>11</sup> Numerous industrial polymerizations are conducted in emulsion, mini-emulsion, micro-emulsion and inverse-emulsion.

Difficulties in applying controlled free radical techniques in heterogeneous aqueous media have been reported.<sup>12</sup> The use of RAFT polymerization in conventional emulsions has been reported. Most of the work carried out by different research groups focuses on styrene polymerization but RAFT emulsions of butyl acrylate and methacrylates have also been reported.<sup>4,13,14</sup> Recently, extensive research based on RAFT chemistry and its application in miniemulsion systems has been investigated.<sup>13,15-17</sup> Miniemulsion systems are made up of small and stable nanodroplets of monomer in a size range of 50 – 500 nm, dispersed in an aqueous phase, prior to polymerization.<sup>18</sup> Some reports describe limited success with RAFT in miniemulsion. Problems such as the loss of molecular weight, broad polydispersity values, latex instability, coagulum formation and phase separation have been reported in academic literature.<sup>8,19</sup> The application of the RAFT technique in heterogeneous aqueous systems has emerged as being more complicated than researchers had anticipated. The kinetics involved in emulsion systems are more complex than that in conventional solution polymerization and difficulties in terms of optimizing these controlled systems still remain.<sup>20</sup> The use of the RAFT technique in aqueous media is, therefore, still to be improved. Presently, for many polymer researchers, the application of controlled radical polymerization in heterogeneous aqueous media still remains a challenge.

### **1.4 Objectives of the study**

The idea leading up to this research project originated from the work published by Vosloo *et al.*<sup>21</sup> who studied a novel approach to conducting controlled radical polymerization in waterborne dispersions. To our knowledge, not much research has been reported in the open

literature on RAFT-mediated heterogeneous systems, whereby one prepolymerizes in a homogeneous system and then converts to a heterogeneous system. Therefore, using the research carried out by Vosloo *et al.* as a foundation to this study, their work was expanded upon. Thus, the overall focus of this study can be summarized as follows.

This research project focuses on the synthesis of well-defined high molecular weight AB diblock copolymers of *n*-butyl methacrylate and styrene in heterogeneous media, namely miniemulsion via the RAFT technique. The methodology used here to synthesize the AB diblock copolymers comprises a two-step process. The first step involves the synthesis of the starting block in bulk, also referred to as a polymeric RAFT agent. Bulk polymerization was chosen since it involves only monomer, RAFT agent and initiator. Therefore, it minimizes the possibility of contamination and results in the initial block being of high purity. In the second step the first block is chain extended in miniemulsion upon further addition of fresh monomer and initiator. The majority of the chains contain the thiocarbonyl-thio moiety on the chain ends after the first step, making these chains potentially active for chain extension.

The objectives of the study are as follows:

1. The monofunctional RAFT agent 2-cyanoisoprop-2-yl dithiobenzoate (CIDB) was to be used in the bulk polymerization of *n*-butyl methacrylate to form a polymeric RAFT agent (also referred to as the starting block) with a molecular weight range between 20 000 gmol<sup>-1</sup> – 40 000 gmol<sup>-1</sup>.
2. Preliminary experiments were to be carried out in which the starting blocks (polymeric RAFT agent) synthesized in bulk polymerization were to be chain extended with the same monomer in the second miniemulsion step. The

purpose was to determine whether the starting block (polymeric RAFT agent) was a good candidate for controlling the molecular weight in the miniemulsion and whether chain extension occurred.

3. Preliminary experiments that involved using a more complex system is also investigated. In this case the initial block was to be chain extended with the second monomer in the miniemulsion step, therefore forming the AB diblock copolymers of *n*-butyl methacrylate and styrene. This was to be carried out to determine whether block copolymer formation occurs when using this methodology and whether the polymerization system exhibited living characteristics.
  
4. In an attempt to synthesize AB diblock copolymers of high molecular weight and narrow molecular weight distribution via the methodology mentioned above, the behavior of the RAFT-mediated miniemulsion system are to be more thoroughly investigated by studying the effects of:
  - a) the initiator/RAFT agent concentration ratio on the system
  - b) the type of initiator (oil-soluble vs. water-soluble) on the system
  - c) synthesizing a lower molecular weight starting block in bulk and a lower molecular weight second block in miniemulsion on the system.

The diblock copolymers were characterized and analyzed using the following analytical techniques:

- ✓ Size exclusion chromatography (SEC) analysis to determine the molecular weight and the polydispersity of the diblock copolymers
- ✓ Dynamic light scattering (DLS) to determine the particle size
- ✓ Transmission electron microscopy (TEM) to confirm particle size determined by DLS, and to obtain visual evidence of the particle morphology of the AB diblock copolymers.

### **1.5 Thesis layout**

The thesis comprises five chapters.

## ***Chapter One Introduction and Objectives***

---

### ***Chapter One: Introduction and objectives***

A brief introduction to free radical polymerization and controlled living radical polymerization in heterogeneous systems is given. The objectives of the research project are presented.

### ***Chapter Two: Historical and theoretical background***

A brief historical and theoretical background is given on important aspects related to the study. It includes the use of controlled free radical polymerization in heterogeneous aqueous media, and its application. The different heterogeneous systems are briefly mentioned and a detailed discussion on (mini)emulsion polymerization is given. The main focus in this chapter is on the use of the RAFT technique in heterogeneous aqueous media for the synthesis of AB diblock copolymers.

### ***Chapter Three: Synthesis and characterization of RAFT agents and diblock copolymers***

Experimental details of the synthesis of the dithioester RAFT agent, the synthesis of the starting blocks and the synthesis of the AB diblock copolymers are discussed. The analytical techniques used to characterize the diblock copolymers are described.

### ***Chapter Four: Results and discussion***

The results obtained for the synthesis of AB diblock copolymers are presented and discussed in this chapter. Results of analyses of the polymer lattices obtained from SEC, DLS and TEM, are reported.

### ***Chapter Five: Conclusion and recommendations***

Conclusions to the study are presented and some recommendations for future research are made.

## 1.6 References

- (1) Abetz, Z. V.; Simon, P. F. W. *Adv. Polym. Sci.* **2005**, *189*, 125.
- (2) Werne, T.; Patten, T. E. *J. Am. Chem. Soc.* **1999**, *121*, 7409.
- (3) Chiefari, J.; Chong, Y. K.; Ercole, F.; Krstina, J.; Jeffery, J.; Le, P. T.; Mayadunne, R. T. A.; Meijs, G. F.; Moad, C. L.; Moad, G.; Rizzardo, E.; Thang, S. H. *Macromolecules* **1998**, *31*, 5559 - 5562.
- (4) Moad, G.; Rizzardo, E.; Thang, S. H. *Aust. J. Chem.* **2005**, *58*, 379 - 410.
- (5) Moad, G.; Solomon, D. H. In *The Chemistry of Radical Polymerization*, 2nd ed.; Elsevier: Australia, 2006; pp 1 - 9.
- (6) Le, T. P.; Moad, G.; Rizzardo, E.; Thang, S. H. *PCT Int. Appl. WO9801478A1980115* **1998**.
- (7) Braunecker, W. A.; Matyjaszewski, K. *Prog. Polym. Sci.* **2007**, *32*, 93 - 146.
- (8) Bowes, A.; McLeary, J. B.; Sanderson, R. D. *J. Polym. Sci. Part A: Polym. Chem.* **2007**, *45*, 588 - 604.
- (9) Bussels, R.; Bergman-Gottgens, C.; Meuldijk, J.; Koning, C. *Macromolecules* **2004**, *37*, 9299.
- (10) Qinghua, Z.; Xiaoli, Z.; Fengqiu, C.; Ying, S.; Qiongyan, W. *J. Polym. Sci. Part A: Polym. Chem.* **2007**, *45*, 1585 - 1594.
- (11) Matyjaszewski, K.; Davis, T. P. In *Handbook of Radical Polymerization*; Herk, A. M. V.; Monteiro, M., Eds.; Wiley & Sons: Canada, 2002; pp 301 - 331.
- (12) Matyjaszewski, K.; Qiu, J.; Tsarevsky, N. V.; Charleux, B. *J. Polym. Sci. Part A: Polym. Chem.* **2000**, *38*, 4724 - 4734.
- (13) Butte, A.; Storti, G.; Morbidelli, M. *Macromolecules* **2001**, *34*, 5885 - 5896.
- (14) Monteiro, M. J.; Sjoberg, M.; Vlist, J. V. D.; Gottgens, C. M. *J. Polym. Sci. Part A: Polym. Chem.* **2000**, *38*, 4206 - 4217.
- (15) Tsavalas, J. G.; Schork, F. J.; de Brouwer, H.; Monteiro, M. J. *Macromolecules* **2001**, *34*, 3938 - 3946.
- (16) Lansalot, M.; Davis, T. P.; Heuts, J. P. A. *Macromolecules* **2002**, *35*, 7582 - 7591.

## ***Chapter One Introduction and Objectives***

---

- (17) Liu, S.; Hermanson, K. D.; Kaler, E. W. *Macromolecules* **2006**, *39*, 4345 - 4350.
- (18) Landfester, K. *Macromol. Rapid Commun.* **2001**, *22*, 897 - 936.
- (19) de Brouwer, H.; Tsavalas, J. G.; Schork, F. J.; Monteiro, M. J. *Macromolecules* **2000**, *33*, 9239 - 9246.
- (20) Matyjaszewski, K.; Davis, T. P. In *Handbook of Radical Polymerization*; Herk, A. M. V.; Monteiro, M., Eds.; Wiley & Sons: Canada, 2002; pp 301 - 331.
- (21) Vosloo, J. J.; De Wet-Roos, D.; Tonge, M. P.; Sanderson, R. D. *Macromolecules* **2002**, *35*, 4894 - 4902.



## *Chapter Two*

### *Theoretical background*

This chapter deals with background relevant to this study. Free radical polymerization and controlled free radical polymerization is discussed. In this chapter, the three living polymerization techniques, namely, atom transfer radical polymerization (ATRP), nitroxide mediated polymerization (NMP) and reversible addition chain transfer (RAFT) are mentioned. A detailed discussion on the RAFT technique is given. A brief overview on the different types of heterogeneous aqueous systems is also described. Since this study entails the use of miniemulsion polymerization, a detailed discussion on miniemulsion polymerization systems is presented. The use of the RAFT technique in miniemulsion for the synthesis of well-defined block copolymers is also discussed.

## *Chapter Two Theoretical Background*

---

### **2. Free radical polymerization**

#### **2.1 Introduction**

In the early 20<sup>th</sup> century many researchers showed great interest in the development and understanding of free radical polymerization.<sup>1</sup> At this time, many chemists believed that polymers were molecules that were held together by colloidal forces. In the 1920's Staudinger investigated polymer materials and realized that these compounds have a high molecular weight and a specific chain structure. Later, the concept of chain polymerization was projected by Staudinger and coworkers.<sup>1</sup> By 1935 polymers were accepted as having functional groups at their chain ends, formed by initiation and termination reactions.

Today, free radical polymerization is one of the most widely used processes for the production of high molecular weight polymers, both on industrial scale and laboratory scale. Compared to other polymerization techniques such as ionic polymerization, free radical polymerization offers many attractive features from an industrial point of view. These reactions can be carried out in undemanding conditions and can tolerate impurities that could be present in solvents that have not been purified. High molecular weight polymers can be synthesized without the removal of stabilizers that are often present in monomers. Free radical polymerization can tolerate small amounts of oxygen and can be used with a variety of monomers, such as styrene, methacrylates and vinyl acetates. A wide range of functional groups can also be tolerated by this process.<sup>2</sup> One of the most important industrial advantages of free radical polymerization is that it can be performed in homogeneous systems (bulk or solution polymerization) and in heterogeneous aqueous media (emulsion or miniemulsion polymerization). However, free radical polymerization has limitations, particularly in its lack of control over the polymer structure. This makes it difficult to synthesize well-defined polymer structures, with defined end-groups or special macromolecular architectures such as block copolymers.

The simplicity and versatility of free radical polymerization makes it one of the most

## ***Chapter Two Theoretical Background***

---

---

widespread polymerization methods in industry for the synthesis of homopolymers and copolymers with unique physical and chemical properties.

### **2.1.2 Chain reaction steps**

In order to understand the complex kinetics involved in free radical polymerization it is important to understand the three primary chain-reaction steps namely initiation, propagation and termination. These elementary steps will now be discussed briefly.

#### 1. Initiation

This is the initial step that involves the formation of primary radicals. In this stage the free radical active centre is formed. There are several mechanisms by which the radicals can be generated, including by thermal, redox, photochemical, electrochemical and radiolysis methods.<sup>3</sup>

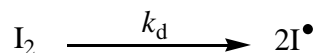
Thermal initiators are divided into two main classes, namely the azo and the peroxy compounds. Upon heating, these compounds decompose and release radicals. An example of an azo initiator that releases radicals when heated is AIBN (azobisisobutyronitrile). Thermal initiators that show first-order decay kinetics each have a half life. This is the time period after which half of the initiator molecules initially present are decomposed.<sup>4</sup> Thermal initiators are mainly used in free radical polymerization. Photoinitiators can also be used to generate radicals. In this case, they decompose upon irradiation with UV or visible light. There are two classes of photoinitiation namely photoinitiation by intramolecular bond cleavage and photoinitiation through hydrogen abstraction. Redox initiators comprise an oxidizing and a reducing agent. Intermediate free radicals are formed by the reaction of the two compounds. These initiators are often classed according to their solubility in water or organic liquids, or the manner in which the radicals are generated. In industry, these initiator systems are favored due to the low activation energies required for radical formation. These initiators can therefore be used at intermediate or low temperatures.<sup>4</sup>

## Chapter Two Theoretical Background

---

---

The initiator dissociation reaction is as follows:



Scheme 2.1: Decomposition of an initiator.

Here,  $I_2$  is the initiator compound that fragments into two radicals,  $I^\bullet$ . The radicals that are generated are called primary radicals. The initiator decomposition rate coefficient,  $k_d$ , is unique for each initiator. This value is dependent on the solvent and the temperature of the polymerization system.

In free radical polymerization, the decrease in the initiator concentration  $[I_2]$  in the polymerization system can be expressed as:

$$\frac{-d[I_2]}{dt} = k_d [I_2] \quad (2.1)$$

An expression that describes the initiator concentration as a function of time can be derived from equation (2.1) and is given as:

$$[I_2] = [I_2]_0 \cdot e^{-k_d t} \quad (2.2)$$

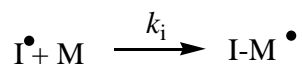
where  $[I_2]$  is the initiator concentration at time  $t$ ,  $[I_2]_0$ , the initial initiator concentration,  $k_d$  is the rate coefficient for the initiator decomposition and  $t$ , the time.<sup>5</sup>

The rate of primary radical formation is also important in kinetic studies of free radical polymerization. The rate of generation of radicals that are able to initiate the polymerization can be expressed as:

$$R_d = -2f \frac{d[I_2]}{dt} = 2fk_d [I_2] \quad (2.3)$$

where  $f$  is the initiator efficiency.

Primary radicals react with the monomer to form initiating radicals.



Scheme 2.2: Addition of a primary radical to monomer.

Here,  $k_i$  is the initiation rate coefficient and  $M$  is a monomer molecule.

## Chapter Two Theoretical Background

---

---

These initiating radicals react further with monomer to form propagating radicals. The initiator efficiency ( $f$ ) is the measure of the number of radicals that survive side processes to actually initiate.

This value can be given by

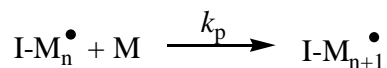
$$f = \frac{\text{[Rate of initiation of propagating chains]}}{n \text{ [Rate of initiator decomposition]}}$$

where  $n$  is the number of moles of radicals generated per mole of initiator.

It is important to note that primary radicals can undergo other side reactions with other species present in the system such as solvent, thereby forming other new secondary radical species.<sup>5</sup>

### 2. Propagation

This step follows after the initiation step. The propagation step consists of the successive addition of a number of monomer molecules to the primary radical. A new radical is generated with each sequential addition of monomer molecule.<sup>6</sup>



Scheme 2.3: Propagation of propagating radicals by monomer addition.

$k_p$  is the rate coefficient of propagation and is chain-length dependent.<sup>7</sup> For most monomers, the rate coefficient of propagation is pressure-dependent.<sup>8</sup> The rate of propagation is given by the equation:

$$v_p = k_p [M] [P^\bullet] \quad (2.4)$$

where  $[M]$  and  $[P^\bullet]$  are the concentrations of the monomer the propagating radical respectively.

### 3. Termination

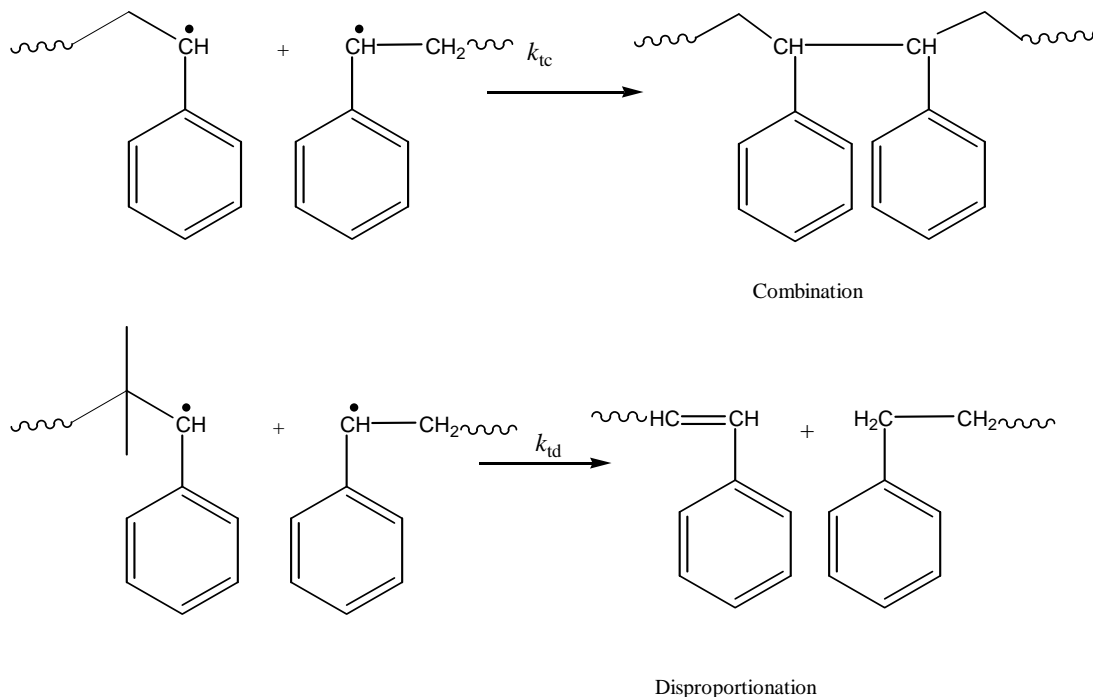
This is believed to be the most complex reaction in radical polymerization.<sup>4</sup> In this step two radicals are destroyed and therefore chain propagation can no longer take place.

The termination of the polymer can occur in two different processes namely:

1. Combination or disproportionation

## Chapter Two Theoretical Background

### 2. Primary radical termination



Scheme 2.4: Two radical termination mechanisms: combination and disproportionation.

Radical disproportionation and radical combination are bimolecular termination reactions. These termination processes dominate in free radical polymerization and are illustrated in Scheme 2.4. Combination or coupling occurs when two chain ends find each other and react, forming a single polymer chain.<sup>9</sup> The rate of termination by combination can be given as:

$$v_t = k_{tc} [P^\bullet]^2 \quad (2.5)$$

where  $k_{tc}$  is the rate coefficient of termination by combination and  $[P^\bullet]$  the concentration of the propagating radical.

In termination by disproportionation, a hydrogen atom is abstracted from a growing chain and transferred to another one. Disproportionation leads to one saturated end-group molecule and one containing an unsaturated end-group.<sup>9</sup> The rate of termination by disproportionation can be expressed as:

$$v_t = 2k_{td} [P^\bullet]^2 \quad (2.6)$$

## Chapter Two Theoretical Background

---

---

where  $k_{td}$  is the rate coefficient of termination by disproportionation and  $[P^\bullet]$  the propagating radical concentration.

The overall  $k_t$ , rate coefficient of termination, includes both the averages of the two rate coefficients and is expressed as:

$$k_t = \langle k_{td} \rangle + \langle k_{tc} \rangle \quad (2.7)$$

The other termination mechanisms mentioned, such as primary radical termination, involve the reaction of a propagating radical with an initiator-derived radical or a transfer-agent-derived radical. Chain termination can also occur by “stable” radicals such as oxygen and nitroxides, and by non-radical species such as phenols and quinones that react with the propagating radicals. These can act as *inhibitors* by terminating chains.<sup>9</sup>

### 4. Transfer reactions

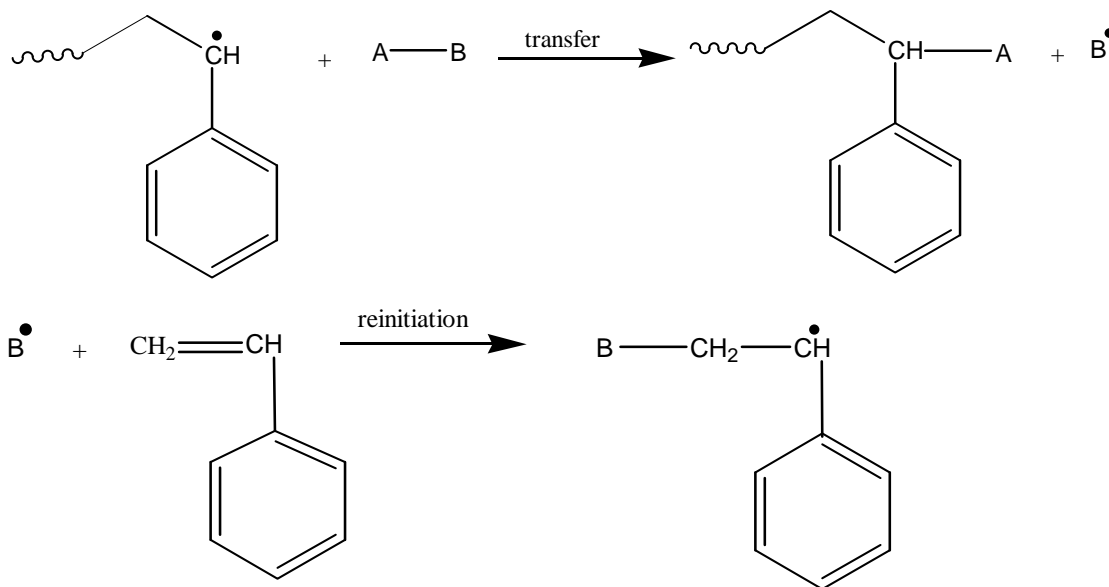
The chain transfer process was first recognized by Flory in 1937.<sup>10</sup> Chain transfer occurs in competition with propagation and affects the reactivity of the radical centres. Side reactions can occur due to the active centre of the radical polymerization that is highly reactive. Therefore, the radical is able to transfer to species in the reaction system by a transfer reaction. A number of transfer reactions exist. During the propagation step the propagating radicals may chain transfer to various species such as solvent, monomer, polymer and chain transfer agent. The formation of new propagating chains will occur if transfer to monomer occurs. Transfer to polymer results in chains of varying lengths as well as branched or crosslinked molecules. These transfer reactions therefore affect both the structures and the molecular weights of the final products.<sup>11</sup> These side reactions are important in free radical polymerizations as they can affect the polymerization system by, for example limiting the molecular weight.

The chain transfer process is well illustrated in Scheme 2.5 below. The reaction of a propagating radical with a transfer agent (A-B), forming a dead chain and a new radical ( $B^\bullet$ ), that is able to initiate a polymer chain, is called a chain transfer reaction. The

## Chapter Two Theoretical Background

---

transfer agent can either be an additive such as a thiol, or it can be an initiator, polymer or a solvent.



Scheme 2.5: The chain transfer process with styrene.

Chain transfer agents are used in synthesis reactions both in industry and in the laboratory. They are added to polymerization systems to reduce chain lengths and control molecular weight. They also control the distribution of the chain lengths and polymer end groups. In industry, alkyl mercaptans are often used as they are active transfer agents.<sup>11</sup>



### **2.2 Homogeneous and heterogeneous free radical polymerization**

Free radical polymerization can be performed in various media and in homogeneous or heterogeneous systems. These systems are now briefly discussed.

#### **2.2.1 Homogeneous systems**

Bulk and solution polymerizations are examples of homogeneous systems. In these polymerization techniques the monomer, solvent and initiator remain in one phase. The polymer that forms is soluble in either the monomer or the solvent.

Bulk polymerization involves the addition of monomer and a monomer-soluble initiator. Polymers of high molar mass and high rates of polymerization can occur if a high monomer concentration is used. With increasing conversion, the viscosity of the reaction mixture increases rapidly. This results in problems such as difficulty in stirring. Heat removal also becomes difficult and can result to auto acceleration. The bulk polymerization process has the advantage that polymers of high molar mass can be produced and the final polymer formed is of high purity.

Solution polymerization is the process whereby one polymerizes the monomer in solution. The solution reduces the viscosity of the system and problems such as heat transfer and auto-acceleration are eliminated. One of the requirements for solution polymerization is that the monomer and the formed polymer must be sufficiently soluble in the solvent of choice. The choice of the solvent plays an important role. The reduced monomer concentration can result in a decrease in both the rate and degree of polymerization. The final polymer obtained is often precipitated from the solution.

#### **2.2.2 Heterogeneous systems**

In industry and in academia, the application of nanoparticles dispersed in a continuous phase has become popular and of great interest as has many potential applications in material science. There exist several systems which differ in terms of the mechanism of particle nucleation, the kinetics of polymerization and the final particle size of the

## ***Chapter Two Theoretical Background***

---

---

polymer.

Heterophase aqueous polymerization results in the formation of polymer particles that are present in the continuous phase. The product is a dispersion of submicron-size polymer particles. Suspension polymerization, microemulsion polymerization, conventional emulsion polymerization and miniemulsion polymerization are different heterogeneous systems that will now be described briefly.

In suspension polymerization, water insoluble monomer is dispersed in a continuous aqueous phase as droplets. The suspension is maintained both by the use of stabilizers and by continuous agitation of the oil-soluble initiator that is dissolved in the monomer and the solution suspended as droplets in the aqueous medium. Polymerization of the monomer occurs within the droplets. These small droplets can be considered as microreactors that are suspended in water. The final polymer that is formed is in the form of beads, which can be obtained by filtration. The monomer droplets are usually 1 – 10  $\mu\text{m}$  in diameter, which is the same size as the beads.<sup>12</sup>

A conventional emulsion polymerization system consists of water, monomer, surfactant and water soluble initiator. Droplet nucleation and micellar nucleation may occur, depending on the monomer solubility, surfactant type and amount, as well as other factors. In these systems the polymerization results in particles of submicron size that remain suspended in the aqueous medium, forming a latex. The final particle diameter typically ranges from 100 – 500 nm. Microemulsion systems exist if the concentration of the surfactant is greatly increased or if the monomer concentration is reduced in an emulsion system. Microemulsions are thermodynamically stable systems with particle size of 10 – 100 nm.<sup>13</sup> Miniemulsion polymerization systems occur if the monomer droplet size in conventional emulsion polymerization is reduced such that the loci of polymerization are the monomer droplets. The aim in miniemulsion is to produce a latex which is a one to-one-copy of the original droplets. The monomer droplets are reduced to submicron sizes using a shear force. The final particle diameter range is 30 – 500 nm. Based on particle size and stability, miniemulsion polymerization lies between

## ***Chapter Two Theoretical Background***

---

---

conventional emulsion and microemulsion polymerizations.<sup>14</sup>

The main focus in this study is based on miniemulsion polymerization. The following section gives a detailed overview of miniemulsion polymerization. Since miniemulsion polymerization is seen as a derivative of emulsion polymerization, it has similar advantages in terms of the mechanism and kinetics.<sup>3</sup> The differences in the mechanism and kinetics of these two systems will also be discussed and compared.

### **2.3 Miniemulsion Polymerization**

#### **2.3.1 History**

The first miniemulsion polymerizations were carried out by Ugelstad *et al.* in 1973.<sup>14</sup> An emulsifier system consisting of anionic surfactant, sodium lauryl sulfate (SDS), and a long fatty alcohol costabilizer cetyl alcohol (CA), was used to polymerize styrene. Droplets smaller than 1 micron were formed by mixing the oil phase, consisting of monomer, into the aqueous phase followed by polymerization. It has been reported that the resulting particle size distribution was similar to the initial droplet size distribution.<sup>14</sup> This implied that the locus of polymerization was inside the droplets.

Throughout the past decade, much research has been carried out on styrene miniemulsion polymerization. At first styrene was used as the sole monomer; however, later, a variety of monomers were studied, such as butyl acrylate, methyl methacrylate and vinyl acetate. A number of copolymerization systems have also been studied, including St/MMA and VAc/ BA.<sup>3,14</sup>

#### **2.3.2 Miniemulsion preparation**

Miniemulsions are specially formulated heterophase systems consisting of stable nanodroplets in a continuous phase. High-shear devices are required to form nanodroplets with a size range of 50 – 500 nm. The droplets are the predominant loci for nucleation. In an ideal miniemulsion system, the polymer particles are a one-to-one copy of the original droplets, i.e. droplet nucleation is the dominant nucleation mechanism.<sup>15</sup> This was experimentally demonstrated by Ugelstad and coworkers in 1973.<sup>13</sup>

A miniemulsion is prepared by mechanically mixing the oil phase consisting of monomer, costabilizer and initiator (oil soluble) together with the aqueous phase consisting of water and surfactant. The mixture is then placed under shear in a high energy homogenizer, a sonicator or a mechanical homogenizer. High shear devices are used to break up the emulsion into submicron-size monomer droplets. At first, simple

## Chapter Two Theoretical Background

---

stirring was a method used for mechanical homogenization of the miniemulsions. Early articles report that homogeneous small particles were difficult to obtain due to the insufficiency of the energy transferred in these systems.<sup>16</sup> Today there are different methods available for the emulsification process, such as the use of sonifiers, high pressure homogenizers and rotor-stator systems. Large scale equipment such as high pressure homogenizers are used in industry where larger quantities or volume of liquids are used. For laboratories where small quantities of liquid are used, sonicators are ideal. Cavitation is the mechanism that is of importance in ultrasound emulsification.<sup>17,18</sup> The ultrasound waves cause the monomer droplets to break up, resulting in small monomer droplets. Droplet disruption and deformation by this mechanism is still not fully understood.

During the homogenization process the droplets change size rapidly until they reach a steady state. At the beginning the polydispersity of the droplets is high. With the application of the fission-fusion process, the polydispersity of the droplet decreases with sonication time. The miniemulsion eventually might reach a steady state. This is well illustrated by a reproduction of a figure by Landfester in Figure 2.1.<sup>17</sup>

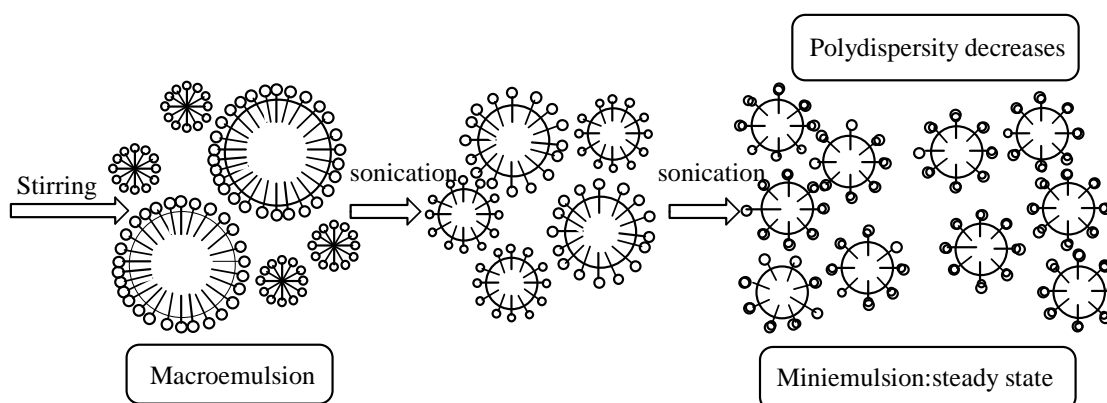


Figure 2.1: Formation of a miniemulsion.<sup>17</sup>

Many articles have reported that the droplet size is dependent on the sonication time.<sup>17</sup> The decrease in droplet size is partly associated with the geometry of the sonicator tip.

## ***Chapter Two Theoretical Background***

---

---

Around the sonicator tip, only a small region of the fluid is affected by the ultrasound waves. Additional stirring is necessary if the sonicator is used. This allows for the fluid to pass the sonication region. Several passes are needed in order to assure that the monomer droplets are broken up.<sup>19,20</sup>

### **2.3.3 Particle nucleation in emulsion and miniemulsion systems**

Emulsion polymerization and miniemulsion polymerization share many similarities but also have their differences. The mechanism of particle nucleation is one of the distinguishing differences between these two systems and will be discussed below.

Particle nucleation is still not well understood in emulsion polymerization due to the complexities of the process. In miniemulsion polymerization, particle nucleation is less complex than in emulsion polymerization due to the monomer droplets usually being the locus of polymerization. The nucleation mechanism is dependant on the water solubility of the initiator, the concentration of the surfactant, the temperature, and the monomer present in the system.<sup>21</sup> Depending on the type of system being used, usually one mechanism will dominate.

The three main forms of particle nucleation that exist in emulsion systems are: homogeneous nucleation, micellar nucleation and droplet nucleation.<sup>12</sup>

In homogeneous nucleation, the aqueous phase radicals polymerize to form oligomers. These oligomers precipitate when they reach a critical chain length at which they become insoluble in the aqueous phase. The precipitated oligoradicals are stabilized by the adsorbed surfactant. Homogeneous nucleation is the primary mechanism of particle formation for relatively water-soluble monomers and low surfactant concentration.<sup>14</sup> This nucleation mechanism sometimes occurs in emulsion polymerization systems. It is possible for homogeneous nucleation to occur in miniemulsions, depending on the monomer used, however homogeneous nucleation can be limited by changing kinetic parameters such that the growing oligoradicals are captured before they reach a critical chain length.<sup>3</sup>

## ***Chapter Two Theoretical Background***

---

---

In micellar nucleation, polymerization is initiated by initiator radicals that are generated in the aqueous phase and enter the monomer swollen surfactant micelles. When the concentration of the surfactant exceeds its critical micelle concentration (CMC), the excess surfactant molecules aggregate together and form small clusters that are called micelles.<sup>22</sup> The micelles become the reaction locus. Therefore, micellar nucleation occurs when the surfactant concentration is above the critical micelle concentration (CMC). Micellar nucleation is the primary particle formation mechanism for highly water-insoluble monomers and is favored by systems with high surfactant concentration.<sup>22</sup> This mechanism often occurs in emulsion polymerization, and is unlikely to occur in miniemulsion systems since the surfactant concentration is well below the CMC.<sup>3</sup>

The dominant mechanism for an ideal miniemulsion system is that of droplet nucleation.<sup>23,24</sup> In this nucleation process the aqueous phase radicals enter the monomer droplets and propagate to form polymeric particles. Colloidal stability is obtained by the presence of the surfactant that adsorbs on the monomer droplet surfaces and polymeric particles. In emulsion polymerization, droplet nucleation is usually ignored, due to the large particle diameter (1 – 10  $\mu\text{m}$ ) and the small number of droplets present.

Both homogeneous and micellar nucleation mechanism are limited in miniemulsions. The reason for this is that, in these systems, most of the surfactant is adsorbed by the droplets that have a large total surface area. This results in little surfactant being present to form micelles. Due to the large total surface area of all droplets, the probability of a propagating radical entering the droplets is greater.

### **2.3.4 Mechanism and kinetics of nucleation in emulsion and miniemulsion systems**

#### **2.3.4.1 Emulsion systems**

To date, many theoretical descriptions based on the kinetics of emulsion polymerization have been developed. The most commonly applied is based on the work of Smith and Ewart.<sup>12</sup> The description of emulsion polymerization kinetics can be characterized by three intervals.

## Chapter Two Theoretical Background

---

**Interval I:** This is the initial stage during which particle nucleation or formation occurs. Micelles and monomer droplets are present. Radicals are generated in the water phase and enter the micelles. In this interval the particle size and number increase and thus the polymerization rate increases. At the end of this interval, monomer conversion is low (2% - 10%), and most of the monomer is in the droplets that are relatively large (1 – 10  $\mu\text{m}$ ).<sup>13</sup>

**Interval II:** This is often the main step of particle growth. In this stage monomer droplets and particles are present. Micelles have disappeared by either becoming particles or they act as monomer and surfactant reservoirs. Monomer molecules migrate from the monomer droplets to the monomer-swollen polymer particles. The particle size increases while the particle number and the monomer concentration is stable, thus the polymerization rate is constant. This interval usually extends from 2% – 10% to 30% – 70% conversion.<sup>3</sup>

**Interval III:** This is the final stage. No more monomer droplets or micelles are present. The monomer is only present in the particles. The particle size and number are usually constant but sometimes  $\bar{n}$ , the average number of radicals per particle increases and the rate increases for a while. The concentration of the monomer decreases and therefore the rate of polymerization decreases. This is the stage in which most miniemulsions spend time.

Figure 2.2 below illustrates the three intervals in emulsion polymerization systems.

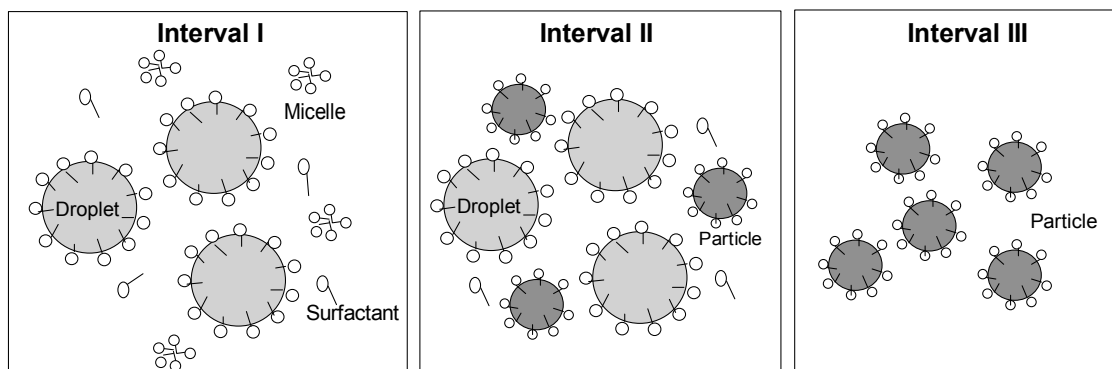


Figure 2.2: The three intervals in emulsion polymerization.



## Chapter Two Theoretical Background

---

The kinetics and mechanisms in emulsion systems are influenced by compartmentalization. This is the process where two radicals in a particle undergo rapid termination. Due to the compartmentalization, the rate of termination in these systems decreases since radicals are present in separate particles. Because of the high concentration of particles the rate of polymerization increases relative to solution systems and higher molecular weights can be obtained, due to longer radical life time. This is a key feature in these systems compared to other polymerization processes such as bulk or solution polymerization.

The rate of polymerization,  $R_p$ , in heterogeneous systems can be expressed as:

$$R_p = k_p[M]_p \bar{n} N_c / N_A \quad (2.8)$$

where  $k_p$  is the rate coefficient of propagation,  $[M]_p$ , the concentration of monomer in the particles,  $N_c$ , the number of particles per unit volume,  $N_A$ , Avagadro's constant and  $\bar{n}$ , the average number of radicals per particle.

$\bar{n}$  is an important factor in emulsion systems. It determines both the rate of polymerization and the molar mass. During the polymerization process, the average number of radicals per particle does not stay constant. The value of  $\bar{n}$  is determined by a number of factors, such as the rate of radical generation, the number of polymer particles, radical exit and termination reactions. For a simple zero-one system

$$\bar{n} = \frac{\rho}{2\rho + k} \quad (2.9)$$

where  $\bar{n}$  is the average number of radicals per particle,  $\rho$  is the rate coefficient for radical entry,  $k$ , the pseudo-first-order rate coefficient for radical exit.  $\bar{n}$  is dependent on  $k$  and  $\rho$ . (Note: if  $\rho \gg k$  then  $\bar{n}$  is approximately 0.5. This is often assumed, but it does not hold in this present study). The earliest mathematical model of emulsion polymerization was that of Smith and Ewart.<sup>12</sup>

Smith-Ewart outlined three cases:

## ***Chapter Two Theoretical Background***

---

---

*Case I:  $\bar{n} \ll 0.5$*

This case applies when radical exit is high relative to entry.

*Case II:  $\bar{n} = 0.5$*

This applies when the rate of radical exit from the particles is insignificant. Termination is instantaneous and, at any time, the particles have either one or zero radicals. This system is referred to a zero-one system and is typical in styrene emulsion polymerization systems.

*Case III:  $\bar{n} \gg 0.5$*

This applies when the rate of termination in the particles is small relative to the entry rate, and often when the particle volume is relatively large.

$\bar{n}$  can be described in two basic ways, which differ in the way that the radicals terminate in the particles. A ***zero-one system*** is one whereby entry of a radical into a particle that contains a growing radical results in termination between the two radicals that is so fast that it is not rate determining. Therefore the average number of radicals per particle cannot exceed 0.5. This describes Smith Ewart's Case I and Case II. Zero-one conditions are uncommon at high conversions where the viscosity in the particles is high. Other systems are ***non-zero-one systems***, where multiple radicals can co-exist within a particle without instantaneous termination. The termination in these systems is diffusion controlled and rate determining.  $\bar{n}$  is usually greater than 0.5, but a system with low  $\bar{n}$  can also be pseudo-bulk if the radical desorption results in the desorbed radical re-entering another particle.

### **2.3.4.2 Phase transfer events in emulsion polymerization**

In emulsion polymerization, propagation, transfer and termination are important basic kinetic events. In emulsion polymerization, the two new kinetically important phase transfer events of radical exit and entry of radicals into and from particles need to be considered.<sup>25</sup>

## Chapter Two Theoretical Background

---

---

For kinetic analysis, specific models for entry and exit have been developed. The mathematical equations have been given as they are of use at a later stage in this study.

- **Model for entry**

Entry is the process whereby free radicals that are generated in the aqueous phase migrate into the particles. In order for a radical to enter a particle it first needs to propagate with monomer present in the aqueous phase to form a surface-active radical, which is able to enter the hydrophobic particles. Radical entry into the particles is modeled according to the mechanism proposed by Maxwell-Morrison, where the rate determining step is the growth of the polymer radical in the aqueous phase to a critical degree of polymerization,  $z$ .<sup>26</sup>

The (pseudo)-first-order rate coefficient for radical entry is given by  $\rho$ . This is the average number of entry events into a particle per second. This value is dependent on the type of initiator, initiator concentration, particle number density, particle size and surface charge density. The rate coefficient for radical entry is expressed as:

$$\rho \approx \frac{2k_d [I] N_A}{N_c} \left\{ \frac{\sqrt{2k_d [I] k_{t, \text{aq}}}}{k_{p, \text{aq}} C_W} + 1 \right\}^{1-z} \quad (2.10)$$

where  $k_d$  is the decomposition rate coefficient of the initiator,  $[I]$ , the initiator concentration,  $N_A$ , Avagadro's constant,  $N_c$ , particle number,  $k_{t, \text{aq}}$ , the aqueous phase termination rate coefficient,  $k_{p, \text{aq}}$ , the aqueous phase propagation rate coefficient,  $C_W$ , the concentration of the monomer in the aqueous phase and  $z$ , the length of the  $z$ -mers.

- **Model for exit**

Exit is the process where radicals desorb or exit the particles, therefore reducing the average number of radicals per particle,  $\bar{n}$ . The radicals that result from chain transfer to monomer or chain transfer agent are capable of desorbing. The surface-active species that have entered the particle are unable to exit due to their insolubility in the aqueous phase. The pseudo-first-order rate coefficient,  $k$ , is the number of exit events from a particle per

## Chapter Two Theoretical Background

---

---

second. The equation for the exit rate coefficient is expressed as:

$$k = 2k_{tr}C_p \frac{k_{dM}}{k_{dM} + k_{p1}C_p} \quad (2.11)$$

where  $k_{dM}$  is the rate coefficient for a single molecule desorbing from the interior of a particle,  $C_p$ , the monomer concentration in the particles and  $k_{p1}$ , the propagation rate coefficient for a monomeric radical. Note: if we combine equation 2.11 with equation 2.13, then  $k$  is dependent on the particle radius.

The equation for the first-order rate coefficient for exit assuming complete aqueous phase termination,  $k_{ct}$ , is given as

$$k_{ct} = k_{tr}C_p \frac{k_{dM}}{k_{dM} + k_{p1}C_p} \quad (2.12)$$

The subscript “ct” in equation 2.12 is for complete termination. The second term of the equation is the probability that a radical resulting from transfer will escape rather than propagate.

Radical exit is further complicated by the process of re-entry. An exited radical is able to re-enter another particle.

- Model for desorption of monomeric radical

The rate coefficient for desorption of a monomeric radical from a particle is expressed as:

$$k_{dM} = \frac{3D_W}{qr_s^2} = \frac{3D_W}{r_s^2} \frac{C_W}{C_P} \quad (2.13)$$

where  $k_{dM}$  is the rate coefficient for a single molecule desorbing from the interior of a particle,  $D_W$  is the diffusion coefficient of the desorbing species in the water phase,  $q$  is the partition coefficient for monomeric radicals between the particle and the water phase,  $r_s$ , the swollen particle radius,  $C_p$ , the monomer concentration in the particles. Note: from equation 2.13,  $k_{dM}$  is dependent on the radius of the particle.

## ***Chapter Two Theoretical Background***

---

theoretically investigated and the equations can be modified.<sup>27</sup> At this stage, the equations given are considered for the simple zero-one system used in Chapter 4.

### **2.3.5 Miniemulsion systems**

As mentioned before, in miniemulsion polymerization the monomer droplets produced are very small in size (0.01 – 0.5  $\mu\text{m}$ ). Studies have been carried on the kinetics of these systems. There exist three distinguished intervals in a miniemulsion polymerization.

**Interval I:** Particle nucleation occurs in this interval. During this interval, propagating radicals enter the droplets in the system. This interval proceeds until the average number of radicals per particle ( $\bar{n}$ ) is 0.5, if zero-one conditions apply.  $\bar{n}$  can however exceed 0.5 and in this case non zero-one kinetics holds. This interval ends when all the droplets have nucleated. Interval I in miniemulsions is usually shorter than that in emulsions.

**Interval III:** In this interval only monomer in the droplet is left for polymerization. Monomer inside the droplets is available for polymerization. In this interval the monomer concentration often decreases exponentially only if  $\bar{n}$  and  $N_c$  are constant.

**Interval IV:** During this interval an increase in viscosity inside the droplet can occur. This is due to the Trommsdorff-Norrish effect, where an increase in the viscosity of the particles occurs. An increase in the average number of radicals per particle occurs and often  $\bar{n} > 0.5$ .

Compared to emulsion polymerization systems, in miniemulsion polymerization, Interval II, where monomer droplets exist, is clearly absent. The reason for this is that monomer transport is negligible – polymerization of the monomer occurs inside the small droplets. Inside the polymerization locus, there is no period where the monomer concentration is constant.<sup>3</sup>

Figure 2.3 illustrates a typical miniemulsion system.

## Chapter Two Theoretical Background

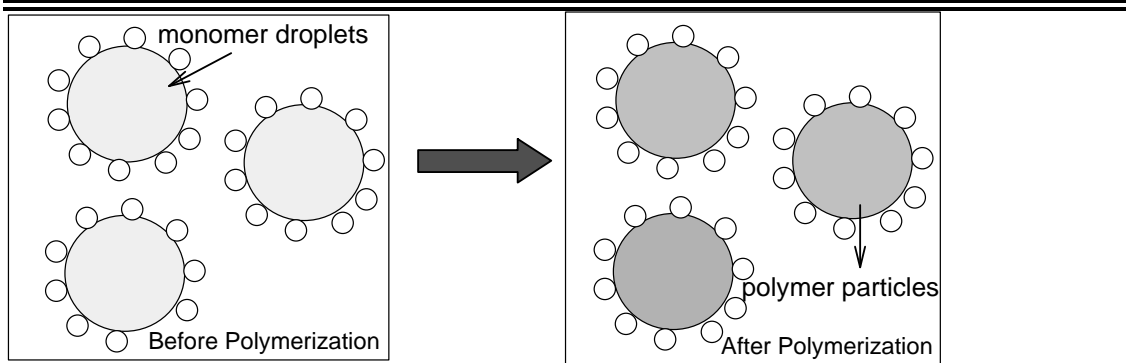


Figure 2.3: Miniemulsion polymerization showing the final latex particles.

### 2.3.6 Particle stability in miniemulsion systems

Miniemulsions are produced by high shear to break up the emulsion into submicron monomer droplets. The submicron droplets that are formed are thermodynamically unstable.<sup>14</sup> Particle stability can be associated with the following:

- droplet coalescence
- Ostwald ripening
- superswelling

In miniemulsion polymerization the role of the surfactant and the costabilizer is of importance. In these aqueous systems, coalescence and collision of particles result in destabilization. A surfactant is defined as being a surface active agent and is characterized by its tendency to adsorb at surfaces and interfaces. The fundamental property of a surfactant is its tendency to accumulate at interfaces between phases.<sup>22</sup> Surfactants are often classified by their polar head group.

There are four classes namely anionic surfactants, cationic surfactants, non-ionic surfactants and zwitterionic surfactants.<sup>22</sup> The role of the surfactant in miniemulsions is to retard droplet or particle coalescence that is caused by Brownian motion. The surfactant stabilizes the droplets by adsorbing at the surfaces of the droplets, providing either an electrostatic stabilization effect in the case of ionic surfactants, or a steric stabilization

## ***Chapter Two Theoretical Background***

---

---

effect, in the case of non-ionic surfactants, or by both stabilization effects in the case of polyelectrolytes. The amount and type of surfactant used in the system also plays an important role in determining the particle size of the final polymer.<sup>17</sup>

In literature, most miniemulsions have been stabilized using ionic surfactants, SDS or CTAB. El-Aasser used cationic surfactants in miniemulsion polymerization and obtained stable, well-defined latexes with narrow particle size distributions.<sup>17</sup> Landfester and coworkers reported that cationic surfactants in styrene miniemulsions produced similar particle sizes to anionic surfactants used in miniemulsions.<sup>28</sup> The use of non-ionic surfactants, such as polyoxyethylene-23 lauryl ether (Brij-35), formed well-defined stable miniemulsions. Polymerizable surfactants, such as vinylbenzylsulfosuccinic acid sodium salt have also been used by Guyot and coworkers.<sup>29</sup> These surfactants also produced stable miniemulsions.

A costabilizer, by definition, is a surface-active agent that reduces the interfacial energy but cannot form micellar aggregates by itself. In miniemulsion systems, Ostwald ripening is a process whereby nanodroplets are destabilized. The costabilizer retards monomer diffusion from the smaller to the larger droplets.<sup>3</sup> In order to obtain small droplets with the Laplace pressure smaller than or equal to the osmotic pressure, the droplet must be prepared using a high-shear device. The presence of large droplets leads to degradation if not further stabilized. If the small droplets are not stabilized against Ostwald ripening, they will disappear.<sup>17</sup> The costabilizer leads to an increase in osmotic pressure in the monomer droplets, which suppresses the monomer diffusion, resulting in small stable droplets. Costabiliser that is confined within the monomer droplets, causes a change in the droplet size which further increases the osmotic pressure with a decrease in the droplet radius. An increase in the osmotic pressure in the small monomer droplets prevents growth of the large droplets by stopping monomer diffusion, therefore the smaller droplets have increased stability.

## Chapter Two Theoretical Background

---

The role of the costabilizer is therefore to prevent or suppress Ostwald ripening. In order for the costabilizer to be efficient it requires the following properties: a high monomer solubility and a low water solubility.<sup>13</sup> The monomer droplet stability can be understood in terms of the free energy. The reason and importance for the particular properties of the costabilizer can be seen in the equation below, which can be used to calculate the efficiency of the costabilizer. The equation consists of two terms, namely the partial molar free energy of mixing and the interfacial partial molar free energy:

$$\frac{\Delta\overline{G}_i}{RT} = \ln \varphi_i = (1 + m_{ij})\varphi_j + \chi_{ij}\varphi_j^2 + \frac{2\overline{V}_i\gamma}{RT r} \quad (2.14)$$

where  $\Delta\overline{G}_i$  is the partial molar free energy of mixing,  $m_{ij}$  is the ratio of costabilizer molecules to monomer molecules,  $\chi_{ij}$  is the interaction parameter between the costabilizer and the monomer,  $\overline{V}_i$  is the molar volume of the monomer,  $\varphi_i$  and  $\varphi_j$  are the volume fractions of the monomer and the costabilizer,  $\gamma$ , the interfacial tension between continuous and dispersed phases and  $r$  is the radius of the droplet.<sup>13</sup>

In early work carried out by Asua *et al.*<sup>30</sup> it was observed that the use of fatty alcohols produced stable miniemulsions. However, later it was noted that the use of a low molecular weight, water-insoluble compound, hexadecane, retarded molecular diffusion. This is due to the slow rate of diffusion of the water-insoluble compound through the aqueous phase, which prevents migration.<sup>30</sup>

In literature, the most commonly used costabilizers are hexadecane and cetyl alcohol. However, these are volatile compounds and are undesirable for commercial application.<sup>17</sup> A variety of other costabilizers are mentioned in literature and have been studied in miniemulsion systems. Siloxanes, silanes and polyesters have also been used and have been shown to suppress Ostwald ripening.<sup>13</sup> The more hydrophobic the agent is the more effective it is. Ugelstad *et al.*<sup>31</sup> have shown that an increase in chain length of the



## ***Chapter Two Theoretical Background***

---

---

hydrophobe increases the stability of the miniemulsions. The use of polymer as a hydrophobe has been reported.<sup>17</sup> Due to their high water insolubility and monomer compatibility, it resulted in stabilization of the droplets. The use of water-insoluble comonomers has also been shown to improve the droplet stability of miniemulsions.<sup>32</sup>

Superswelling is also a cause of instability in miniemulsions, however, this is usually seen in controlled miniemulsion polymerization systems. In superswelling, as the superswelling equilibrium point approaches, a large amount of monomer is transferred from a large number of droplets to a small number of particles that contain oligomers. This causes the monomer droplets to shrink and the particles to swell. Superswelling results in the broadening of the particle size distribution, which causes an unstable miniemulsion system. Luo *et al.*<sup>33</sup> postulated the existence of superswelling. Their work showed that superswelling is dependent on the reaction recipe. By increasing the costabilizer level or by using a non-ionic surfactant, superswelling can be suppressed.

### **2.4 Controlled free radical polymerization**

#### **2.4.1 History and developments**

Initially, and for a long period of time, the control of radical addition reactions has been difficult due to unavoidable termination reactions. Kharasch and Jensen<sup>34</sup> were one of the first to be successful in studying systems whereby they added halogenated compounds to alkenes via radical intermediates under photochemical conditions ATRA (Atom Transfer Radical Addition).

During the 1960s, Minisci<sup>35</sup> and Asscher and Vosfi<sup>36</sup> further studied these ATRA reactions; they introduced metal-catalyzed reactions which subsequently became more important in organic synthesis. Researches are still continuing to carry out studies based on ATRA reactions, which could improve stereocontrol and tacticity control in both radical polymerization and living radical polymerization.<sup>37</sup>

## ***Chapter Two Theoretical Background***

---

In 1956, the concept of living polymerizations was first discovered and described by Szwarc.<sup>38</sup> Both polymer chemistry and polymer physics were greatly influenced by this discovery, which led to major developments in the world of polymer science. His advances and improvements are believed to be the “foundation of modern nanotechnology”.<sup>39</sup> Szwarc defined living polymerization as a chain-growth process without chain breaking reactions. Traditionally, anionic polymerization is an example of a living polymerization process that gives chemists the possibility to synthesize well-defined polymers with nano-structured morphologies and complex architectures. Living anionic polymerization, based on ionic species, was the first technique used to synthesize polymers with controlled topology. The main drawback of this technique is however that it requires stringent process conditions and is limited to only a number of monomers.<sup>37</sup>

Cationic ring opening polymerization of tetrahydrofuran was the first system whereby dormant and active species were spectroscopically observed. During this time, many other approaches were used in anionic polymerization based on the exchange between active and dormant chains. At that time, original living anionic polymerization still showed control. The new systems that were studied showed less control and chain breaking did not occur. The results obtained, confirmed that it was difficult to control the molecular weight and to obtain a linear increase in molecular weight with increasing conversion. However, the understanding of the kinetics involved in these systems was useful for improved living radical polymerization.<sup>40</sup>

Borsig *et al.*<sup>41</sup> was one of the first to observe controlled radical polymerization when he polymerized MMA and Sty initiated by cyclic tetraarylethane derivatives. A linear increase in molecular weight with conversion was observed. Block copolymer formation was also observed. Braun<sup>42</sup> also studied these systems, but did not find a linear increase in molecular mass with conversion. Initiation efficiencies were low and high polydispersities were obtained.

In 1982, the concept of controlled/living radical polymerization was introduced to the

## ***Chapter Two Theoretical Background***

---

scientific community and first discussed by Otsu.<sup>37</sup> He studied the use of iniferters: agents that initiate, transfer and terminate. The model he studied was based on MMA polymerization initiated by benzyl dithiocarbamates. The results obtained showed low initiation efficiency, molecular weights did not evolve linearly with conversion and high polydispersities were obtained. Although the work of Otsu (entailing the use of iniferters) resulted in deficiencies, block copolymers were synthesized even though contamination by homopolymer was present.

In 1985, the use of nitroxides as stable radicals for controlling radical polymerization was patented.<sup>43</sup> This was the work of Solomon and Rizzardo, but not recognized at that time. Later, another controlled radical polymerization technique based on addition-fragmentation was proposed and fully understood by Rizzardo and Moad.<sup>44</sup> It was only in 1993 that the concept of living radical polymerization came to the forefront, after the work of Georges *et al.*<sup>45</sup> who further investigated the work of Rizzardo.

Recently, the discoveries of many controlled radical polymerization systems have captured the interest of many chemists. The understanding of these controlled free radical polymerization reactions, the calculation and quantitative measurements of parameters such as rate and equilibrium constants and concentration of the species involved in these reactions, has progressed significantly over recent years. Unique materials that were previously unattainable are now accessible.

Today, living techniques such as Stable Free Radical Polymerization (SFRP), Nitroxide mediated Polymerization (NMP), Atom Transfer Radical Polymerization (ATRP) and Reversible Addition chain Transfer (RAFT) are modern living radical polymerization techniques that are currently most popular. These techniques are being used to control polymer topologies, compositions and functionalities.<sup>46,47</sup>

### **2.4.2 Controlled free radical polymerization mechanisms**

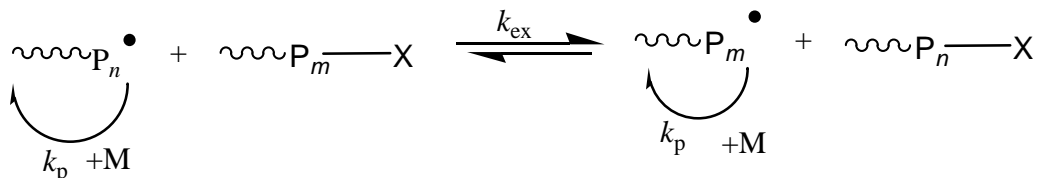
In all controlled free radical polymerization processes, there is ideally a low occurrence



## Chapter Two Theoretical Background

---

- Degenerative transfer



Scheme 2.7: Controlled free radical polymerization via degenerative transfer.

The second scheme is based on degenerative transfer. In these systems, fast exchange between the active and dormant species is needed in order to have good control of the molecular weight and polydispersity. The dormant species in these systems is the transfer agent. Unlike the deactivation/activation process, an external source of free radicals is needed to initiate the polymerization. In these systems, the concentration of the transfer agent is usually larger than that of the initiator. This system is not based on PRE.<sup>37</sup>

RAFT is an example of reversible transfer and is a very commonly used technique to produce living polymers. Reversible transfer involves the exchange between active and dormant chains and, at any time, some chains are active. In this technique, the radical concentration is not directly affected by the transfer mechanism. The number of radicals is determined by the initiator decomposition and termination rates. In order to obtain good control, the concentration of the initiator is usually small compared to the control agent, since each radical generated will eventually terminate and form a dead chain.

The following are the main features and characteristics of living radical polymerization systems:

- Polymers of narrow MWD can be synthesized.
- The molecular weight increases linearly with conversion and can be predicted.
- Polymers with low polydispersity and high functionality can be synthesized.
- Polymerization can proceed until all the monomer has been consumed. Further addition of monomer allows the polymerization to continue.
- Polymers of complex architectures such as block, star, graft, comb and brush copolymers are accessible.

## ***Chapter Two Theoretical Background***

---

---

Other advantages include:

- Experimental conditions are the same as for free radical polymerization.
- Controlled radical polymerization can be performed in homogeneous systems (bulk and solution polymerization) as well as heterogeneous systems (miniemulsion and emulsion polymerization).

During the past few years, the three main controlled radical polymerization techniques have been studied extensively and now provide a tool to prepare polymers with well-defined structures, controlled molecular weights and narrow molecular weight distributions.

In this study, the controlled radical polymerization technique used is the RAFT process. The RAFT process itself is discussed briefly in the following section.

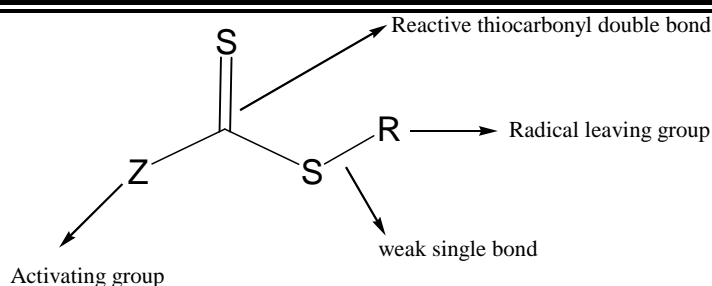
### **2.5 Reversible addition fragmentation chain transfer (RAFT)**

Moad and coworkers reported a new controlled radical polymerization technique, RAFT, in 1998.<sup>49-51</sup> The RAFT process is an exceptionally versatile technique that allows for the synthesis of polymers of predictable molecular weight and narrow polydispersity.<sup>52</sup> In the RAFT technique, the polymerization is carried out in the presence of dithio compounds. These compounds act as RAFT agents and give the polymerization living characteristics. The RAFT process can be applied to a range of monomers, solvents, functional groups and reaction conditions (solution, bulk, emulsion, miniemulsion polymerization). Block copolymers of type AB, ABA, and gradient block copolymers can also be synthesized by thiocarbonyl-thio terminated polymers.<sup>53,54</sup>

#### **2.5.1 General structure of the RAFT agent**

The RAFT process involves free radical polymerization in the presence of a transfer agent. The structure of the RAFT agent plays an important role. In order for the RAFT process to function effectively, the choice of the Z and the R groups must be considered.

## Chapter Two Theoretical Background



Scheme 2.8: General structure of a RAFT agent.

There exists four classes of thiocarbonyl-thio RAFT agents. This depends on the nature of the Z group. The classes are identified according to the group or atom used to form the C-Z bond.

Class	Z
Dithioesters	Alkyl or aryl
Trithiocarbonates	Substituted sulfur
Xanthates	Substituted oxygen
Dithiocarbamates	Substituted nitrogen

When choosing an efficient RAFT agent for the polymerization system, the effect of the Z and the R group need to be considered. The thiocarbonyl-thio radical is strongly influenced by the Z group. The Z group is the activating group. This group is able to modify the rate of free radical addition to the C=S double bond and it simultaneously modifies the stability of the formed intermediate radical. The Z group activates the double bond towards radical addition. The effect of the Z group with a variety of monomers has been investigated.<sup>55,56</sup> Studies have shown that the phenyl Z group is ideal for most monomers since it balances the stability of the radical intermediate and its reactivity towards fragmentation. The benzyl Z group allows for fragmentation to occur more easily and almost no retardation occurs in styrene polymerization. The R group is the leaving group and can also stabilize the radical intermediate, however to a lesser extent than the Z group. The leaving group R should be carefully chosen, and is dependent on the monomer that is used in the system.<sup>2</sup> Different leaving groups will have different reactivities and so the kinetics of the system will be influenced. The R group

## Chapter Two Theoretical Background

should be a good leaving group relative to the radical of the propagating species and a good reinitiating group towards the monomer used. When choosing a R group, factors such as polarity factors, steric factors and radical stability should be considered. More stable, more electrophilic and more bulky radicals are better leaving groups.

The nature of the Z and R groups, the monomer and the polymerization conditions are all factors that determine the effectiveness of the RAFT agent.

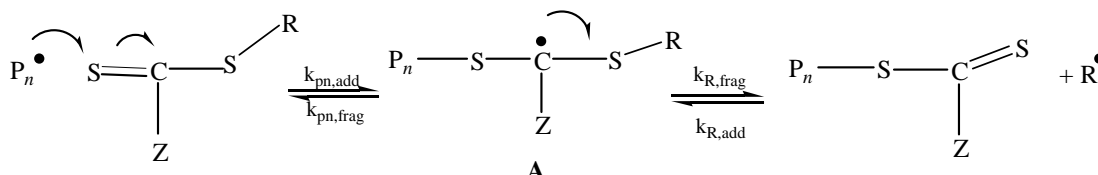
### 2.5.2 RAFT mechanism

The key feature of the RAFT mechanism is a sequence of addition-fragmentation equilibria.<sup>2,49</sup> In this mechanism, initiation, propagation and termination occurs as in conventional radical polymerization. A general accepted RAFT mechanism is given below.

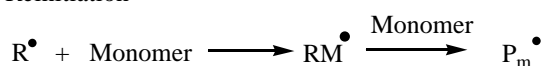
#### 1. Initiation and propagation



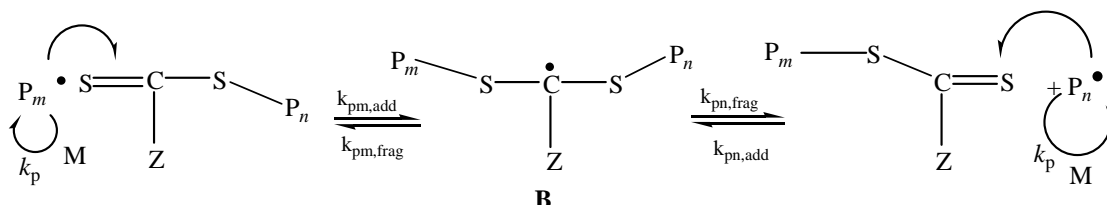
#### 2. Addition to the RAFT agent



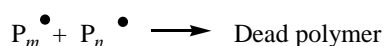
#### 3. Reinitiation



#### 4. Chain equilibrium



#### 5. Termination



Scheme 2.9: The RAFT mechanism.



## Chapter Two Theoretical Background

---

- (1) In the RAFT mechanism the first step is initiation. The decomposition of the initiator leads to the propagating radical forming.
- (2) The propagating radical  $P_n^\bullet$  adds to the RAFT agent  $[S=C(Z)SR]$  and fragmentation of the intermediate radical leads to the formation of a new radical  $R^\bullet$  and a polymeric RAFT agent.
- (3)  $R^\bullet$  reacts with monomer and reinitiates the polymerization. This results in a new propagating radical  $P_m^\bullet$  forming.
- (4) Equilibrium between the active propagating species  $P_n^\bullet$  and  $P_m^\bullet$  with dormant polymeric RAFT compound allows chains to have an equal probability to grow. which allows for polymers of narrow polydispersity to be produced. The intermediate radical species (B) has been observed via electron spin resonance (ESR) mechanism.<sup>51,57</sup>

The RAFT mechanism is often complicated by a number of side reactions that can occur. This results in the formation of by-products, retardation and inhibition. Inhibition typically occurs at the start of the reaction while retardation can last throughout the reaction. Retardation is mainly caused when an inappropriate RAFT agent is used.

There has been ongoing debate on the mechanism causing retardation.<sup>27,58</sup> From Scheme 2.9, retardation might occur due to:

1. slow fragmentation of the intermediate radical species (A) formed from the addition to the original RAFT agent
2. slow reinitiation by  $R^\bullet$ , the leaving group
3. preferred addition of the leaving radical  $R^\bullet$  to the RAFT agent rather than to the monomer
4. slow fragmentation of the intermediate radical species (B) formed from the addition to the polymeric RAFT agent
5. preferred addition of  $P_n^\bullet$  and  $P_m^\bullet$  to the RAFT agent rather than monomer

## Chapter Two Theoretical Background

---

6. Evidence of cross termination between propagating and adduct radicals was proposed by Monteiro and coworkers to explain rate retardation in RAFT-mediated systems.<sup>59,60</sup> There is evidence that this causes retardation, however the argument of slow fragmentation vs. cross termination is still being debated.

In the RAFT process, the final molecular weight of the polymer can be predicted and controlled. This is an important feature of the RAFT process.

In RAFT systems, the concentration of the chains at 100 % conversion can be determined by the following equation, assuming termination by disproportionation

$$[chains] = [RAFT] + 2.f \cdot ([I] - [I]_0) \quad (2.15)$$

The first term in the equation describes the concentration of the dormant chains while the second term describes the number of chains derived from the decomposed initiator. Since RAFT polymerization involves the formation of free radical intermediates, radical-radical termination cannot be avoided. This results in the formation of dead chains. The amount of dead polymer chains formed is dependent on the number of chains initiated by the initiator-derived radicals. The concentration of the initiator with respect to the RAFT agent should be kept small in order to have a minimum amount of dead chains.<sup>61</sup>

The RAFT process is characterized by a roughly linear increase in molecular weight with conversion. Therefore, by knowing the initial concentration of the RAFT agent and the initial concentration of the monomer, the equation below allows one to calculate the theoretical molecular weight:

$$\bar{M}_{n_{theo}} = FW_{RAFT} + \frac{x[M_0]FW_M}{[RAFT]_0} \quad (2.16)$$

$$\bar{M}_{n_{theo}} = FW_{RAFT} + \frac{x[M_0]FW_M}{[RAFT]_0 + 2.f \cdot [I_0](1 - e^{-k_d t})} \quad (2.17)$$

where  $FW_{RAFT}$  is the molecular weight of the RAFT agent,  $[RAFT]_0$ , the initial concentration of the RAFT agent,  $[M_0]$ , the initial concentration of the monomer,  $[I_0]$ ,

## ***Chapter Two Theoretical Background***

---

---

the initial concentration of the initiator,  $FW_M$ , the molecular weight of the monomer,  $x$ , the fractional conversion at time  $t$ ,  $f$ , the initiator efficiency, and  $k_d$ , the initiator dissociation constant.

Equation 2.16 excludes the contribution of the initiator-derived chains to the final chain concentration. Equation 2.17 includes the time-dependent concentration of the initiator-derived chains to the final chain concentration.

### **2.5.3 Controlled free radical polymerization in heterogeneous aqueous media**

A challenge confronting many polymer chemists is the application of controlled free radical polymerization in heterogeneous aqueous media. As has been stated, controlled free radical polymerization has been shown to be a viable method for the synthesis of polymers with well-controlled molecular structure. Many studies have been carried out on homogeneous living free radical polymerization using various mechanisms such as NMP, ATRP, and RAFT.<sup>62</sup> Recently, efforts have been made to carry out controlled free radical polymerization in water-based conventional systems such as emulsion or miniemulsion polymerization. The range of possible industrial applications and products will be improved if controlled free radical polymerization can be carried out successfully in these dispersed media.

The advantages of heterogeneous aqueous systems over homogeneous systems are the following:

- inexpensive
- high polymerization rates
- The use of organic solvents is eliminated which results in no volatile organic compounds (VOC) being present, which makes it an environmental friendly process.
- The final product is in latex form. The viscosity of the polymer is low for high-polymer-solid content, which makes it easy for the polymer to be handled and processed.
- efficient heat transfer

## ***Chapter Two Theoretical Background***

---

---

- high conversions with low monomer residuals are obtained.
- A wide range of experimental conditions can be used.
- Polymer materials of complex architecture and novel particle morphologies can be synthesized, which is of great interest in the coating industry and other industries.

The following section focuses on the use of controlled radical polymerization in heterogeneous media. Emphasis is based on the RAFT process in these systems since the research carried out in this study is based on the RAFT process in miniemulsion polymerization.

### **2.5.4 RAFT in heterogeneous aqueous systems**

The use of living radical polymerization in bulk or solution polymerization has been investigated and is now well understood. The use of controlled free radical polymerization in aqueous media has been extensively carried out but a better understanding of the complex kinetics and the mechanisms involved in these systems still challenges many researchers.

These systems are complicated by a number of important variables, such as partitioning of the activating species in different environments, rate of transportation of the species to the locus of polymerization, choice of initiator, surfactant and cosurfactant.<sup>63</sup> Despite all of these complications that must be taken into consideration, a very significant kinetic advantage of these aqueous systems is compartmentalization that occurs in either the droplets or the particles. Compartmentalization reduces bimolecular termination, increases the rate of polymerization and results in better control of the molecular weight distribution.

### **2.5.5 Stability of RAFT in heterogeneous aqueous media**

The use of NMP, ATRP and RAFT in emulsion polymerization has been studied by many researchers and has found to be very successful.<sup>64,65</sup> Research on the use of

## ***Chapter Two Theoretical Background***

---

---

dithioester compounds in controlling emulsion polymerization has been studied.

Successful results were reported in early work on RAFT-mediated emulsion polymerization of butyl methacrylate using cumyl dithiobenzoate as RAFT agent.<sup>49</sup> However, the use of RAFT in emulsion systems has been found to present difficulties. Colloidal instability in heterogeneous aqueous media has been an issue that has troubled polymer chemists for many years and researchers have spent much effort on trying to explain the possible reasons for the occurrence of this behavior in these systems. Some of the reasons mentioned are due to polymerization occurring in droplets, water sensitivity of some reagents and slow transport of the hydrophobic RAFT agent across the aqueous phase. The success of RAFT-mediated emulsion polymerization depends on the choice of RAFT agent and the polymerization conditions.<sup>66,67</sup>

The use of controlled free radical polymerization in miniemulsions has also been approached. The first living technique introduced into miniemulsion systems was the RAFT technique.<sup>68</sup> A lack of stability was first seen, similar to those observed in emulsion systems. The stability of miniemulsions before and during polymerization is a key issue that is currently being investigated. This issue needs to be addressed because of its effects on the polymerization kinetics and the properties of the latex products. It was initially believed that by using controlled living techniques in miniemulsions colloidal stability would improve as there is no need for controlling agents to be transferred from the monomer droplets to the polymerization locus. However, slow rates of polymerization as well as colloidal instability in the form of broad particle size distributions have been observed.<sup>69</sup>

One of the instability problems observed with RAFT in emulsion and miniemulsion polymerization is phase separation in the form of a RAFT colored layer during the polymerization. This resulted in non-living behavior and latex instability.<sup>70,71</sup> One of the reasons for this is the transport of the RAFT agent to the polymerization sites. Other possible reasons are the exit of short radicals from the polymerization sites and the slow

## ***Chapter Two Theoretical Background***

---

---

formation of higher molecular weight polymer.<sup>72</sup>

de Brouwer *et al.*<sup>68</sup> reported unstable latexes when dithiobenzoate RAFT agents were used in cationic and anionic stabilized miniemulsion systems. Phase separation in the form of a red organic layer was observed on the surface of the reaction mixture. The red layer consisted of species containing dithiobenzoate groups. GPC revealed that this layer comprised of low molecular weight polymer and monomer. When non-ionic surfactants such as Igepal 890 and Brij 98 were used instead of ionic surfactants then no phase separation was observed.<sup>70</sup> De Brouwer *et al.*<sup>68</sup> used the RAFT technique and synthesized block copolymers prepared by chain extension using a CFRP technique in miniemulsion. Nucleation mechanisms other than droplet nucleation led to particles containing no RAFT agent. This resulted in block copolymers with broader molecular weights and mixtures of block copolymers and homopolymers.

Luo *et al.*<sup>33</sup> postulated the existence of a superswelling state that occurs early in living polymerizations due to the presence of oligomers. Superswelling occurs if low molecular weight oligomers are formed in the early stages of polymerization. These oligomeric species are effective swelling agents and can destabilize the miniemulsions. Superswelling is likely to occur in a system where nucleation is slow and monomer transport is fast. The work of Luo *et al.* concluded that a possible way to eliminate superswelling is by increasing levels of cosurfactant or/and by using polymeric surfactant.<sup>33</sup> Recently, another derivation based on the Lifshitz-Slyozov-Wagner (LSW) theory has been proposed and further details can be found in the literature.<sup>73</sup>

### **2.6 The use of free radical and controlled free radical polymerization in block copolymer synthesis**

As described in Section 2.5, the versatility of controlled free radical polymerizations is clearly evident. The majority of the literature focuses on the use of these controlled techniques to synthesize block copolymers. These applications of block copolymers

## ***Chapter Two Theoretical Background***

---

range from surfactants, dispersants, coatings, adhesives, cosmetics and materials for microelectronics, to sophisticated applications such as controlled drug release in cardiovascular stents, bone and tissue engineering, antimicrobial surfaces and biomaterials in the medical field.<sup>48</sup>

Until recently, living ionic polymerization (cationic and anionic) were the only techniques used for block copolymer synthesis. However, these techniques do have several drawbacks, such as being compatible with only a limited number of monomers and they do not tolerate low levels of impurities such as moisture or oxygen. These techniques are also expensive.

The synthesis of block copolymers using free radical polymerization is of industrial importance due to facile copolymerization and low requirements of monomer and solvent purity. However, this technique resulted in poor control of the molecular weight. High polydispersities and low diblock copolymer formation efficiency limits their applicability as high-performance materials. The development of controlled free radical techniques such as NMP<sup>74</sup>, ATRP<sup>75</sup> and RAFT<sup>49</sup> for the synthesis of block copolymers has gained interest.

In the following section, the use of the RAFT process in block copolymer synthesis will be discussed.

### **2.6.1 The RAFT process and block copolymers**

The RAFT technique has been successfully used in the synthesis of block copolymers, gradient copolymers, star-shaped block copolymers and polymer brushes. AB-type block copolymers have been synthesized by Chong and coworkers using the RAFT process.<sup>54</sup> The results indicated the versatility of this process in block copolymer formation. ABC triblock copolymers have also been synthesized by sequential RAFT polymerization. In this case a third monomer is added to the existing AB diblock copolymer. ABA triblock copolymers were also synthesized by starting with a difunctional transfer agent. In this case two arms of polymer B are propagated simultaneously. The obtained PBMA

## *Chapter Two Theoretical Background*

---

---

polymer was used in a second step in which the second monomer, methyl methacrylate, was added. PMMA-*b*-PBMA-*b*-PMMA triblock copolymers were synthesized.<sup>54</sup> From the RAFT mechanism one finds that since most of the chains have the S=C(Z)S- group, it is possible to sequentially add a second monomer, this results in the formation of a block copolymer.

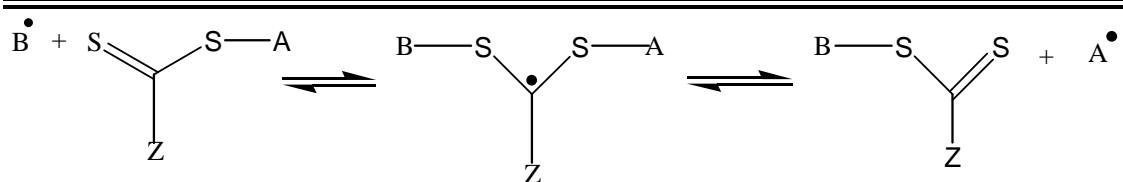
A very important factor that must be considered when synthesizing block copolymers using the RAFT technique is the choice of the starting block. The starting block should be chosen on the basis of its relative quality as a leaving group, so that it is capable of reinitiating further polymerization with the second monomer. It is important that the starting block acts as a better leaving group than the block formed in the second step. In order to form a narrow AB block copolymer, the first formed thiocarbonyl-thio compound (S=C(Z)S-A) should have a high effective transfer constant in the subsequent polymerization step to give the B block. A better leaving group is required from propagating radical A<sup>•</sup> than from propagating radical B<sup>•</sup>.

An example is demonstrated in the scheme below for the polymerization of MMA and styrene.

A block copolymer consisting of poly(styrene) (PSt) and poly(methyl methacrylate) (PMMA) blocks can be successfully synthesized by first polymerizing MMA. Subsequently, Sty has to be added to the first block, followed by the addition of fresh initiator to reinitiate polymerization. Performing the synthesis in this order leads to fragmentation occurring in the direction of the right hand side. This results in a well-defined block copolymer with narrow MWD. In this specific case the PMMA block is a better leaving group than the PSt block. If the order of addition of monomer was to be reversed (starting with the styrene block followed by the addition of methyl methacrylate), broad block copolymer products would be formed due to the polystyryl propagating radicals that are poor leaving groups compared to the polymethacryl propagating radical. This causes the intermediate radical to partition strongly in favor of the starting materials.



## Chapter Two Theoretical Background



Scheme 2.10: Intermediate structure formed during AB block copolymerization.

When synthesizing block copolymers, the order in which the monomers are polymerized should be:

Methacrylates => styrenes => acrylates

A further advantage of the RAFT process is that it can be used to produce block copolymers in both homogeneous and heterogeneous systems.

The use of the RAFT process to produce block copolymers in heterogeneous aqueous media has been demonstrated by Butté *et al.*<sup>76</sup> and de Brouwer *et al.*<sup>68</sup> Reasonable results were obtained using dithiobenzoate RAFT agents. In the work of Butté, an oligomeric RAFT agent (Z=Ph R= -(STY)<sub>n</sub>C(CH<sub>3</sub>)<sub>3</sub>) was synthesized in bulk polymerization. This oligomeric RAFT agent was used in a miniemulsion of styrene. The polymerization showed good control, however high polydispersities (> 2) were obtained. Much is still to be investigated regarding why high PDI values are obtained in these systems and further improvements in the polydispersity values need to be studied.

Most of the literature focuses on the synthesis of block copolymers using seeded RAFT-mediated emulsion polymerization. Bowes *et al.*<sup>77</sup> synthesized block copolymers of styrene and butyl acrylate via RAFT-mediated miniemulsion. AB diblocks were synthesized using a trithiocarbonate monofunctional RAFT agent and ABA triblocks were synthesized using a trithiocarbonate difunctional RAFT agent. The polymer based on the first monomer acted as a seed latex for the second block. The use of the monofunctional RAFT agent produced butyl-acrylate-styrene diblocks of high polydispersity (> 2) while the difunctional RAFT agent also produced ABA triblocks of high polydispersity (> 2).

Recently, in the work of Qinghua *et al.*,<sup>78</sup> block copolymers of dodecafluoroheptyl

## ***Chapter Two Theoretical Background***

---

---

methacrylate (DFMA) and butyl methacrylate (BMA) were prepared by RAFT miniemulsion polymerization. The poly (BMA-b-DFMA) was prepared in two sequential steps by chain extension of PBMA macro-RAFT with DFMA. In the first step, BMA was polymerized in miniemulsion using a dithiobenzoate RAFT agent, cyano-2-isoprop2-yl dithiobenzoate. This latex was used as a seed latex for the second step, where DFMA monomer and KPS initiator were added to the miniemulsions. The final PDI of the block copolymer was lower than 1.3.

In conclusion, the ability to work in a heterogeneous environment using controlled free radical polymerization is a growing field of interest in the world of polymer science. Further research in the field of controlled free radical polymerization in heterogeneous systems is needed in order for it to reach its full potential. There are still many challenges facing polymer chemists in this field of research. However, in the near future, many novel and interesting structures that can only be prepared by these controlled/living techniques should find use in many industrial applications.

## Chapter Two Theoretical Background

---

---

### 2.7 References

- (1) Moad, G.; Solomon, D. H. In *The Chemistry of Radical Polymerization*, 2nd ed.; Elsevier: Australia, 2006; pp 1 - 9.
- (2) Moad, G.; Rizzardo, E.; Thang, S. H. *Aust. J. Chem.* **2005**, *58*, 379 - 410.
- (3) Qui, J.; Charleux, B.; Matyjaszewski, K. *Prog. Polym. Sci.* **2001**, *26*, 2083 - 2134.
- (4) Matyjaszewski, K.; Davis, T. P. In *Handbook of Radical Polymerization*; Yamada, B.; Zetterlund, P. B., Eds.; Wiley & Sons: Canada, 2002; pp 117 - 186.
- (5) Moad, G.; Solomon, D. H. In *The Chemistry of Radical Polymerization*, 2nd ed.; Elsevier: Australia, 2006; pp 49 - 166.
- (6) Moad, G.; Solomon, D. H. In *The Chemistry of Radical Polymerization*, 2nd ed.; Elsevier: Australia, 2006; pp 167 - 232.
- (7) Olaj, O. F.; Vana, P.; Zoder, M. *Macromolecules* **2002**, *35*, 1208 - 1214.
- (8) Russell, G. T.; Gilbert, R. G.; Napper, D. H. *Macromolecules* **1992**, *25*, 2459 - 2469.
- (9) Moad, G.; Solomon, D. H. In *The Chemistry of Radical Polymerization*, 2nd ed.; Elsevier: Australia, 2006; pp 233 - 278.
- (10) Moad, G.; Solomon, D. H. In *The Chemistry of Radical Polymerization*, 2nd ed.; Elsevier: Australia, 2006; pp 279 - 331.
- (11) Mark, H. F.; Bikates, N. M.; Overberger, C. G.; Menges, G. In *Encyclopedia of Polymer Science and Engineering*, 2nd ed.; Wiley & Sons: New York, 1998; Vol. 13, pp 708 - 867.
- (12) Lovell, P. A.; El-Aasser, M. S. In *Emulsion Polymerization and Emulsion Polymers*; El-Aasser, M. S.; Sudol, E. D., Eds.; Wiley & Sons: New York, 1997; pp 38 - 57.
- (13) Schork, F. J.; Luo, Y.; Smulders, W.; Russum, J. P.; Butté, A.; Fontenot, K. *Adv. Polym. Sci.* **2005**, *175*, 129 - 255.
- (14) Lovell, P. A.; El-Aasser, M. S. In *Emulsion Polymerization and Emulsion Polymers*; Sudol, E. D.; El-Aasser, M. S., Eds.; Wiley & Sons: New York, 1997; pp 700 - 722.

## ***Chapter Two Theoretical Background***

---

- (15) Landfester, K.; Betchold, N.; Forster, S.; Antonietti, M. *Macromol. Rapid Commun.* **1999**, *20*, 81.
- (16) Abismail, A.; Cansekier, J. P.; Wilhelm, A. M.; Delmas, H.; Gourdon, C. *Ultrason. Sonochem.* **1999**, *6*, 75 - 83.
- (17) Landfester, K. *Macromol. Rapid Commun.* **2001**, *22*, 897 - 936.
- (18) Mason, T. J. *Ultrason. Sonochem.* **1992**, *30*, 192 - 196.
- (19) Blythe, P. J.; Klein, A.; Sudol, E. D.; El-Aasser, M. S. *Macromolecules* **1999**, *32*, 4225 - 4231.
- (20) Landfester, K.; Bechthold, N.; Tiarks, F.; Antonietti, M. *Macromolecules* **1999**, *32*, 5222 - 5228.
- (21) Matyjaszewski, K.; Davis, T. P. In *Handbook of Radical Polymerization*; Herk, A. M. V.; Monteiro, M., Eds.; Wiley & Sons: Canada, 2002; pp 301 - 331.
- (22) Holmberg, K.; Jonsson, B.; Kronberg, B.; Lindman, B. In *Surfactants and Polymers in Aqueous Solution*, 2nd ed.; Wiley & Sons: USA, 2004; pp 1 - 37.
- (23) Lovell, P. A.; El-Aasser, M. S. In *Emulsion Polymerization and Emulsion Polymers*; Lovell, P. A., Ed.; Wiley & Sons: New York, 1997; pp 3 - 35.
- (24) Tang, P. L.; Sudol, E. D.; Silebi, C. A.; El-Aasser, M. S. *J. Appl. Polym. Sci.* **1991**, *42*, 2019.
- (25) Gilbert, R. G. In *Emulsion Polymerization: A Mechanistic Approach*; Ottewill, R. H.; Rowell, R. L., Eds.; Academic Press: London, 1995; pp 25 - 77.
- (26) Maxwell, I. A.; Morrison, B. R.; Napper, D. H.; Gilbert, R. G. *Macromolecules* **1991**, *24*, 1629 - 1640.
- (27) Luo, Y.; Wang, R.; Yang, L.; Yu, B.; Li, B.; Zhu, S. *Macromolecules* **2006**, *39*, 1328 - 1337.
- (28) Landfester, K.; Bechthold, N.; Tiarks, F.; Antonietti, M. *Macromolecules* **1999**, *32*, 2679 - 2683.
- (29) Boisson, F.; Uzulina, I.; Guyot, A. *Macromol. Rapid Commun.* **2001**, *22*, 1135.
- (30) Asua, J. M. *Prog. Polym. Sci.* **2002**, *27*, 1283 - 1346.
- (31) Ugelstad, J.; El-Aasser, M. S.; Vanderhoff, J. W. *Polym. Lett. Ed.* **1973**, *503* - 513.
- (32) Reimers, J.; Schork, F. J. *Polym. React. Eng.* **1996**, 135 - 152.

## ***Chapter Two Theoretical Background***

---

- (33) Luo, Y.; Tsavalas, J.; Schork, F. J. *Macromolecules* **2001**, *34*, 5501 - 5507.
- (34) Kharasch, M. S.; Jensen, E. V. *Science* **1945**, *102*.
- (35) Minisci, F. *Acc. Chem. Res* **1975**, *8*, 165.
- (36) Asscher, M.; Vosfi, D. *J. Chem. Soc.* **1963**, 3921.
- (37) Matyjaszewski, K.; Davis, T. P. In *Handbook of Radical Polymerization*; Matyjaszewski, K., Ed.; Wiley & Sons: Canada, 2002; pp 361 - 406.
- (38) Swarc, M.; Levy, M.; Milkovich, R. *J. Am. Chem. Soc.* **1956**, *78*, 2656.
- (39) Wade, A.; Matyjaszewski, K. *Prog. Polym. Sci.* **2007**, *32*, 93 - 146.
- (40) Litvinenko, G.; Muller, H. E. *Macromolecules* **1997**, *30*, 1253 - 1266.
- (41) Borsig, E.; Lazar, M.; Capla, M.; Florian, S. *Angew. Makromol. Chem* **1969**, *9*, 89.
- (42) Braun, D. *Macromol Symp* **1996**, *63*, 111.
- (43) Solomon, D. H.; Rizzardo, E.; Cacioli, P. **1986**, *4*, 429.
- (44) Moad, C. L.; Moad, G.; Rizzardo, E.; Thang, S. H. *Macromolecules* **1997**, *29*, 7717 - 7726.
- (45) George, M. K.; Veregin, P. N.; Kazmaier, P. M.; Hamer, G. K. *Macromolecules* **1993**, *26*, 2987 - 2988.
- (46) Beers, K. L.; Gaynor, S. G.; Matyjaszewski, K. *Macromolecules* **1998**, *31*, 9413 - 9415.
- (47) Hawker, C. J.; Elce, E.; Dao, J.; Volksen, W.; Russell, T. P.; Barclay, G. G. *Macromolecules* **1996**, *29*, 2686 - 2688.
- (48) Braunecker, W. A.; Matyjaszewski, K. *Prog. Polym. Sci.* **2007**, *32*, 93 - 146.
- (49) Chiefari, J.; Chong, Y. K.; Ercole, F.; Krstina, J.; Jeffery, J.; Le, P. T.; Mayadunne, R. T. A.; Meijs, G. F.; Moad, C. L.; Moad, G.; Rizzardo, E.; Thang, S. H. *Macromolecules* **1998**, *31*, 5559 - 5562.
- (50) Le, T. P.; Moad, G.; Rizzardo, E.; Thang, S. H. *PCT Int. Appl. WO9801478A1980115* **1998**.
- (51) Hawthorne, D. G.; Moad, G.; Rizzardo, E.; Thang, S. H. *Macromolecules* **1999**, *32*, 5457 - 5459.
- (52) Darling, T. R.; Davis, T. P.; Fryd, M.; Gridnev, A. A.; Haddleton, D. M.; Ittel, S. D.; Matheson, R. R.; Moad, G.; Rizzardo, E. *J. Polym. Sci. Part A: Polym*

## ***Chapter Two Theoretical Background***

---

- Chem* **2000**, 38, 1706 - 1708.
- (53) Mayadunne, T. A. R.; Rizzardo, E.; Chiefari, J.; Krstina, J.; Moad, G.; Postma, A.; Thang, S. H. *Macromolecules* **2000**, 33, 243 - 245.
- (54) Chong, Y. K.; Le, P. T.; Moad, G.; Rizzardo, E.; Thang, S. H. *Macromolecules* **1999**, 32, 2071 - 2074.
- (55) Mayadunne, R. T. A.; Rizzardo, E.; Chiefari, J.; Chong, Y. K.; Moad, G.; Thang, S. H. *Macromolecules* **1999**, 32, 6977 - 6980.
- (56) Barner-Kowollik, C.; Quinn, J. F.; Nguyen, T. L. U.; Heuts, J. P. A.; Davis, T. P. *Macromolecules* **2001**, 34, 7849 - 7857.
- (57) Calitz, F. M.; Tonge, M. P.; Sanderson, R. D. *Macromolecules* **2003**, 36, 5 - 8.
- (58) Barner-Kowollik, C.; Coote, M. L.; Davis, T. P.; Radom, L.; Vana, P. *J. Polym. Sci. Part A: Polym Chem* **2003**, 41, 2828 - 2832.
- (59) Monteiro, M.; de Brouwer, H. *Macromolecules* **2001**, 34, 349 - 352.
- (60) Wang, A. R.; Zhu, S.; Kwak, Y.; Goto, A.; Fukuda, T.; Monteiro, M. S. *J. Polym. Sci. Part A: Polym Chem* **2003**, 41, 2833 - 2839.
- (61) Moad, G.; Chiefari, J.; Chong, Y. K.; Krstina, J.; Mayadunne, T. A.; Postma, A.; Rizzardo, E.; Thang, S. H. *Polym. Int* **2000**, 49, 993 - 1001.
- (62) Chong, B. Y. K.; Le, T. P. T.; Moad, G.; Rizzardo, E.; Thang, S. H. *Macromolecules* **1997**, 30, 324.
- (63) Matyjaszewski, K.; Davis, T. P. In *Handbook of Radical Polymerization*; Herk, A. M. V.; Monteiro, M., Eds.; Wiley & Sons: Canada, 2002; pp 301 - 331.
- (64) Smulders, W.; Gilbert, R. G.; Monteiro, M. J. *Macromolecules* **2003**, 36, 4309 - 4318.
- (65) Monteiro, M. J.; Sjoberg, M.; Vlist, J. V. D.; Gottgens, C. M. *J. Polym. Sci. Part A: Polym. Chem.* **2000**, 38, 4206 - 4217.
- (66) Monteiro, M. J.; de Barbeyrac, J. *Macromolecules* **2001**, 34, 4416 - 4423.
- (67) Shim, S. E.; Lee, H.; Choe, S. *Macromolecules* **2004**, 37, 5565 - 5571.
- (68) de Brouwer, H.; Tsavalas, J. G.; Schork, F. J.; Monteiro, M. J. *Macromolecules* **2000**, 33, 9239 - 9246.
- (69) Butte, A.; Storti, G.; Morbidelli, M. *Macromolecules* **2000**, 33, 3485 - 3487.
- (70) Tsavalas, J. G.; Schork, F. J.; de Brouwer, H.; Monteiro, M. J. *Macromolecules*

## ***Chapter Two Theoretical Background***

---

---

- 2001**, *34*, 3938 - 3946.
- (71) Monteiro, M. J.; Hodgson, M.; de Brouwer, H. *J. Polym. Sci. Part A: Polym. Chem.* **2000**, *38*, 3864 - 3874.
- (72) McLeary, J. B.; Klumperman, B. *Roy. Soc. Chem.* **2006**, *2*, 45 - 53.
- (73) Qi, G.; Schork, F. J. *J. Am. Chem. Soc.* **2006**, *22*, 9076 - 9078.
- (74) Puts, R. D.; Sogah, D. Y. *Macromolecules* **1996**, *29*, 3323 - 3325.
- (75) Xia, J.; Matyjaszewski, K. *Macromolecules* **1997**, *30*, 7697 - 7700.
- (76) Butte, A.; Storti, G.; Morbidelli, M. *Macromolecules* **2001**, *34*, 5885 - 5896.
- (77) Bowes, A.; McLeary, J. B.; Sanderson, R. D. *J. Polym. Sci. Part A: Polym. Chem.* **2007**, *45*, 588 - 604.
- (78) Qinghua, Z.; Xiaoli, Z.; Fengqiu, C.; Ying, S.; Qiongyan, W. *J. Polym. Sci. Part A: Polym. Chem.* **2007**, *45*, 1585 - 1594.

## *Chapter Three*

# *Synthesis and characterization of RAFT agent and diblock copolymers*

This chapter deals with the synthesis of the monofunctional RAFT agent, 2-cyanoisoprop-2-yl dithiobenzoate chosen for this study. The RAFT agent was characterized using  $^1\text{H}$  NMR,  $^{13}\text{C}$  NMR and ESMS. The two-step route taken for the synthesis of the AB diblock copolymers of *n*-butyl methacrylate and styrene is also discussed.



### **3.1 Introduction**

Controlled free radical polymerization is one of the most convenient ways of preparing well-defined block copolymers. The extension of controlled free radical polymerization to copolymerization is important in both industry and in academia. An unlimited range of polymers with unique chemical and physical properties can be synthesized by copolymerization of two different monomers. The RAFT controlled/living technique is currently the most versatile process used in heterogeneous systems and has produced successful results in synthesizing block copolymers.<sup>1,2</sup> For this reason, the RAFT process was chosen in this study to synthesize block copolymers in a miniemulsion system.

The synthesis of polymers of complex architecture in an environmentally friendly medium has become a challenge for polymer chemists. In this present study, the polymerization was conducted in heterogeneous media, namely miniemulsion with water as the continuous phase. Emulsion polymerization remains the preferential method of choice in industrial applications and only recently has miniemulsion polymerization has gained popularity. Academic literature also reported that the use of these controlled techniques has produced block copolymers of higher block purities than in solution processes due to the reduced amount of bimolecular termination.<sup>1</sup> Reasonable results have been reported for the synthesis of block copolymers via RAFT-mediated miniemulsion polymerization. However, it still remains a challenging subject. Polymer chemists are confronted with many problems (colloidal instability, large particle size, broad particle size distributions) in these systems which are dependent on several reaction variables such as the type of RAFT agent, type and amount of surfactant, amount of hydrophobe, monomer and type of initiator used.<sup>3-5</sup>

To date, interesting results have been reported using dithioester RAFT agents in both miniemulsion and seeded miniemulsion polymerization systems using styrene, acrylate and methacrylate monomers.<sup>6-9</sup> Both of these systems should be efficient since each droplet is expected to act like a nano-reactor, therefore, transport of the monomer through the aqueous phase could possibly be eliminated. In addition, the RAFT agent will be in the reaction locus from the start of the polymerization. Most

### ***Chapter Three Synthesis and Characterization of RAFT agent and diblock copolymers***

---

---

polymer chains will therefore have an equal lifetime (provided that all the droplets are nucleated fast) and the RAFT agent will be expected to be homogeneously distributed among the particles, thus the same average molar mass will be expected in the particles.

The use of highly hydrophobic RAFT agents such as macro-RAFT agents to stabilize a miniemulsion system has shown to be promising.<sup>1,10,11</sup> Polymers with RAFT groups at the end of the polymer chains can be chain extended into block copolymers. The RAFT functionalized polymer acts as a macro-RAFT agent in the chain extension step. This methodology for the synthesis of block copolymers has been reported in the literature.<sup>11</sup> Reasonable results were obtained in these systems, however, obtaining an ideal RAFT miniemulsion polymerization system is rare and broad molecular weight distributions and polydispersities as high as 2 were reported.<sup>5,12</sup> The possible reasons for obtaining broad molecular weight distributions and high polydispersity values in these miniemulsion systems is still an area of research that needs to be investigated.

In this study the RAFT technique was used for the synthesis of diblock copolymer latices of *n*-butyl methacrylate and styrene in miniemulsion. The synthesis comprises a two step process. The first step involves the synthesis of the first block that is prepared in bulk polymerization using a monofunctional RAFT agent, 2-cyanoisoprop-2-yl dithiobenzoate (CIDB). Bulk polymerization was chosen since it comprises monomer, RAFT agent and initiator, and therefore the starting block is of high purity and contamination is minimized. It must be noted that the starting block acts as a polymeric RAFT agent. The RAFT-functionalized polymer obtained in the first step has a RAFT moiety at the end that can be chain extended. The second step involves the chain extension process of the first block upon further addition of fresh monomer and initiator, in a miniemulsion system.

This chapter focuses on the experimental details of the synthesis and characterization of the RAFT agent and the synthesis of the diblock copolymers. The first part of this chapter reports on the experimental procedures carried out for the synthesis of the RAFT agent. The second part reports the procedure used for the synthesis of the initial blocks (polymeric RAFT agent) and the block copolymers.

## **3.2 RAFT agent synthesis**

### **3.2.1 Background**

In Chapter 2, the RAFT process was addressed in detail. As was mentioned, RAFT agents are classed into four groups depending on the activating Z group: dithioesters, trithiocarbonates, dithiocarbamates and xanthates.

The RAFT agent chosen for this study was the dithiobenzoate RAFT agent, 2-cyanoisoprop-2-yl dithiobenzoate (CIDB). Dithiobenzoates are a common class of RAFT agents and have a common structure of Z being a phenyl group and R an alkyl or aryl group. This RAFT agent has been shown to be effective in the presence of the monomers used in this study<sup>9,13</sup>, namely *n*-butyl methacrylate and styrene, and was therefore chosen.

A common type of RAFT agent is that of dithiocarboxylic ester derivatives. Rizzardo *et al.*<sup>14</sup> patented the use of dithiocarboxylic esters in free radical polymerization leading to controlled characteristics.<sup>14</sup> Dithiobenzoate RAFT agents are often synthesized by forming dithioesters from dithiobenzoic acids. A number of methods have been reported for the synthesis of dithioesters and dithiocarboxylic acids.<sup>15</sup> Dithiocarboxylic acid can be synthesized by carrying out a Grignard reaction whereby an alkyl/aryl halide reacts with CS<sub>2</sub>, forming a thiocarbonyl-thio salt. Dithiocarboxylic acid can also be prepared by the reaction of P<sub>4</sub>S<sub>10</sub> with benzoic acid. Dithioesters can be prepared by the reaction of P<sub>4</sub>S<sub>10</sub> with a carboxylic acid in the presence of a thiol.<sup>15</sup>

However, the most effective way of synthesizing dithioesters is by the Grignard reaction. For the synthesis of dithioesters, Grignard reactions are applied to alkyl/aryl halides, which are then converted into a magnesium salt. This reacts further with CS<sub>2</sub> to form a thiocarbonyl-thio salt, which reacts with an alkyl halide to give the dithioester. It is important that no water is present when carrying out these reactions as Grignard reagents are very reactive and decompose in the presence of moisture.<sup>16</sup> For the synthesis of the RAFT agent chosen in this study, dithiobenzoic acid was synthesized using a Grignard reaction. This method was chosen as it provides dithiobenzoic acid of high purity.

## ***Chapter Three Synthesis and Characterization of RAFT agent and diblock copolymers***

---

---

### **3.2.2 Materials**

The following materials were used as received: 2,2'-azobisisobutyronitrile (Riedel de Haen), bromobenzene (Fluka, > 99.5%), carbon disulfide (Aldrich, 99%), diethyl ether (Saarchem, 98%), dimethyl sulfoxide (Saarchem, 99%), distilled deionized water (Millipore Milli-Q purification), ethyl acetate (KIMIX, 99%), *n*-hexadecane (Aldrich, 99%), HCl (32% ACE), iodine crystals (Aldrich, 99%), magnesium turnings (Acros, 99.9%), potassium persulfate (Aldrich, 99.99%), sodium lauryl sulfate (Sigma, 99%).

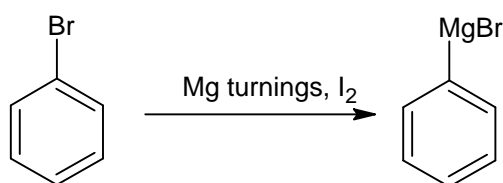
THF (Sigma-Aldrich, 99%) was distilled from LiAlH<sub>4</sub> (ROMIL, 99%).

### **3.2.3 Experimental procedure**

#### **3.2.3.1 Synthesis of dithiobenzoic acid**

Magnesium turnings (2.43 g, 0.1 mol) and a catalytic amount of iodine crystal was placed in 250 mL round-bottom reaction flask with a stirrer bar. A condenser with a dripping funnel, a thermometer and a calcium chloride drying tube were fitted. Bromobenzene (12.7 mL, 0.12 mol) and dry, distilled THF (25 mL, 0.313 mol) were placed in a dripping funnel. The THF was first distilled from LiAlH<sub>4</sub>. The temperature of the reaction was kept below 40 °C using an ice bath to prevent excessive heat formation as this can destroy the Grignard reagent.

At first, a small amount of THF and bromobenzene was added dropwise until the yellow color of the reaction mixture changed to clear grey. The reaction flask was heated slightly using a heat gun in order to start the reaction. The remaining solvent was added very slowly, dropwise, to the reaction mixture. At first, the brown-yellow color of the iodine disappeared. This is an indication of the onset of the reaction. After the addition of the bromobenzene and THF the final color of the mixture was metallic grey/olive green. The reaction mixture was stirred for an additional hour.

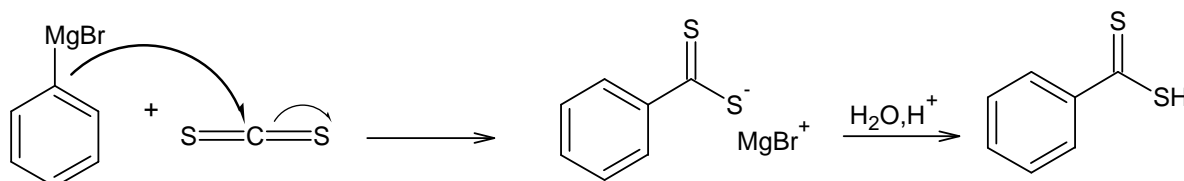


Scheme 3.1: Formation of Grignard reagent.

### ***Chapter Three Synthesis and Characterization of RAFT agent and diblock copolymers***

---

CS<sub>2</sub> (6 mL, 0.099 mol) was then placed in a clean dripping funnel and added slowly over 30 minutes to the Grignard mixture. The temperature of the exothermic reaction mixture was kept below 40 °C, using an ice bath. During the addition of the CS<sub>2</sub>, the reaction mixture changed color from green/grey to a deep red. Once all the CS<sub>2</sub> was added, the reaction mixture was stirred for an additional hour. The Grignard mixture was then hydrolyzed by the addition of ice cold DDI (distilled deionized water), until no more heat evolved. The excess magnesium was filtered off. The mixture was then acidified by the dropwise addition of a 32% HCl solution (20 mL). The color of the reaction mixture changed from dark red to the bright purple color of the dithiobenzoic acid. The final pH of the mixture was 1. The organic layer was washed with diethyl ether 75 mL (x 2). The diethyl ether organic mixture was then concentrated under vacuum on a rotary evaporator. The final product, dithiobenzoic acid, was a deep purple color. Dithiobenzoic acid is an unstable compound and must be stored at -4 °C. This product was used immediately in the following step.



Scheme 3.2: Formation of dithiobenzoic acid.

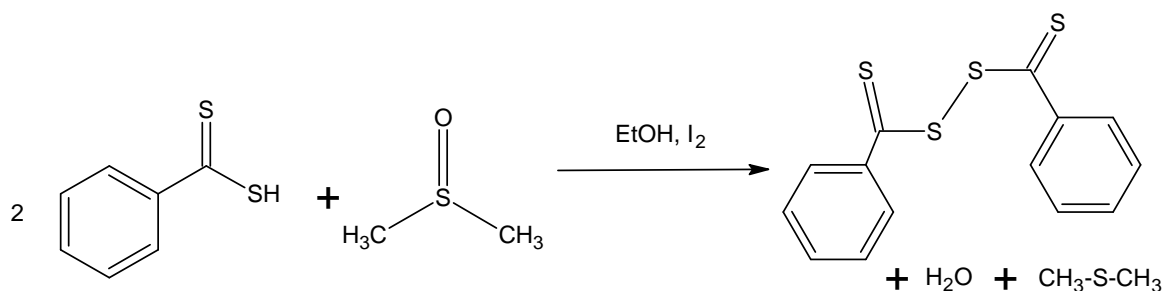
#### **3.2.3.2 Synthesis of bis(thiobenzoyl) disulfide**

Dithiobenzoic acid (12.48 g, 0.081 mol) and a catalytic amount of iodine were placed in a 250 mL three-neck round bottom flask with a stirrer bar fitted with a condenser.

Twice the molar ratio of DMSO (11.5 mL, 0.162 mol) to dithiobenzoic acid was used. Ethanol (15 mL) and DMSO were placed in a dripping funnel and added dropwise over an hour to the dithiobenzoic acid at room temperature. An ice bath was used to prevent excessive heat formation and to aid crystallization. Before the last few drops of DMSO and ethanol were added the formation of purple crystals could be seen. The reaction mixture was then cooled in a refrigerator overnight to promote further crystallization. The crystals were filtered and washed with cold ethanol, then dried under vacuum at room temperature. Bis(thiobenzoyl) disulfide crystals are relatively

## Chapter Three Synthesis and Characterization of RAFT agent and diblock copolymers

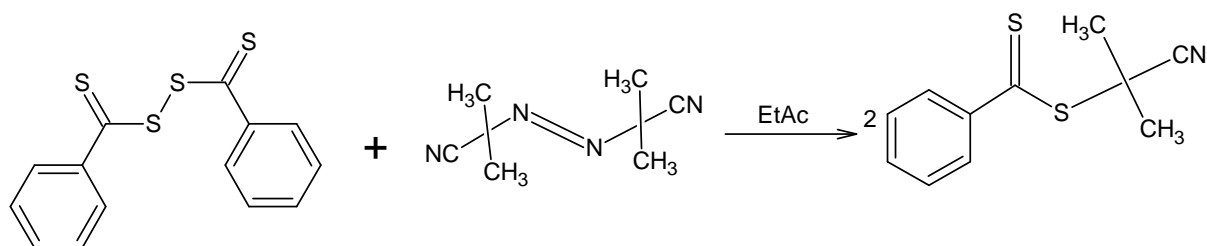
stable and decompose only slowly in the presence of light and heat. They can be stored in a refrigerator for a long period of time.



Scheme 3.3: Formation of bis(thiobenzoyl) disulfide.

### 3.2.3.3 Synthesis of 2-cyano isoprop-2-yl dithiobenzoate (CIDB)

Bis(thiobenzoyl) disulfide (4.96 g, 0.032 mol), AIBN (2,2'-azobisisobutyronitrile) (3.632 g, 0.022 mol) and ethyl acetate (100 mL) were placed in a 250 mL reaction vessel containing a stirrer bar and immersed into an oil bath. The mixture was refluxed under argon in ethyl acetate for 24 hours at 80 °C. After the reaction mixture was concentrated under vacuum on the rotary evaporator, the product was purified by column chromatography on silica using ethyl acetate and petroleum ether (2:1) as the solvent system.



Scheme 3.4: Synthesis of 2-cyano-isoprop-2-yl dithiobenzoate.

### 3.2.3.4 Characterization of RAFT agent

$^1\text{H}$  NMR and  $^{13}\text{C}$  NMR spectra were recorded on a Varian Unity Inova 400 MHz spectrometer. ESMS was carried out on a Waters-Micromass QTOF API instrument.

The chemical structure of the dithioester was verified using  $^1\text{H}$  NMR,  $^{13}\text{C}$  NMR and ESMS (Electron Spray Mass Spectroscopy). The RAFT agent was successfully

## Chapter Three Synthesis and Characterization of RAFT agent and diblock copolymers

synthesized. The product was obtained as a red oil. The respective spectra are shown in Appendix A.

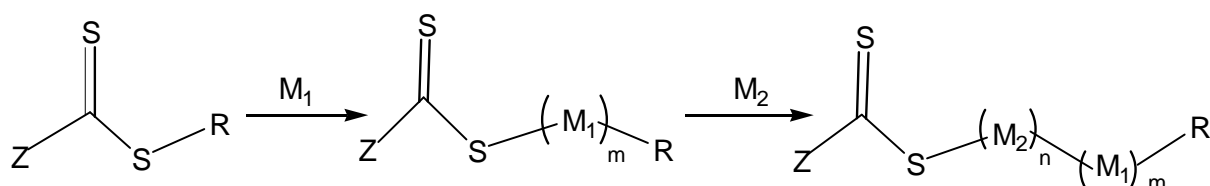
**$^1\text{H}$  NMR:** ( $\text{CDCl}_3$ ):  $\delta$  ppm values: 7.24 (t, 2H, o-ArH), 7.6 (t, 1H, p-ArH), 7.9(d, 2H, m-ArH), 1.92 (s, 6H,  $(\text{CH}_3)_2$ ).

**$^{13}\text{C}$  NMR:** ( $\text{CDCl}_3$ )  $\delta$  ppm values: 26.2 ( $(\text{CH}_3)_2$ ), 45( $\text{C}(\text{CH}_3)_2$ ), 225 (C=S), 123 (C=N), 130; 134, 140, 144 (Ar-C).

**ESMS:** The ESMS spectrum of the RAFT agent is given in Appendix A. A low resolution electron spray mass spectrometer was used and the analysis was carried out in the positive mode. The ESMS spectrum shows the molecular mass of the RAFT agent and its abundance relative to impurities. The theoretical  $m/z$  values were calculated using the isotopic values from the periodic table. The theoretical  $m/z$  of the base peak is 222 while the experimental  $m/z$  of the base peak is 221.24. If the proton was included ( $\text{M}^+$ ), the calculated  $m/z$  value would be 222.24. The most intense peak at 100% abundance (base peak) is the RAFT agent. Other smaller peaks are small traces of impurities.

### 3.3 Block copolymer synthesis

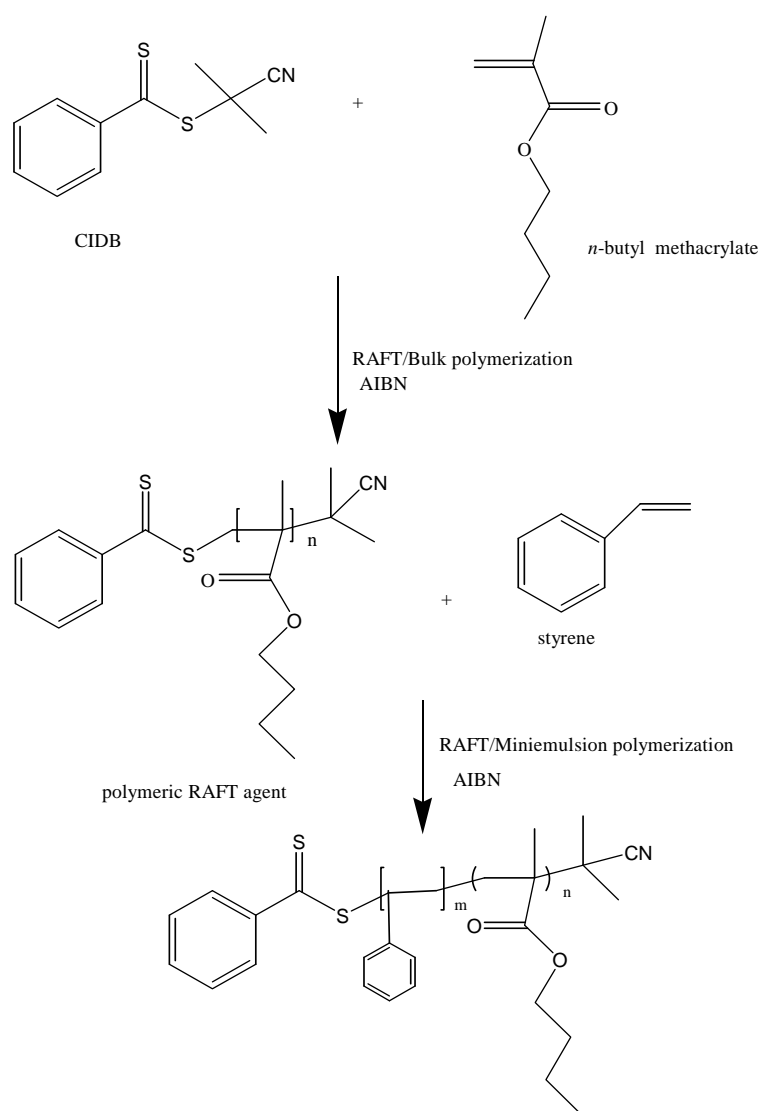
There are a number of routes that exist for the synthesis of diblock copolymers. One of the first and most common ways of synthesizing diblock copolymers is by the use of a monofunctional RAFT agent. This approach was used in this study. Here the block copolymer contains the RAFT functionality at the end of the chain. Upon the addition of the first monomer, the monomer effectively inserts itself between the C=S moiety and the activating group. Upon further addition of the second monomer and initiator, the second monomer effectively inserts itself between the C=S moiety and the end of the first block. This is illustrated below:



Scheme 3.5: Block copolymer formation via a monofunctional RAFT agent.

### Chapter Three Synthesis and Characterization of RAFT agent and diblock copolymers

Scheme 3.6 illustrates the reaction scheme followed in this study for the synthesis of the AB diblock copolymers of *n*-butyl methacrylate and styrene using the monofunctional RAFT agent. The first step involves the synthesis of the polymeric RAFT agent in bulk, which forms the starting block of the AB diblock copolymer, which should be sufficiently hydrophobic. In the second step, the starting block (polymeric RAFT agent) is chain extended in miniemulsion upon further addition of styrene and fresh initiator.



Scheme 3.6: Representation of the two-step reaction procedure for the synthesis of AB diblock copolymers.



### **3.3.1 Step I: Preparation of the initial block (polymeric RAFT agent) via RAFT/bulk polymerization**

In all bulk polymerizations, the monomers, *n*-butyl methacrylate and styrene, were washed three times with 0.3 M KOH in order to remove any inhibitor present. The monomers were then distilled under reduced pressure. The *n*-butyl methacrylate and styrene monomers were stored in the refrigerator at 2 °C. All AIBN used in this study was recrystallised from methanol and stored at 2 °C.

#### **3.3.1.1 Experimental procedure**

For the synthesis of the initial poly(*n*-butyl methacrylate) block (polymeric RAFT agent), *n*-BMA monomer, the monofunctional RAFT agent, CIDB, and the initiator, AIBN, were placed in a 100 mL three-neck round bottom flask equipped with a condenser and a stirrer bar.

The reaction mixture was purged with nitrogen for 10 minutes at room temperature in order to remove any dissolved oxygen. The reaction vessel was then submerged in an oil bath and the reaction was carried out at 80 °C for 70 minutes. The reaction mixture was then cooled to room temperature. Methanol was then added slowly to the bulk mixture and the polymer precipitated from the methanol. The crude polymer was then washed with methanol in order to remove residual monomer and excess unreacted RAFT agent. The polymer was dried in a vacuum oven at room temperature for 24 hours. In bulk polymerization, the viscosity increases significantly as polymerization progresses. All the bulk polymerizations were stopped at 30% conversion. SEC analysis of the final polymer sample was carried out in order to determine the molecular weight and polydispersity of the polymer.

The procedure for the synthesis of the initial poly(styrene) block in bulk was the same as described above for the poly(*n*-butyl methacrylate) block. The final molecular weight and polydispersity were determined by SEC.

Several batches of starting blocks (polymeric RAFT agent) had to be synthesized. Table 3.1 shows the bulk polymerization formulations of the different batches of the initial PBMA and PSt blocks synthesized.

## ***Chapter Three Synthesis and Characterization of RAFT agent and diblock copolymers***

---

---

Table 3.1: Bulk polymerization reaction compositions for the synthesis of initial blocks (polymeric RAFT agents)

<b>Batch number</b>	<b>Monomer</b>	<b>RAFT agent</b>	<b>RAFT (mol)</b>	<b>Initiator AIBN (mol)</b>
Batch 1	<i>n</i> -BMA	CIDB	$2.40 \times 10^{-4}$	$9.90 \times 10^{-5}$
Batch 2	<i>n</i> -BMA	CIDB	$1.81 \times 10^{-4}$	$9.05 \times 10^{-5}$
Batch 3	<i>n</i> -BMA	CIDB	$1.81 \times 10^{-4}$	$9.05 \times 10^{-5}$
Batch 4	Sty	CIDB	$1.81 \times 10^{-4}$	$9.00 \times 10^{-5}$
Batch 5	<i>n</i> -BMA	CIDB	$7.70 \times 10^{-4}$	$38 \times 10^{-5}$

### **3.3.2 Step II: Preparation of diblock copolymers via RAFT/mini-emulsion polymerization**

Mini-emulsion polymerization was used in the second step for the synthesis of the diblock copolymers.

The pre-emulsion was prepared by mixing the continuous aqueous phase and the oil phase, separately. The components of the oil phase: monomer, oil-soluble initiator (AIBN), costabilizer hexadecane, and the initial block (polymeric RAFT agent synthesized in bulk, step I), were mixed in a 100 mL round-bottom flask for 24 hours to ensure that the polymer had completely dissolved in the monomer. For all of the experiments, a costabilizer, hexadecane, was used to prevent or suppress Ostwald ripening (as discussed in Chapter 2, Section 2.3.6) and an anionic surfactant, SDS, was used. The components of the water phase: surfactant SDS and DDI water, were mixed in a 100 mL beaker. For the case where oil-soluble initiator AIBN was used, the initiator was dissolved in the oil phase. For the polymerization where the water-soluble initiator, potassium persulfate (KPS) was used, the initiator was dissolved in the water phase. The oil phase and the water phase were then mixed together, forming

### ***Chapter Three Synthesis and Characterization of RAFT agent and diblock copolymers***

---

---

the pre-emulsion, and stirred at 300 rpm for an additional 20 minutes prior to sonication.

The pre-emulsion was homogenized using a Sonics and Material Vibra Cell 750VCX ultrasonicator. The sonication process was carried out for 15 minutes at 90% amplitude and a cut-off probe temperature of 40 °C. The total energy was in the range of 80 – 85 kJ. The latex was then placed in a 100 mL three-neck round bottom flask fitted with a condenser and nitrogen feed. The contents of the flask were purged with nitrogen for 10 minutes before the flask was submerged into a thermostatic oil bath at 75 °C and polymerization allowed to commence. The miniemulsion mixture was stirred at 300 rpm. The temperature at which all of the miniemulsion reactions were carried out was 75 °C.

During the polymerization, samples were drawn at specific intervals. These samples were dried and analysed by SEC. The conversion was determined gravimetrically. The final latex was stored for further analysis. Table 3.2 gives details of experimental formulations of the miniemulsion reactions investigated in this study.

## ***Chapter Three Synthesis and Characterization of RAFT agent and diblock copolymers***

---

---

Table 3.2: Block copolymer miniemulsion compositions

<b>Reaction*</b>	<b>Polymeric RAFT agent</b>	<b>Monomer</b>	<b>Polymeric RAFT agent (mol)</b>	<b>Initiator (mol)</b>
1	PBMA (batch 1)	<i>n</i> -BMA	$5.08 \times 10^{-5}$	$1.26 \times 10^{-5}$
2	PSt (batch 4)	Sty	$8.60 \times 10^{-5}$	$4.30 \times 10^{-5}$
3	PBMA (batch 1)	Sty	$4.60 \times 10^{-5}$	$2.3 \times 10^{-5}$
4	PBMA (batch 2)	Sty	$5.07 \times 10^{-5}$	$2.50 \times 10^{-6}$
5	PBMA (batch 2)	Sty	$5.24 \times 10^{-5}$	$5.30 \times 10^{-6}$
6	PBMA (batch 2)	Sty	$5.05 \times 10^{-5}$	$2.50 \times 10^{-6}$
7	PBMA (batch 3)	Sty	$4.80 \times 10^{-5}$	$5.0 \times 10^{-6}$
8	PBMA (batch 5)	Sty	$1.28 \times 10^{-4}$	$1.30 \times 10^{-5}$

\*All reactions consisted of 10 g monomer, 0.3 g (3 wt % relative to monomer) HD, 0.3 g (3 wt % relative to monomer) SDS surfactant. An oil-soluble initiator, AIBN, was used in reactions 1-6, 8. In reaction 7, a water-soluble initiator, KPS, was used. All latices had a 20% solid content.

### **3.4 Analytical techniques used for the characterization of block copolymers**

#### **3.4.1 Size Exclusion Chromatography (SEC)**

SEC was used to monitor the evolution of the molar masses of the polymer latices.

The SEC instrument used in this study consisted of a Water 717 plus Autosampler controller and a Water 1515 Isocratic HPLC pump. A Waters 2414 refractive index detector was used at 30 °C. The UV detector used was a Waters 2487 dual and absorbance detector. The SEC was calibrated with ten narrow polydispersity Easivial

### ***Chapter Three Synthesis and Characterization of RAFT agent and diblock copolymers***

---

---

polystyrene standards (Polymer Labs), with a molecular weight range of 580 – 3053000 g mol<sup>-1</sup>. The flow rate used was 1 mL/min using HPLC grade THF (0.012% BHT stabilized) as solvent. Samples were prepared by dissolving the polymer in THF. The samples were then filtered through a 0.45 µm filter membrane.

#### **3.4.2 Dynamic Light Scattering (DLS)**

DLS was used to determine the particle size before and after polymerization. The Zetasizer system determines size by first measuring the Brownian motion of the particles and relates this to the size of the particles in the sample.

Latex samples were prepared by dissolving a few drops of latex in DDI water. DLS was carried out on a Malvern-Nano instrument fixed at 90 degrees at 25 °C. The Zetasizer Malvern system was calibrated using nanosphere size standards of polymer microspheres (Malvern instruments) in water with a mean diameter of 60 nm.

#### **3.4.3 Transmission Electron Microscopy (TEM)**

TEM analysis was carried out on the latices to visualize the particle morphology on a nanometer scale.

TEM analysis was carried out at the University of Cape Town, Electron Microscope Unit A. The apparatus used was as a Leo 912 microscope attached to a digital camera. Samples were prepared by diluting the latex in water. The diluted samples were stained with 2% uranyl acetate solution and mounted on a copper grid. The negative uranyl acetate stain increases the contrast for electrons between the domains and defines the particle edges.<sup>17</sup>

### 3.5 References

- (1) Butte, A.; Storti, G.; Morbidelli, M. *Macromolecules* **2001**, *34*, 5885 - 5896.
- (2) Ferguson, C. J.; Hughes, R. J.; Pham, B. T. T.; Hawket, B. S.; Gilbert, R. G.; Serelis, A. K.; Such, C. H. *Macromolecules* **2002**, *35*, 9243 - 9245.
- (3) Farcet, C.; Charleux, B.; Pirri, R. *Macromolecules* **2001**, *34*, 3823 - 3826.
- (4) Tsavalas, J. G.; Schork, F. J.; de Brouwer, H.; Monteiro, M. J. *Macromolecules* **2001**, *34*, 3938 - 3946.
- (5) de Brouwer, H.; Tsavalas, J. G.; Schork, F. J.; Monteiro, M. J. *Macromolecules* **2000**, *33*, 9239 - 9246.
- (6) Smulders, W.; Gilbert, R. G.; Monteiro, M. J. *Macromolecules* **2003**, *36*, 4309 - 4318.
- (7) Hutson, L.; Krstina, J.; Moad, C. L.; Moad, G.; Morrow, G. R.; Postma, A.; Rizzardo, E.; Thang, S. H. *Macromolecules* **2004**, *37*, 4441 - 4452.
- (8) Bowes, A.; McLeary, J. B.; Sanderson, R. D. *J. Polym. Sci. Part A: Polym Chem* **2007**, *45*, 588 - 604.
- (9) Qinghua, Z.; Xiaoli, Z.; Fengqiu, C.; Ying, S.; Qiongyan, W. *J. Polym. Sci. Part A: Polym Chem* **2007**, *45*, 1585 - 1594.
- (10) Vosloo, J. J.; De Wet-Roos, D.; Tonge, M. P.; Sanderson, R. D. *Macromolecules* **2002**, *35*, 4894 - 4902.
- (11) Zhou, X.; Ni, P.; Yu, Z.; Zhang, F. *J. Polym. Sci. Part A: Polym Chem* **2007**, *45*, 471 - 484.
- (12) Butte, A.; Storti, G.; Morbidelli, M. *Macromolecules* **2000**, *33*, 3485 - 3487.
- (13) Liu, S.; Hermanson, K. D.; Kaler, E. W. *Macromolecules* **2006**, *39*, 4345 - 4350.
- (14) Le, T. P.; Moad, G.; Rizzardo, E.; Thang, S. H. *PCT Int. Appl. WO9801478A1980115* **1998**.
- (15) Perrier, S.; Takolpuckdee, P. *J. Polym. Sci. Part A: Polym Chem* **2005**, *43*, 5347 - 5393.
- (16) Loudon, G. M. In *Organic Chemistry*, 2nd ed.; Benjamin/Cummings: Canada, 1984; pp 272 - 318.
- (17) Ferguson, C.; Russell, G.; Gilbert, R. *Polymer* **2002**, *43*, 6371 - 6382.

## *Chapter Four Results and discussion*

The reversible addition fragmentation transfer (RAFT) technique was investigated using 2-cyanoisoprop-2-yl dithiobenzoate, (CIDB) as transfer agent for the synthesis of diblock copolymers. AB diblock copolymers of *n*-butyl methacrylate and styrene were synthesized whereby the starting blocks (polymeric RAFT agent) were synthesized in homogeneous media namely bulk polymerization, and further chain extended in heterogeneous aqueous media, namely miniemulsion polymerization. The results obtained for the synthesis of the AB diblock copolymers are discussed in this chapter. The polymer latices were analyzed by size exclusion chromatography (SEC), dynamic light scattering (DLS) and transmission electron microscopy (TEM).

### **4.1 Introduction**

The synthesis of AB diblock copolymers of high molecular weight via the RAFT process is the main challenge and focus of this study. This chapter presents and discusses the results obtained for the synthesis of AB diblock copolymers of *n*-butyl methacrylate and styrene via the two-step process described in Chapter 3, Scheme 3.6. Chapter four comprises two parts. The first part is divided into three sections: Sections 4.2, 4.3, 4.4. The second part is divided into three sections: Sections 4.5, 4.6, 4.7.

Section 4.2 discusses the results obtained for the synthesis of the initial poly(*n*-butyl methacrylate) and poly(styrene) blocks, end functionalized with a RAFT dithioester group. These starting blocks were synthesized in bulk polymerization. The obtained RAFT functionalized polymers act as polymeric RAFT agents which were later chain extended upon further addition of monomer in miniemulsion.

Results of the initial approach used to synthesize AB diblock copolymers were discussed in Section 4.3. This approach investigates a simple system where the initial poly(*n*-butyl methacrylate) blocks were chain extended with *n*-butyl methacrylate and initial poly(styrene) blocks are chain extended with styrene in miniemulsion.

In Section 4.4 a more complex system was investigated. In this case, the initial poly(*n*-butyl methacrylate) block was chain extended with styrene in miniemulsion, thereby forming AB diblock copolymers of *n*-butyl methacrylate and styrene. Sections 4.3 and 4.4 describe the results of the preliminary experiments carried out to demonstrate the ability of block copolymer formation via the methodology illustrated in Chapter 3, Scheme 3.6.

In Sections 4.5 and 4.6, the RAFT-mediated miniemulsion system in Section 4.4 was more thoroughly investigated. In Section 4.5, the effect of the initiator/RAFT agent concentration ratio on the system was investigated. The type of initiator (water-soluble vs. oil-soluble) was also investigated and discussed in Section 4.6. Based on conclusions



## Chapter Four Results and Discussion

obtained from Section 4.5 and Section 4.6, the effect of changing the molecular weight of the initial block was investigated. This is discussed in Section 4.7.

### 4.2 Initial poly(*n*-butyl methacrylate) and poly(styrene) blocks (polymeric RAFT agents) via RAFT-mediated bulk polymerizations

Initial PBMA and PSt blocks were synthesized in bulk using a CIDB RAFT agent, AIBN initiator and either *n*-butyl methacrylate or styrene monomer at 80 °C. Details on the experimental formulations used for the different batches of initial blocks synthesized in bulk were given in Chapter 3, Section 3.3.

#### 4.2.1 Results

The results obtained for the synthesis of the initial PBMA and PSt blocks are summarized in the Table 4.1. Note that the initial block synthesized in bulk functions as a polymeric RAFT agent in the subsequent miniemulsion step.

Table 4.1: Initial poly(*n*-butyl methacrylate) and poly(styrene) blocks (polymeric RAFT agents) synthesized by bulk polymerization at 80 °C for 70 minutes, initiated by AIBN.

Batch	Polymeric RAFT agent	Conversion (%)	$\bar{M}_{n,theo}$ * gmol <sup>-1</sup>	$\bar{M}_{n,SEC}$ * gmol <sup>-1</sup>	PDI
Batch 1	PBMA	30	43000	47100	1.19
Batch 2	PBMA	30	43000	39300	1.18
Batch 3	PBMA	30	43700	39400	1.19
Batch 4	PSt	20	32100	23300	1.20
Batch 5	PBMA	30	19000	23500	1.12

\*  $\bar{M}_{n,theo}$  values were calculated using equation 4.1 and  $\bar{M}_n$  values obtained from SEC are based on PSt standards.

The predicted  $\bar{M}_n$  values of the initial poly(*n*-butyl methacrylate) blocks showed good agreement with the SEC  $\bar{M}_n$  values. Low polydispersity values of 1.18 – 1.19 were obtained for the initial poly(*n*-butyl methacrylate) blocks. As for the initial poly(styrene)

## Chapter Four Results and Discussion

blocks, the SEC  $\bar{M}_n$  was lower than the predicted  $\bar{M}_n$  values. The final polydispersity of the initial block was 1.2. The polydispersity values for both starting blocks were well below the benchmark of 1.5 for controlled radical polymerization. This indicated that the CIDB RAFT agent was efficient for the monomers used in the bulk polymerization. The molecular weight distributions of the initial blocks appeared to be narrow and are illustrated in the following sections. UV-RI analysis was used to confirm the preservation of the end functionality of the starting block.

### 4.3 Chain extension via RAFT-mediated miniemulsion polymerization

#### 4.3.1 Chain extension of the initial poly(*n*-butyl methacrylate) block with *n*-butyl methacrylate and the initial poly(styrene) block with styrene in miniemulsion

As a starting point for this study, the behavior of a simple system was investigated. In this case, the initial poly(*n*-butyl methacrylate) block synthesized in the bulk polymerization step was chain extended with *n*-butyl methacrylate monomer, and the initial poly(styrene) block was chain extended with styrene in miniemulsion. The reason for using this approach to the study was to observe whether the system showed living behavior, whether chain extension efficiently occurred and whether the initial poly(*n*-butyl methacrylate) and poly(styrene) blocks were good candidates to mediate a well controlled miniemulsion polymerization in the second step.

#### 4.3.2 Results

The results obtained for these reactions are summarized in Table 4.2.

Table 4.2: Characteristics of the polymer formed in the final latices obtained for the chain extension reactions in RAFT-mediated miniemulsion polymerization at 75 °C for 2 hours.

Reaction	Monomer	Polymeric RAFT agent	Conversion (%)	$\bar{M}_{n,theo}$ * g mol <sup>-1</sup>	$\bar{M}_{n,SEC}$ * g mol <sup>-1</sup>	PDI
1	<i>n</i> -BMA	Batch 2	87	216600	163000	2.05
2	Sty	Batch 4	75	85000	66100	1.92

\*  $\bar{M}_{n,theo}$  values were calculated using equation 4.1 and  $\bar{M}_n$  values obtained from SEC are based on PSt standards.

## Chapter Four Results and Discussion

High conversion (87%) was obtained within 2 hours for the chain extension of poly(*n*-butyl methacrylate) with *n*-butyl methacrylate in miniemulsion (reaction 1). The number average molecular weight increased from 39 300 gmol<sup>-1</sup> to 216 600 gmol<sup>-1</sup> within 2 hours. Polydispersity values increased throughout the polymerization starting from 1.18 and stabilizing at about 2. The SEC  $\overline{M}_n$  values were lower than the predicted  $\overline{M}_n$  values for this reaction where *n*-butyl methacrylate was the monomer used. The difference in values might be explained by the fact that the molar masses were determined by GPC against polystyrene standards. Unreliable results in terms of the absolute molecular weights were therefore expected for the chain extension of the initial poly(*n*-butyl methacrylate) block with *n*-butyl methacrylate.

Figure 4.1 shows the SEC traces obtained for the chain extension of initial poly(*n*-butyl methacrylate) block with *n*-butyl methacrylate. The SEC trace for the initial poly(*n*-butyl methacrylate) block is represented by the bold, solid line in the chromatogram.

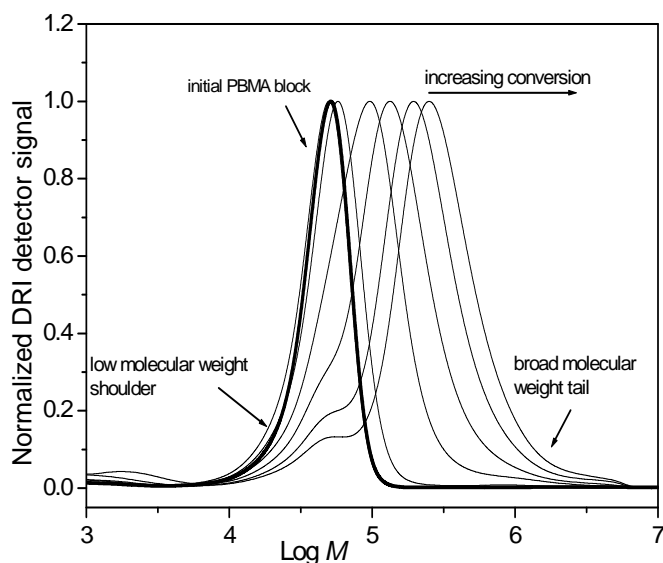


Figure 4.1: Normalized SEC chromatograms for the chain extension of initial poly(*n*-butyl methacrylate) block with *n*-butyl methacrylate in RAFT-mediated miniemulsion polymerization at 75 °C for 2 hours, initiated by AIBN, using PBMA-RAFT agent batch 2.

A shift in the molecular weight distribution from the initial poly(*n*-butyl methacrylate) block ( $\overline{M}_n = 39\,300\text{ gmol}^{-1}$ ) is seen in the chromatogram, indicating that most chains

## ***Chapter Four Results and Discussion***

---

were reinitiated in the second step. Note: not all of the chains underwent chain extension as the initial block already contains some terminated (inactive) chains.

In RAFT-mediated miniemulsion systems, propagating chains are initiated either by primary radicals that originate from the azo-initiator (in this case AIBN) or by radicals from the leaving group of the RAFT agent. The polymeric radicals terminate by either reacting with the RAFT agent or with the same initiating group (initiator or leaving group of RAFT agent). Therefore, numerous different structures exist in these systems. The chains that contain the active RAFT agent (Z-C-S(S)) attached to the chain ends are highly preferable since they can possibly be chain extended upon further addition of new monomer, resulting in block copolymer formation. However, growing polymer chains that have terminated are unfavorable and result in dead chains. The “hump” in the low molecular weight region that does not grow with conversion is ascribed to dead chains from the initial poly(*n*-butyl methacrylate) block synthesized in bulk. These chains are unable to reinitiate in the chain extension step. In the SEC chromatogram (Figure 4.1) a low molecular weight shoulder lower than the initial block is seen and grows, this is likely to be new chains. In the high molecular weight region a tail is seen in the distribution that shifts towards higher molecular weight with increasing conversion. The sharp decrease seen at the end of the high molecular weight distribution suggests that some chains are at the exclusion limit of the column. Several reasons for the behavior of these miniemulsion systems are discussed in Section 4.4. Both the existence of the low molecular weight shoulder and the high molecular weight tail have an effect on the polydispersity of the final polymer. These are some of the reasons for the high polydispersity values obtained in the miniemulsion reactions studied here.

A dual detector system, UV(Ultraviolet)-RI(refractive index) coupled to GPC, was used to identify the polymer chains that contained the active RAFT agent group. The UV signal at 320 nm primarily detected the chains that contained the RAFT-functional group while the UV 254 nm signal detected the phenyl group of the styrene or the RAFT agent. The UV and RI overlay is shown in Figure 4.2. The signals from the two detectors had the same shape in the main distribution, likely because these were arbitrarily normalized.

## Chapter Four Results and Discussion

It should be noted that when processing the SEC results, in order to compare the UV and RI signals, before normalization, the UV signal is multiplied by a factor  $M$  (molecular weight). The RI detector is a concentration sensitive detector and the signal intensity is a function of monomer units passing the detector. The UV detector is approximately sensitive to a single chromophore per polymer chain at a wavelength of 320 nm. In the low molecular weight region, no UV 320 nm absorbance was seen. This is ascribed to dead chains from the initial block that have no RAFT agent functionality and cannot reinitiate in the chain extension step. In the high molecular weight region, noise was seen in the UV 320 nm signal. The noise in the high molecular weight region ( $\text{Log } M$  6.5 –  $\text{Log } M$  7), where the tail appears, was due to the UV 320 nm signal being multiplied by a large value of molecular weight.

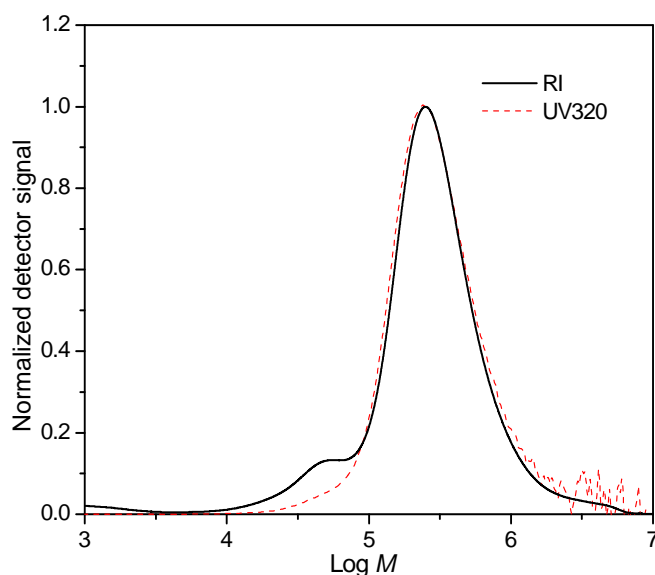


Figure 4.2: UV and RI overlay of the final sample of the chain extension of an initial poly(*n*-butyl methacrylate) block with *n*-butyl methacrylate in RAFT-mediated miniemulsion polymerization at 75 °C for 2 hours, initiated by AIBN.

For the chain extension of the initial poly(styrene) block with styrene in miniemulsion, the reaction was stopped at 60 minutes due to the high viscosity of the reaction mixture, which made sampling and handling of the reaction mixture difficult. The polymerization reached 70% conversion after one hour. The number average molecular weight increased

## Chapter Four Results and Discussion

from 23 300  $\text{gmol}^{-1}$  to 66 100  $\text{gmol}^{-1}$ . The predicted  $\overline{M}_n$  was lower than that of the theoretical  $\overline{M}_n$ . The polydispersity increased throughout the polymerization, stabilizing at 1.98.

In Figure 4.3, a shift in the molecular weight distribution from the initial poly(styrene) block ( $\overline{M}_n = 23\ 000\ \text{gmol}^{-1}$ ) was evident. This indicated that the system was living and that chain extension did occur. A bimodal distribution was seen. The distinct low molecular weight shoulder seen is low molecular weight chains (new chains) at low conversion. The “hump” seen that does not shift towards a higher molecular weight during the reaction is associated with dead chains from the initial poly(styrene) block.

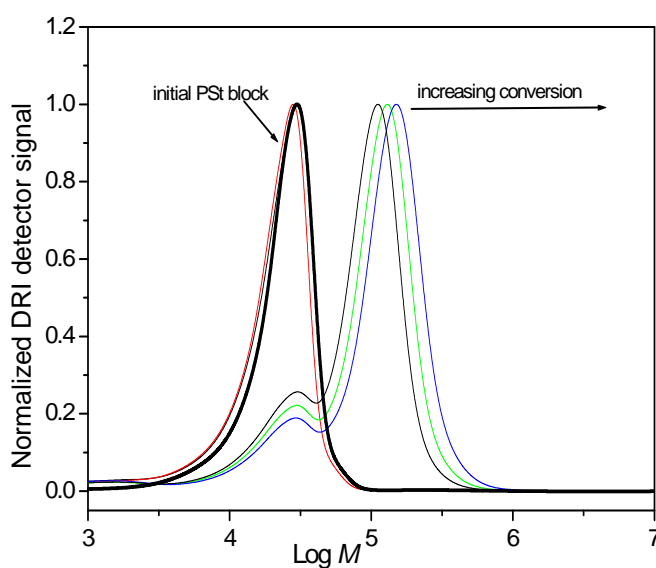


Figure 4.3: Normalized SEC chromatogram for the chain extension of an initial poly(styrene) block with styrene in RAFT-mediated miniemulsion polymerization at 75 °C for 1 hour, initiated by AIBN.

As before, the UV and RI distributions match closely as seen in Figure 4.4. UV 320 nm absorbance is seen in the main distribution, indicating that the thiocarbonyl-thio moiety is present in the chains. The low molecular weight shoulder lacks UV 320 nm absorbance. These are dead chains that do not possess the dithioester moiety. UV 254 nm as before

## Chapter Four Results and Discussion

matches the low molecular weight shoulder and the main distribution indicating that styrene is present in the chains.

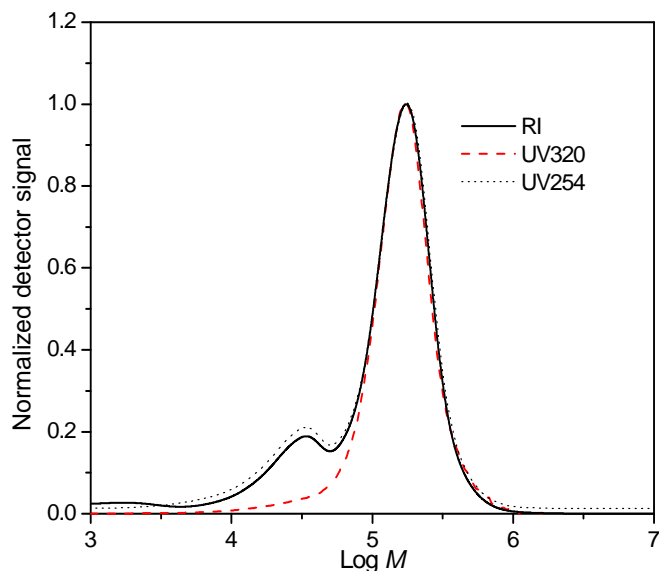


Figure 4.4: UV and RI overlay of the chain extension of an initial poly(styrene) block with styrene in RAFT-mediated miniemulsion polymerization at 75 °C for 1 hour, initiated by AIBN.

### 4.3.3 Dynamic Light Scattering (DLS)

DLS results for reactions 1 and 2 are summarized in Table 4.3.

Table 4.3: DLS results for the chain extension of initial poly(*n*-butyl methacrylate) with *n*-butyl methacrylate (reaction 1) and the chain extension of initial poly(styrene) with styrene (reaction 2) in RAFT-mediated miniemulsion polymerization.

Reaction	Z Average diameter (nm) Before polymerization	Z Average diameter (nm) After polymerization	PDI Before polymerization	PDI After polymerization
1	67	100	0.185	0.118
2	78	101	0.256	0.095

Particle size was determined by DLS before and after polymerization in order to see whether a change in the particle size occurred during the polymerization. Ideally, the final polymer latex should be a copy of the initial miniemulsion in terms of the particle size

## ***Chapter Four Results and Discussion***

---

and particle size distribution.<sup>1</sup> However, in practice, not all of the monomer droplets are nucleated and the final particle size distribution is not an exact copy of the initial monomer droplet size distribution. For both reactions, the final particle sizes are small and well within the range of typical miniemulsions (50 – 500 nm). The DLS size distribution for both reactions appeared to be monomodal and relatively narrow. This is consistent with droplet nucleation.

The SEC results obtained for the simple system correlate with that of Butté *et al.*<sup>2</sup>, who obtained stable systems using dithiobenzoates that were prepolymerized in homogeneous media and chain extended in miniemulsion. Similar work was carried out by Vosloo *et al.*<sup>3</sup>, where pre-formed dithiobenzoate-end-capped styrene oligomers were synthesized in bulk. The bulk mixture was then mixed with a water/surfactant/costabilizer mixture and emulsified, forming a miniemulsion. High polydispersity values were obtained in both of the literature studies (> 1.9). The use of these prepolymerized RAFT agents showed some disadvantages in that the SEC chromatograms show the presence of a low molecular weight shoulder (due to inactive chains) and a high molecular weight shoulder (significant termination and in some cases, the presence of uncontrolled distributions). This resulted in high polydispersity values and broadening of the molecular weight distributions. The polydispersity values obtained in the present study are much higher than those reported in literature. There are other factors in this study that must be taken into consideration, one of them being the higher molecular weights that were targeted compared to those reported in literature. Section 4.4.4 gives a detailed comparative discussion on the results reported in literature and those obtained in this study.

### **4.3.4 Conclusion**

Reasonable results were obtained for the preliminary experiments carried out for the chain extension of the initial poly (*n*-butyl methacrylate) block with *n*-butyl methacrylate and poly(styrene) block with styrene in miniemulsion. Both systems showed living behavior despite the high polydispersity values (there are possible explanations for this, which will be discussed in Section 4.4.4). The results obtained for the simple system



## Chapter Four Results and Discussion

demonstrated the ability to control polymer growth and the possibility of producing block copolymers via this two step process.

### 4.4 Chain extension of initial poly(*n*-butyl methacrylate) block with styrene in miniemulsion

In the following section, a more complex system was investigated. Here, the initial poly(*n*-butyl methacrylate) block was chain extended with styrene in the miniemulsion step, thereby forming AB diblock copolymers. The formulation of the reactions conducted in miniemulsion was tabulated in Chapter 3, Table 3.2

#### 4.4.1 Results

The results obtained for reaction 3 is summarized in Table 4.4.

Table 4.4: Characteristics of poly(*n*-butyl methacrylate)-*b*-poly(styrene) diblock copolymer formed in RAFT-mediated miniemulsion polymerization at 75 °C for 2 hours, initiated by AIBN.

Reaction	Monomer	Polymeric RAFT agent	Conversion (%)	$\bar{M}_{n,theo}^*$ gmol <sup>-1</sup>	$\bar{M}_{n,SEC}^*$ gmol <sup>-1</sup>	PDI
3	Sty	Batch1	87	240000	245000	2.24

\*  $\bar{M}_{n,theo}$  values were calculated using equation 4.1 and  $\bar{M}_n$  value obtained from SEC is based on PST standards.

Figure 4.5 shows a linear evolution of  $\bar{M}_n$  with conversion. In the graph illustrating the evolution of  $\bar{M}_n$  and PDI for the block copolymer miniemulsion polymerization the straight, bold line indicating the predicted  $\bar{M}_n$  was calculated according to Monteiro *et al.*<sup>4</sup> The equation is given below and takes into consideration not only the chains generated by the RAFT agent but also the initiator-derived chains:

$$\bar{M}_{n,theo} = M_{RAFT} + \frac{x[M]_0 M_M}{[RAFT]_0 + 2f[I]_0(1 - e^{-k_d t})} \quad (4.1)$$

## Chapter Four Results and Discussion

where  $\overline{M}_{RAFT}$  is the molar mass of the RAFT agent,  $[M]_0$  and  $[RAFT]_0$  are the initial concentrations of the monomer and the RAFT agent,  $[I]_0$  is the initial initiator concentration,  $k_d$  is the decomposition rate coefficient of the initiator,  $f$  is the initiator efficiency and  $t$  is the reaction time.

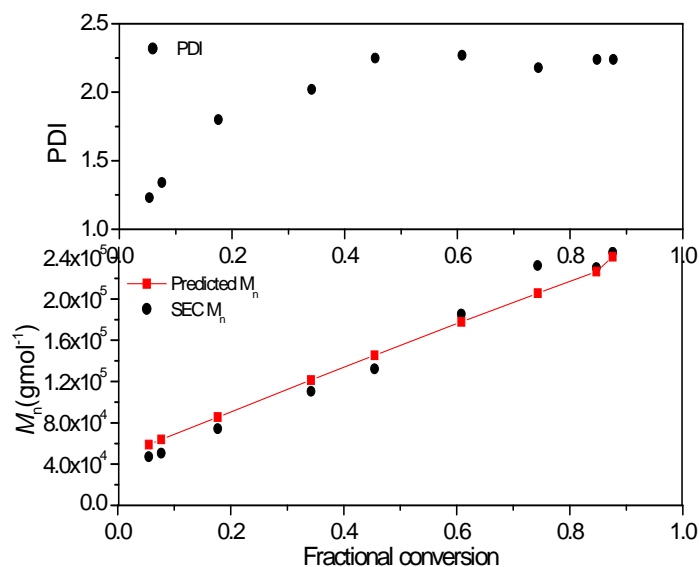


Figure 4.5: Evolution of  $\overline{M}_n$  and PDI for poly(*n*-butyl methacrylate)-*b*-poly(styrene) in RAFT-mediated miniemulsion polymerization at 75 °C for 2 hours, initiated by AIBN, using PBMA-RAFT agent batch 1.

The predicted  $\overline{M}_n$  versus SEC  $\overline{M}_n$  values obtained for this reaction are in good agreement with each other. As is evident, the livingness of the miniemulsion systems was demonstrated by the linear increase of  $\overline{M}_n$  with conversion. Throughout the polymerization, the polydispersity increased with conversion and stabilized at high polydispersity values near a range of 2.2, as seen in Figure 4.5. This is larger than that of the initial block polymer synthesized in bulk (PDI 1.18). In an ideal case, with increasing conversion, the polydispersity should decrease in RAFT-mediated miniemulsion systems since most of these chains grow via the RAFT mechanism.<sup>5</sup> In the results obtained, the polydispersity increased throughout the reaction. Significant bimolecular termination via coupling of the growing polymer chains is a commonly suggested cause for this

## Chapter Four Results and Discussion

occurring<sup>6</sup>. However, it is more likely to be due to other causes which will be discussed in Sections 4.5 and 4.6, where the complex system is investigated more thoroughly. The results obtained agree with results reported in academic literature where methyl methacrylate-styrene and styrene-butyl acrylate block copolymers of much lower molecular weight were synthesized via RAFT-mediated miniemulsion polymerization.<sup>7</sup> High polydispersity values ( $> 2$ ) were reported and significant broadening in the molecular weight distribution was evident.

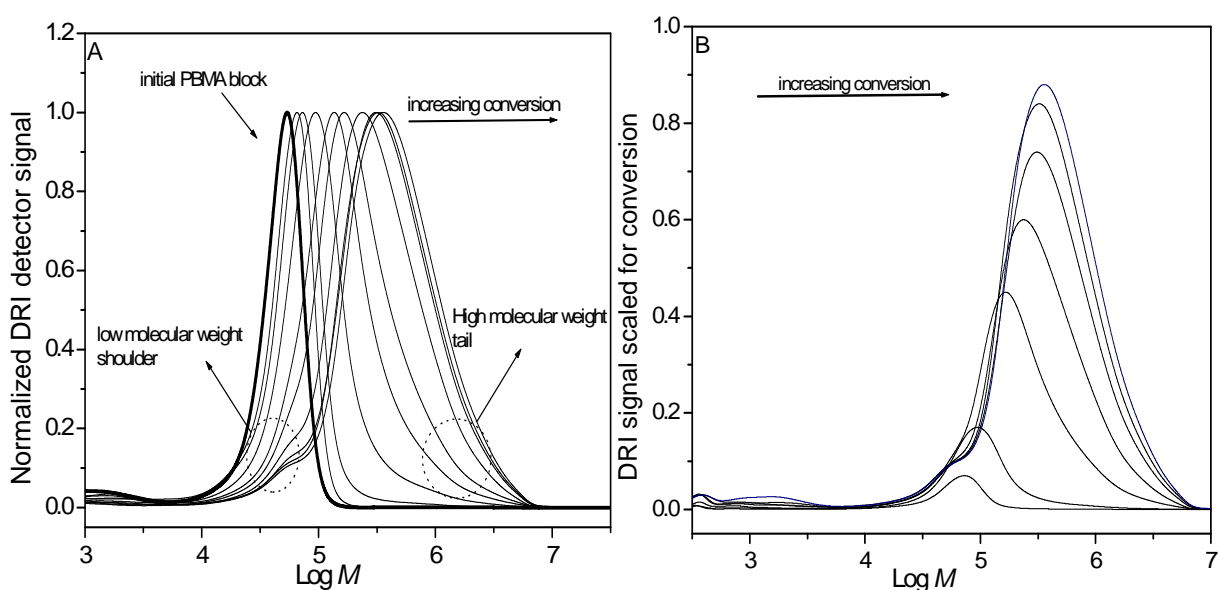


Figure 4.6: (A) Normalized SEC chromatograms for the chain extension of initial poly(*n*-butyl methacrylate) block with styrene in RAFT-mediated miniemulsion at 75 °C, initiated by AIBN, using PBMA-RAFT agent batch 1. (B) Evolution of molar mass distribution with conversion for poly(*n*-butyl methacrylate)-*b*-poly(styrene) in RAFT-mediated miniemulsion at 75 °C initiated by AIBN, using PBMA-RAFT batch 1 (normalized for conversion for amount of polymer present).

An obvious peak shift to higher molecular weights was seen in the SEC chromatograms in Figure 4.6 (A). This indicated that propagation started from the initial RAFT functionalized PBMA block, and generated the PBMA-*b*-PSt diblock copolymer. The SEC chromatogram showed a single distribution and the existence of a low molecular weight shoulder was seen in the SEC chromatogram. Other research groups have reported on the existence of a low molecular weight shoulder in the preparation of diblock copolymers.<sup>8</sup> This shoulder could be short poly(styrene) initiator-derived chains which

## Chapter Four Results and Discussion

eventually grow into longer chains. Significant broadening in the high molecular weight region occurred at conversions greater than 20%, as is indicated on the SEC chromatogram. The possible reasons for this will be discussed in Section 4.5. The SEC chromatogram in Figure 4.6 (B), where the DRI signal is scaled for conversion, confirmed the living behavior of the system. The tailing in the low molecular weight region and the broadening in the high molecular weight region was clearly evident in this chromatogram.

### 4.4.2 Dynamic Light Scattering (DLS)

DLS results for reaction 3 are summarized in Table 4.5.

Table 4.5: DLS results for the poly(*n*-butyl methacrylate)-*b*-poly(styrene) diblock copolymer latex in RAFT-mediated miniemulsion, at 75 °C, initiated by AIBN.

Reaction	Z(Average) diameter (nm) Before polymerization	Z(Average) diameter (nm) After polymerization	PDI Before polymerization	PDI After polymerization
3	82	96	0.133	0.051

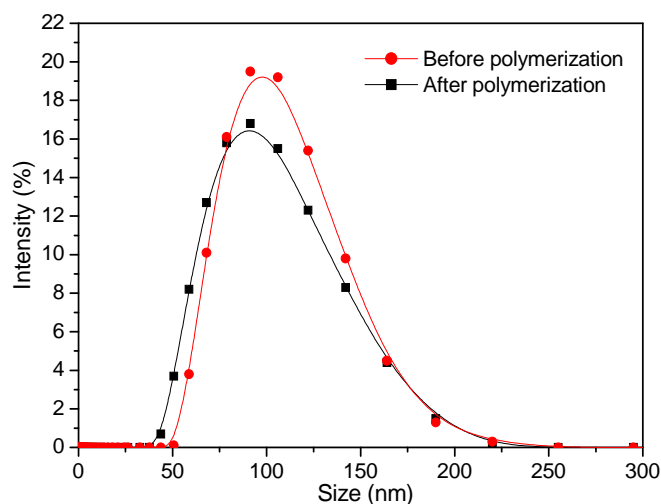


Figure 4.7: DLS size distribution graph of the final poly (*n*-butyl methacrylate)-*b*-poly(styrene) diblock copolymer latex in RAFT-mediated miniemulsion, at 75 °C, initiated by AIBN.

## ***Chapter Four Results and Discussion***

---

DLS analysis was carried out before polymerization (directly after sonication), as well as after the miniemulsion polymerization to observe if there was any change in particle size. Before polymerization, the Z average diameter value obtained was 82 nm. After polymerization, the particle size was 96 nm. A significant change in volume was seen which could be indicative of particle coagulation or uneven particle growth occurring. During sonication particles break up, collide and coalesce when placed under high shear. Once the submicron particles have formed the particles are unstable and an equilibrium (steady state) needs to be established. According to thermodynamics, in order for equilibrium to be achieved, diffusion of monomer from the smaller to the larger droplets might occur after sonication, (this should however be suppressed by the hydrophobe). This usually requires time, and is dependent on the degree of water solubility of the monomer. This causes a change in the particle size and results in miniemulsions with broad particle size distributions.<sup>9</sup> Landfester *et al.*<sup>10</sup> also showed that the final particle size obtained once the droplets have reached equilibrium, is dependent on the concentration of the surfactant, and the time required to reach the steady state depends on the amount of energy applied to the system and other factors, for example, the viscosity inside the droplets.<sup>10</sup>

The DLS size distribution graph showed a monomodal distribution with a low PDI value (0.05) for the final diblock copolymer. The DLS distribution graph for after polymerization showed a broader distribution in the smaller particle size region than the DLS distribution graph for before polymerization. This could indicate that there are more smaller particles present after polymerization than before polymerization. If this were not an artifact in the DLS then this could be indicative of new particle formation or the presence of “lagging” particles (which grow slower as mentioned later) and seen in the TEM images.

### 4.4.3 Transmission Electron Microscopy (TEM)

Particle size, particle size distributions and particle morphology of the poly(*n*-butyl methacrylate)-*b*-poly(styrene) diblock copolymer latices were determined using TEM.

TEM micrographs showing the particle morphology of the poly(*n*-butyl methacrylate)-*b*-poly(styrene) diblock copolymer latex before and after polymerization is seen in Figure 4.8. The TEM images obtained provide more insight into the possible reasons for obtaining broad molecular weight distributions and high polydispersity values in these systems.

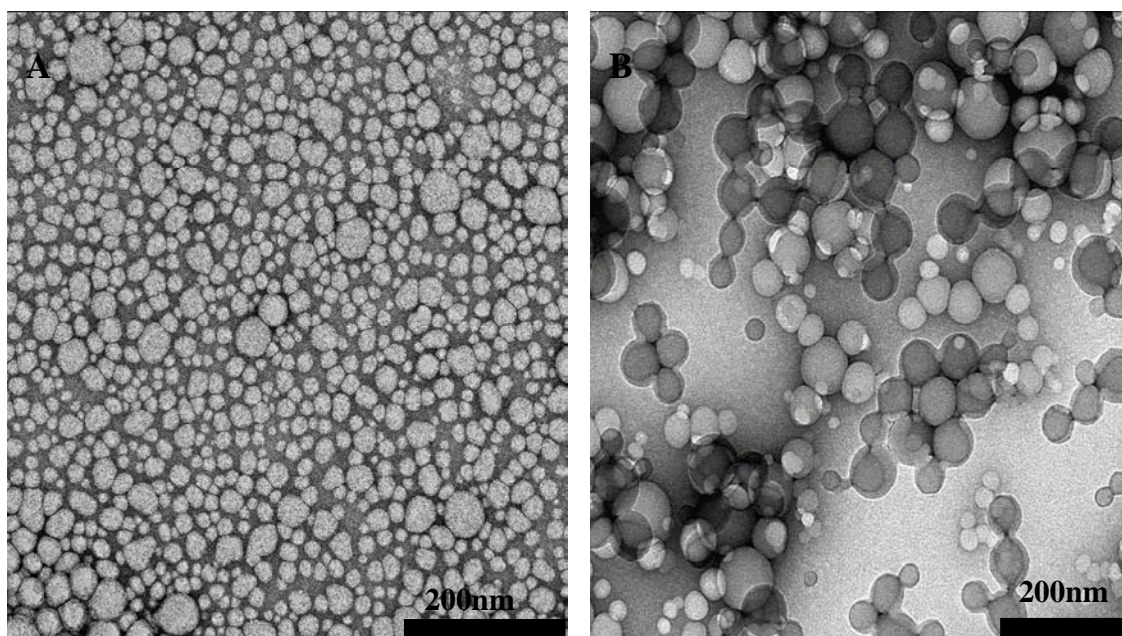


Figure 4.8: TEM image of the poly(*n*-butyl methacrylate)-*b*-poly(styrene) diblock copolymer prepared by RAFT-mediated miniemulsion polymerization at 75 °C for 2 hours, initiated by AIBN (A) before polymerization; (B) after polymerization

The TEM micrograph, Figure 4.8 (A), taken before polymerization (after sonication), showed a non-uniform particle size distribution. This should correspond to the first block “cores”. The majority of particles had particle sizes of 30 – 50 nm, however there were a few larger particles in the range of 80 – 90 nm.

## ***Chapter Four Results and Discussion***

---

Huang *et al.*<sup>9</sup> report on the reasons for the broad particle size distribution in these miniemulsion systems after the sonication process. During the sonication process, particles diffuse, break up and recombine, resulting in both small and large particles, and therefore a broad particle size distribution.

In ideal miniemulsion systems the final polymer particles range between 30 and 500 nm in size.<sup>11,12</sup> A broad particle size distribution was seen in the TEM micrograph (B) of the final poly(*n*-butyl methacrylate)-*b*-poly(styrene) latex. The image showed that the particles were not monodisperse, as shown in the DLS results. Small and large particles were present in the initial latex and in the final block copolymer latex. The small particles were in the range of 50 – 60 nm, while the slightly larger particles were in the range of 70 – 80 nm (corresponding to DLS measurements).

In the image, a population of small particles (20 – 30 nm) was distinguishable. These small particles are possibly secondary particles, however this statement is debatable. This is further investigated in section 4.5. If this were the case, an uncontrolled secondary distribution in the high molecular weight region would have been present in the SEC chromatogram.<sup>13,14</sup> Light scattering results did not indicate the presence of these small particles as this technique is biased towards large particles. The TEM images of the diblock copolymer appeared to exhibit a phase separated morphology. Some of the darker particles seem to have a double layer shell but are a single layer. This might be an indication of phase-separation. This is seen in some areas of in the TEM image. It must be taken into consideration that artifacts can easily occur in TEM. The possibility of microphase separation in these block copolymers could further be investigated in future work; it is not part of the current research objectives.

### **4.4.4 Discussion**

The use of the RAFT process to produce block copolymers in heterogeneous aqueous media has been shown by Butté *et al.*<sup>2</sup> and de Brouwer *et al.*<sup>4</sup> To our knowledge, not much has been reported in the literature on the reasoning for observed behavior of these systems in terms of the high polydispersities and broad molecular weight distributions.

## Chapter Four Results and Discussion

---

Butté *et al.*<sup>2</sup> reported on the use of RAFT in miniemulsion polymerization systems. The work of Butté entails the use of an oligomeric RAFT agent ( $Z=\text{Ph}$   $R=-(\text{STY})_n\text{C}(\text{CH}_3)_3$ ) that was synthesized in bulk polymerization. The oligomeric RAFT agent was used in a miniemulsion polymerization of styrene. The polymerization showed good control, although high polydispersities ( $> 2$ ) were obtained. The existence of a low molecular weight tail was evident in the SEC chromatogram of the styrene miniemulsion. This tail was ascribed to the presence of dead chains from the initial bulk polymerization. These dead chains are terminated chains that are unable to reinitiate in the second miniemulsion step when styrene monomer is added. This was assigned as one of the reasons for the high polydispersity obtained. Block copolymers of PMMA-*b*-PSt were also synthesized using an oligomeric RAFT agent ( $Z=$  pyrrole,  $R=-(\text{MMA})\text{C}(\text{CH}_3)_2\text{CN}$ ), prepared in solution and initiated by AIBN. The PMMA-*b*-PSt was synthesized in miniemulsion. The nature of the living system was seen in the linear increase of  $\overline{M}_n$  with conversion. However, the polydispersity increased with time and high polydispersity values (1.4 – 3) were obtained.

In a recent study, Vosloo *et al.*<sup>3</sup> investigated a system in which dithiobenzoate end-capped styrene oligomers were synthesized in bulk, the bulk mixture was then emulsified and a miniemulsion was formed. The SEC chromatograms obtained showed a bimodal distribution and in some cases a multimodal distribution. A low molecular weight shoulder was seen in the SEC chromatograms. This was ascribed to some oligomers that were not reinitiated in the miniemulsion polymerization or possibly shorter chains that were terminated during the polymerization. Relatively high polydispersity values of 1.9 were obtained in the systems. A high molecular weight shoulder was evident in samples of higher conversion. This was attributed to a fraction of polymerization occurring in an uncontrolled manner due to less RAFT agent present in the particles and numerous termination reactions of different kinds or transfer taking place.

The results obtained thus far in this study reflect the conclusions also reported in literature and discussed above. The chain extension of the initial PBMA block with *n*-butyl methacrylate, PSt block with styrene and PBMA block with styrene all showed the



## ***Chapter Four Results and Discussion***

---

existence of a low molecular weight shoulder, broad molecular weight distribution (tailing in the high molecular weight region) and high polydispersity values.

The low molecular weight shoulder seen in the SEC chromatograms in both this study and in academic literature is ascribed to dead chains (caused by radical-radical termination reactions), which are unable to reinitiate. This could be a partial explanation for obtaining such high polydispersity values ( $> 2$ ) and broadening of the molecular weight distribution in the systems. In the literature, another possible reason for high polydispersity values obtained in these miniemulsion systems is given as being due to the deviation in the behavior of these RAFT-mediated miniemulsion systems from that of an ideal miniemulsion system. In this present study, deviation of this RAFT-mediated miniemulsion system might be one of the reasons for the broadening in the molecular weight distributions. The TEM micrograph obtained for the diblock copolymer before polymerization, taken after the sonication process, shows a non-uniform particle size distribution and a variety of particle sizes in the sample. This could mean that from the start of the polymerization, different particles have different RAFT agent concentrations if the organic phase were to be inhomogeneous. The possibility of this occurring will be discussed in Section 4.5 where the system is investigated in more detail.

In an ideal miniemulsion, particles are said to be “one-to-one copies” of the original droplets, i.e. droplet nucleation is the dominant nucleation mechanism in these systems.<sup>1</sup> Several factors cause miniemulsions to deviate from the ideal systems. The presence of multiple nucleation mechanisms occurring within the system is an additional factor to consider. Homogeneous nucleation and micellar nucleation (micellar nucleation is expected to a lesser extent due to the concentration of surfactant being below the CMC) has been reported and can result in deviation from ideal miniemulsion systems.<sup>15</sup> This will have an effect on the RAFT technique since some of the particles will contain RAFT agent which will polymerize in a controlled manner while some particles might lack RAFT agent (or contain less RAFT agent), resulting in conventional miniemulsion polymerization occurring, thus, uncontrolled polymer growth. A signature of this is a high molecular weight distribution that does not change in molecular weight with conversion.

## ***Chapter Four Results and Discussion***

---

In RAFT-mediated miniemulsion systems, secondary nucleation might occur, resulting in secondary particle formation in the aqueous phase. In order for these secondary particles to form, radicals need to be present in the aqueous phase. These radicals can be initiator fragments, propagating oligomers or radicals that desorb from the particles. No evidence of a secondary distribution was seen in the SEC chromatogram, Figure 4.6. However, in the TEM image, Figure 4.8 (B), a population of small particles (20 – 30 nm) was clearly seen. These particles are possibly secondary particles. In academic literature, other factors such as the nature of the radical leaving group of the RAFT agent can also influence the formation of secondary particles. Butté *et al.*<sup>2</sup> found that the larger the hydrophobic leaving group, the lower the probability of exit of the leaving group from the particle.<sup>2</sup> The exit of the leaving group is one of the important factors in the formation of these particles. In this study, the use of a hydrophobic leaving group should decrease the amount of exit, therefore reducing termination or propagation in the aqueous phase. The use of aqueous radical traps such as sodium nitrite and Fremy's salt (dipotassium nitrosodisulfonate) to eliminate radicals present in the aqueous phase has been reported in literature.<sup>12,16</sup> In preventing radicals from being generated in the aqueous phase, secondary particle growth can be minimized or suppressed.

A further point of importance that needs to be taken into account is the high molecular weights that are targeted in this study. In most RAFT-mediated miniemulsion polymerizations, molecular weights in the range of 20 000 – 30 000 g mol<sup>-1</sup> are usually targeted.<sup>17</sup> However, higher molecular weights are targeted when block copolymers for specific applications, such as when thermoplastic elastomers are synthesized. Yang *et al.*<sup>17</sup> synthesized high molecular weight polystyrene using a polystyrene oligomeric RAFT agent. Results showed that the PDI is dependent on the molecular weight. The higher the molecular weight, the higher the PDI value. This could also be a partial reason for the high PDI values obtained in the miniemulsion systems.

Another important point to consider is the internal viscosity of the particles in the latex. The very high internal viscosity might be unfavorable to the activation-deactivation equilibrium. This results in more side reactions occurring and poor control, since  $k_{\text{add}}$  can

## ***Chapter Four Results and Discussion***

---

decrease, which further results in broadening and in high polydispersity values of the molecular weight distributions.<sup>3</sup>

Vosloo *et al.*<sup>3</sup> proposed a possible explanation for obtaining broad molecular mass distributions and possible loss in control at higher conversions. In an efficient RAFT process, the exchange between the active and the dormant species must be rapid in order to ensure that the rate of deactivation ( $k_{\text{deact}}$ ) is faster than the rate of propagation ( $k_{\text{prop}}$ ). At high conversions the internal viscosity of the particles increases, the deactivation reaction might become affected and might become diffusion controlled. When radical deactivation becomes diffusion controlled, the activation/deactivation equilibrium between the propagating chain and the dormant chain shifts to the direction of the propagating chain. In addition, a decrease in the ratio of the rate coefficients of the deactivating and activating reactions will occur, which will increase the concentration of the active species. The broadening of the molecular weight distribution and high polydispersity values in the system in such a case is mainly due to inefficient control in the system.

The above discussion is a summary of the possible explanations for the observed behavior in these RAFT-mediated miniemulsion systems reported in the literature. These points should be taken into consideration when the RAFT-mediated miniemulsion system in this present study is investigated more thoroughly in the following section.

### **4.4.5 Conclusion**

Reactivation of the initial PBMA block with styrene in miniemulsion was successfully carried out. A majority of the chains were reinitiated in the chain extension step and a strong diblock component was seen. Results of the preliminary experiments proved that the initial PBMA block (polymeric RAFT agent) was a good candidate to mediate a controlled styrene miniemulsion polymerization for which high molecular weight was targeted. The SEC results showed living/controlled behavior for the latices despite the broad molecular weight distributions and the high polydispersity values ( $> 2$ ).

## Chapter Four Results and Discussion

In the second part of the study, the behavior of the RAFT-mediated miniemulsion system was investigated more thoroughly in Section 4.5. A detailed discussion is given for the possible reasons and explanations for the observed broadening of the molecular weight distributions and high polydispersity observed in the RAFT-mediated miniemulsion system.

### 4.5 The influence of the different initiator/RAFT agent molar ratios on the RAFT-mediated miniemulsion system

In RAFT polymerization systems, the molar ratio of initiator to RAFT agent plays an important role in achieving a successful controlled radical polymerization. The change in the ratio of initiator to RAFT agent is normally expected to have a significant influence on the polydispersity of the polymer.<sup>18</sup> In an attempt to synthesize high molecular weight diblock copolymers of narrow molecular weight via the two-step process, the effect of the initiator/RAFT agent molar ratio on the system was investigated.

The formulations of the reactions carried out in miniemulsion were given in Chapter 3, Table 3.2.

#### 4.5.1 Results

Table 4.6 below is a summary of the characteristics obtained for the AB diblock copolymer miniemulsion polymerization reactions.

Table 4.6: Characteristics of the polymer formed in the final latices obtained for the chain extension reactions in RAFT-mediated miniemulsion polymerization at 75 °C for 2 hours.

Reaction	Monomer	Polymeric-RAFT agent	AIBN/Polymeric-RAFT agent (mol ratio)	Conversion (%)	$\bar{M}_{n,theo}$ gmol <sup>-1</sup>	$\bar{M}_{n,SEC}$ gmol <sup>-1</sup>	PDI
4	Sty	Batch 2	1:2	93	$2 \times 10^5$	197000	2.24
5	Sty	Batch 2	1:10	86	$2 \times 10^5$	187000	2.09
6	Sty	Batch 2	1:20	89	$2 \times 10^5$	179500	2.54

$\bar{M}_{n,theo}$  values were calculated using equation 4.1 and  $\bar{M}_n$  values obtained from SEC are based on PSt standards.

## Chapter Four Results and Discussion

The conversion–time profiles of the miniemulsion polymerizations using different initiator/RAFT agent molar ratios are displayed in Figure 4.9 (A). In all three reactions high conversions ( $> 80\%$ ) were obtained within two hours, whereafter the reactions were stopped due to the high viscosity (this was considered rather unusual for emulsion-type systems). From the conversion graph, one finds that in the case of  $[\text{AIBN}]/[\text{RAFT agent}] = (1:2)$ , the monomer conversion increased faster than in reaction 5 ( $[\text{AIBN}]/[\text{RAFT agent}] = (1:10)$ ) and reaction 6 ( $[\text{AIBN}]/[\text{RAFT agent}] = (1:20)$ ); obtaining a higher percentage conversion (93%) than reaction 5 (84%) and reaction 6 (89%) was obtained within two hours.

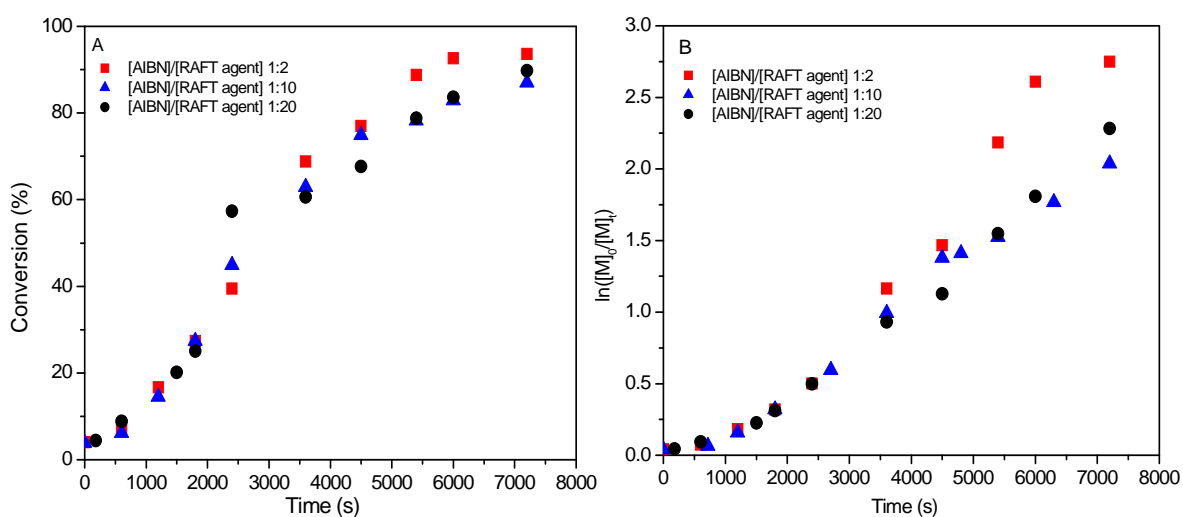


Figure 4.9: (A) Monomer conversion versus reaction time for the synthesis of poly(*n*-butyl methacrylate)-*b*-poly(styrene) in RAFT-mediated miniemulsion at 75 °C for 2 hours, initiated by AIBN, using PBMA-RAFT batch 2. Reaction 4,  $[\text{AIBN}]/[\text{RAFT agent}] = 1:2$ , Reaction 5,  $[\text{AIBN}]/[\text{RAFT agent}] = 1:10$ , Reaction 6,  $[\text{AIBN}]/[\text{RAFT agent}] = 1:20$ .

(B) Semilogarithmic plot of monomer conversion versus reaction time for the synthesis of poly(*n*-butyl methacrylate)-*b*-poly(styrene) in RAFT-mediated miniemulsion at 75 °C for 2 hours, initiated by AIBN, using PBMA-RAFT batch 2. Reaction 4,  $[\text{AIBN}]/[\text{RAFT agent}] = 1:2$ , Reaction 5,  $[\text{AIBN}]/[\text{RAFT agent}] = 1:10$ , Reaction 6,  $[\text{AIBN}]/[\text{RAFT agent}] = 1:20$ .

The semilogarithmic plots indicated the presence of a short induction period, which is probably due to dissolved oxygen which is very common in styrene emulsions. Induction periods are common in these dithiobenzoate RAFT-mediated miniemulsion polymerizations and have been documented.<sup>19,20</sup> The phenomenon of rate retardation in

## ***Chapter Four Results and Discussion***

---

dithiobenzoate-mediated RAFT polymerization, compared to conventional free-radical polymerization has also been reported in academic literature. This topic is, however, beyond the scope of the study and will not be discussed.<sup>20</sup> The slope of the logarithmic plot is proportional to the overall propagating radical concentration in the reaction. In emulsion systems the rate of polymerization is proportional to the product of the particle number and the average number of radicals per particle.<sup>21</sup> For reactions 4, 5 and 6, the semilogarithmic plots were roughly linear up to 70% conversion. At higher conversion, deviation from linearity was seen – the polymerization rate increased, which suggested that either  $\bar{n}$  (average number of radicals per particle) or  $N_c$  (particle number) were increasing, which could at this stage indicate that a transition in the kinetics from zero-one conditions (at low conversion) to non-zero-one (at high conversion) occurred in the system or possibly secondary particle formation was occurring late in these systems.

The Trommsdorff effect could also be a reason for the observed increase in the polymerization rate in miniemulsion systems and is probably what would drive the transition from zero-one conditions, i.e. termination slows down. In all three reactions, high conversions were reached. As conversion increases, the viscosity inside the particles increases and the mobility of the chains is reduced (long chains and more chain entanglements). At a high weight fraction of polymer the system can become glassy and the motion of a radical of any degree of polymerization by centre-of-mass diffusion is slow. As more monomer is consumed, the rate of termination decreases and the number of radicals per particle increases, resulting in an increase in the rate of polymerization.<sup>22</sup>

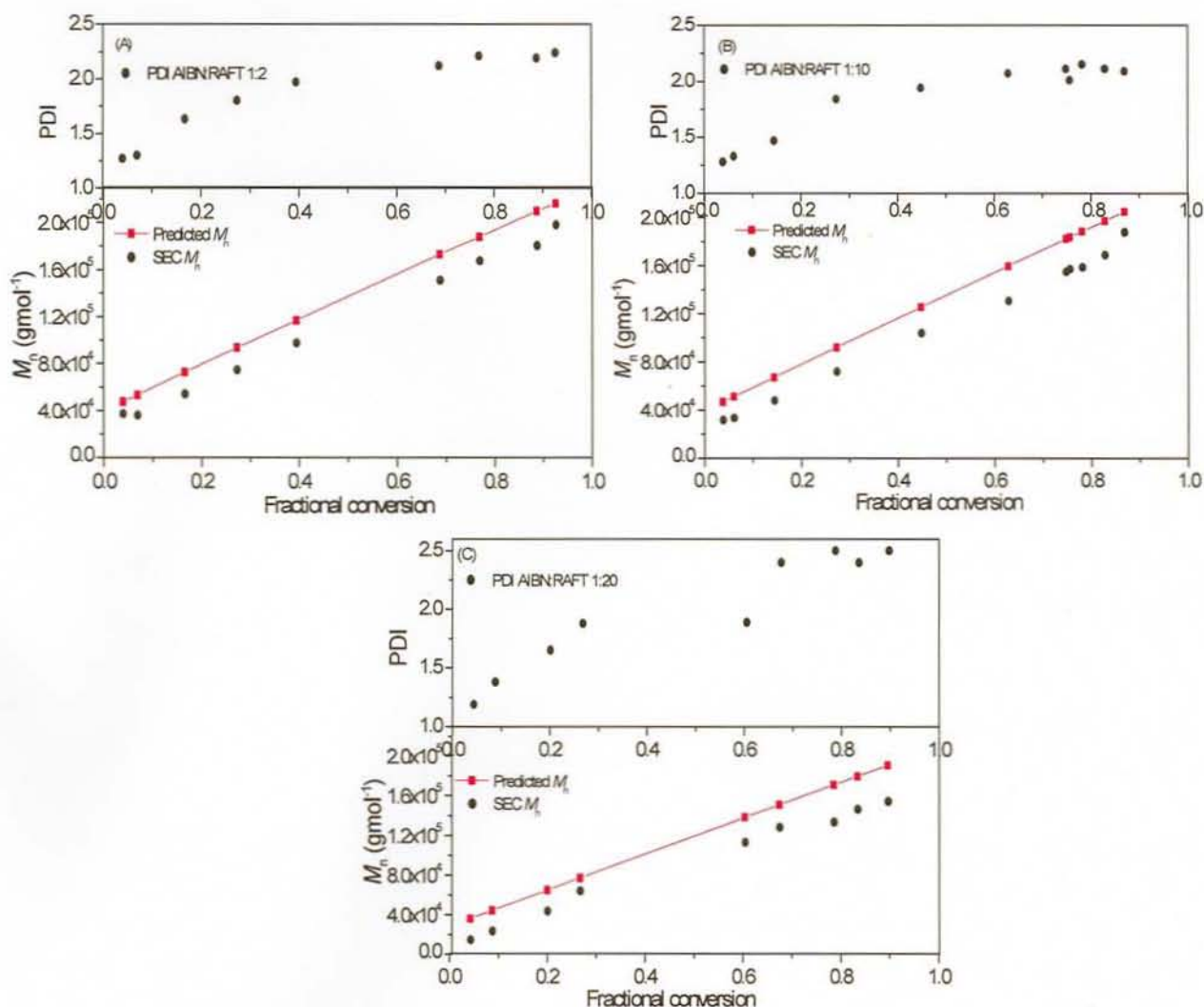


Figure 4.10: Evolution of  $\bar{M}_n$  and PDI for poly(*n*-butyl methacrylate)-*b*-poly(styrene) in RAFT-mediated miniemulsion polymerization at 75 °C for 2 hours using PBMA-RAFT agent batch 2: (A) Reaction 4, [AIBN]/[RAFT agent] = 1:2 (B) Reaction 5, [AIBN]/[RAFT agent] = 1:10 (C) Reaction 6, [AIBN]/[RAFT agent] = 1:20.

In Figure 4.10 (A), the SEC  $\bar{M}_n$  values increased linearly with increasing conversion. The predicted  $\bar{M}_n$  and the SEC  $\bar{M}_n$  values correlated well. This is a strong indication that the miniemulsion system was well controlled. The PDI values increased throughout the polymerization, starting from 1.18 and leveling off at about 2.2. In Figure 4.10 (B), a

## Chapter Four Results and Discussion

---

good agreement of the predicted  $\overline{M}_n$  and SEC  $\overline{M}_n$  values was also observed. The PDI values increased during the reaction starting from 1.18 and stabilizing at 2.1. These PDI values were lower than those of reaction 4. This might be expected, since a lower molar ratio of [AIBN]/[RAFT agent] was used and therefore the number of possible termination reactions occurring are expected to be less.

Figure 4.10 (C), reaction 6, in which a minimal amount of initiator was used, reflects the living process by the linear increase of  $\overline{M}_n$  with conversion. Throughout the polymerization the polydispersity values increased, stabilizing at about 2.54. The PDI values were higher than those obtained in reaction 4 and 5 even though the concentration of the initiator was the lowest.

The linear increase in  $\overline{M}_n$  with conversion for the three reactions confirmed that there was a constant number of growing chains during the polymerization. In Figure 4.10, a trend in all three polymerization reactions of different initiator concentration is seen. At low conversions (approximately 20%) the system performed well (PDI < 1.5) before the polydispersity rapidly increased at higher conversions. This rapid increase in the polydispersity suggested that dead chains and bimolecular termination were not the only reason for this occurring. The kinetic plots in Figure 4.9 appeared to deviate from linearity at higher conversion which suggests that  $\bar{n}$  (which is expected to increase at some point) or  $N_c$  is increasing. An increase in  $N_c$  at higher conversion could mean that secondary particle formation was occurring, which will further increase the PDI of the system since these particles have polymerized in a less controlled manner (due to the little or no RAFT agent expected to be present inside these particles).

In the literature the high polydispersity obtained in similar RAFT-mediated miniemulsion systems is ascribed to termination reactions. For example, in the work reported by Heuts *et al.*<sup>5</sup> group, oligomeric PEPDTA (1-phenylethyl phenyldithioacetate) RAFT agent was used in a styrene miniemulsion with an anionic surfactant, SDS. High polydispersity values were also reported and irreversible termination was considered to be the cause. Yang *et al.*<sup>23</sup> studied the dependence of the final PDI on reaction parameters. Results



## ***Chapter Four Results and Discussion***

---

---

showed that higher initiator levels lead to higher PDI values due to a larger number of irreversible termination reactions. The results obtained in this present study indicated that the high polydispersity was not solely related to the initiator concentration. In the work carried out by Butté *et al.*<sup>2</sup>, an uneven RAFT agent distribution (inhomogeneity in the system) was believed to be the reason for the high polydispersity values in the system. This is more likely to be the reason for the observed polydispersity in this present study.

The SEC chromatograms in Figure 4.11 for poly(*n*-butyl methacrylate)-*b*-poly(styrene) diblock copolymers prepared using different initiator/RAFT agent concentration ratios indicate the living nature of the miniemulsion system. The initial PBMA block is indicated by the bold, solid line.

## Chapter Four Results and Discussion

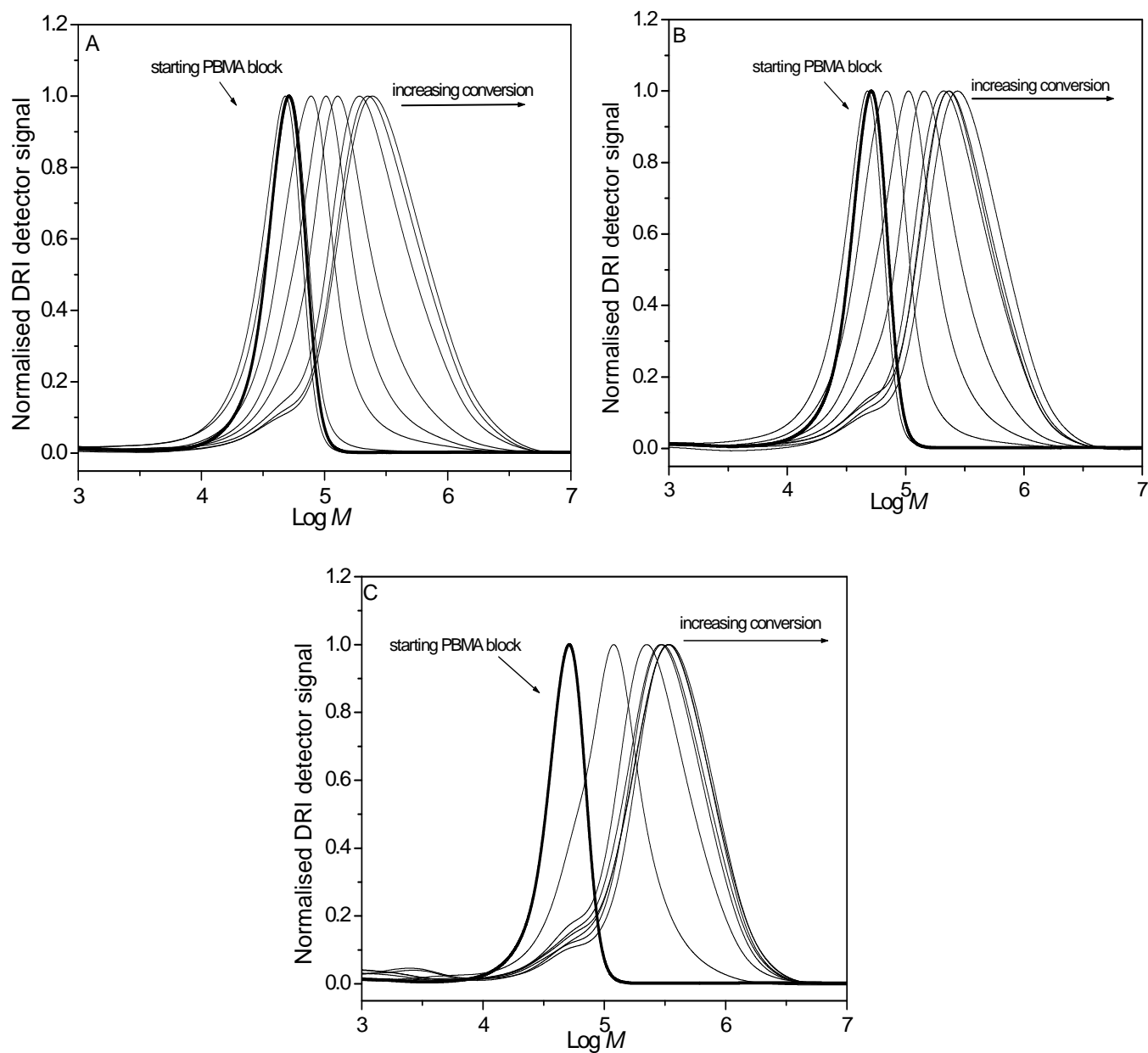


Figure 4.11: Normalized SEC chromatograms for the chain extension of the initial PBMA block with styrene in RAFT-mediated miniemulsion polymerization at 75 °C for 2 hours, initiated by AIBN using PBMA-RAFT batch 2: (A) Reaction 4, [AIBN]/[RAFT agent] = 1:2; (B) Reaction 5, [AIBN]/[RAFT agent] = 1:10 (C); Reaction 6, [AIBN]/[RAFT agent] = 1:20.

## ***Chapter Four Results and Discussion***

---

Figure 4.11 (A) shows the DRI traces for the SEC analysis of the obtained poly(*n*-butyl methacrylate)-*b*-poly(styrene) block copolymer where a high initiator/RAFT agent concentration ratio was used. Chain extension did indeed occur resulting in block copolymer formation. The SEC chromatogram shows that not all of the chains were reinitiated from the starting block which contains some terminated (inactive) chains. At 20% conversion or below, a new low molecular weight component was seen. This could be ascribed to short PSt chains (initiator-derived chains that are not diblocks, which eventually grow to be long) formed upon decomposition of the AIBN initiator. Broadening in the distribution was seen, forming a tail that shifted towards a higher molecular weight with increasing conversion.

The SEC chromatogram in Figure 4.11 (B), showed similar behavior to that in Figure 4.11 (A). The low molecular weight tail was also seen in the chromatogram. At conversions greater than 20%, broadening of the distribution towards the high molecular weight region was seen. Compared to reaction 4, a slightly narrower molecular weight distribution was seen, which might be expected since less initiator was used, thus reducing the amount of bimolecular termination reactions (therefore lowering the polydispersity of the system).

In RAFT-mediated polymerization, for efficient control over the molecular weight, several requirements must be fulfilled. One is that the addition of the propagating radicals to the RAFT agent must be faster than to monomer,  $k_{\text{add}}[\text{RAFT}] \gg k_{\text{p}}[\text{M}]$ . For high targeted molecular weights (low RAFT agent concentration), the criteria do not hold, resulting in poor control in the system due to  $k_{\text{add}}[\text{RAFT}]$  not being significantly larger than  $k_{\text{p}}[\text{M}]$ . For the system under consideration in the present study, the first term is not significantly larger than the second term (for  $k_{\text{add}} = 10^6 \text{ L}\cdot\text{mol}^{-1}\text{s}^{-1}$ ,<sup>24</sup>  $k_{\text{p}} = 565 \text{ L}\cdot\text{mol}^{-1}\text{s}^{-1}$  at 75 °C<sup>25</sup>). The high polydispersity values obtained in all three reactions could be a result of inefficient control with good livingness, which is consistent with the SEC results.

In the extreme case, where a minimal amount of initiator was used, the SEC chromatogram in Figure 4.11 (C) was similar to the SEC chromatograms of reaction 4

## Chapter Four Results and Discussion

and 5. The presence of a low molecular weight tail throughout the distributions and tailing in the high molecular weight region was evident. The molecular weight distributions appeared to be narrower than that of reaction 4, but broader than that of reaction 5. This further suggests that termination is not the only reason for the observed broadening in the molecular weight distributions.

For illustrative purposes, the SEC chromatograms for the DRI scaled to conversion are given in Figure 4.12, for reaction 4 and reaction 5. The continuous broadening of the tail in the high molecular weight region, at conversion greater than about 20%, is clearly seen.

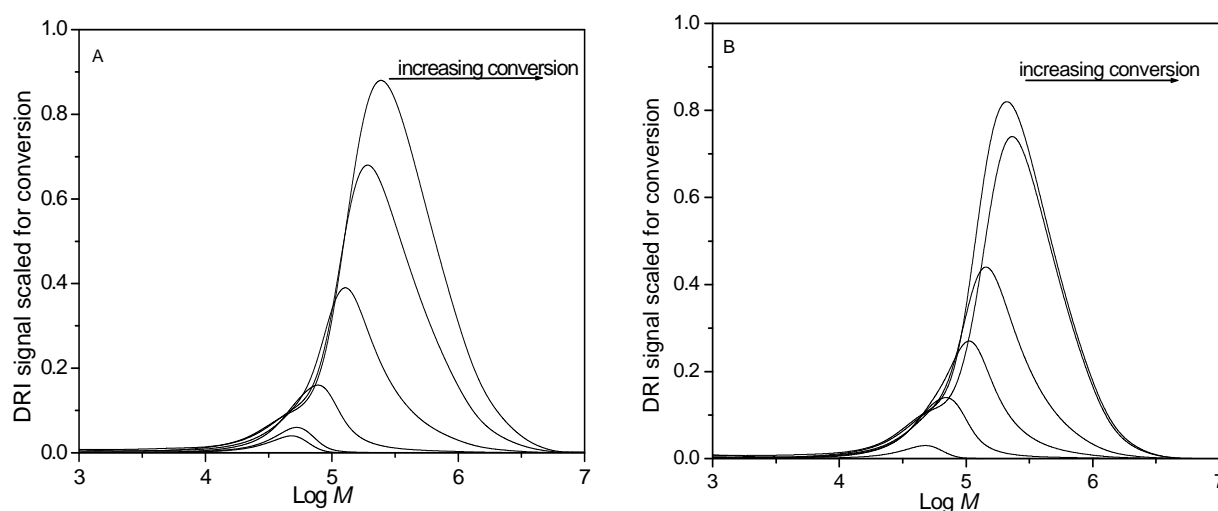


Figure 4.12: DRI signal scaled for conversion for poly(*n*-butyl methacrylate)-*b*-poly(styrene) diblock copolymer in RAFT-mediated miniemulsion polymerization at 75 °C for 2 hours, initiated by AIBN: (A) reaction 4, [AIBN]/[RAFT agent] = 1:2; (B) reaction 5, [AIBN]/[RAFT agent] = 1:10.

The SEC chromatograms displayed in Figure 4.11 show an interesting trend for all three reactions. Significant broadening occurs to high molecular weight at conversions greater than about 20%. It is at this point in Figure 4.10 where a sudden increase in the polydispersity values occurs. Thus, the high molecular weight tail is dominantly responsible for the high PDI values obtained.

## ***Chapter Four Results and Discussion***

---

When changing the initiator concentration of the system, it was expected that bimolecular termination reactions would be reduced (resulting in block copolymers of narrower molecular weight distributions). Not much improvement was seen in the results obtained which indicated that termination reactions are not the sole reason for the observed broadening and high polydispersity values.

In RAFT-mediated miniemulsion systems, inhomogeneity is a factor to be taken into account. Inhomogeneity brings about in the simplest case two scenarios – high RAFT agent concentration and low RAFT agent concentration. *If* we are to assume that the system were inhomogeneous from the start then the RAFT agent will be unevenly distributed among the particles, resulting in particles of high RAFT agent concentration and some of low RAFT agent concentration. *If* the initial mixing is poor from the start, it can be expected that the particles of low RAFT agent concentration will attain a higher conversion and a higher targeted molecular weight more quickly than those particles with a higher RAFT agent concentration. Under such conditions at early conversion, a high molecular weight fraction is expected to be seen in the SEC chromatograms (corresponding to the particles of low RAFT agent concentration). The styrene block (if not much PBMA-RAFT agent is present) will grow faster and should grow fairly quickly to high molecular weight with block extension still occurring. As for the particles of high RAFT agent concentration, the targeted molecular weight will be lower. The initial PBMA block will grow more slowly with styrene, in a controlled manner, with a distribution that does not leave a tail.

The SEC chromatograms in Figure 4.11 show that there is no sign of a high molecular weight tail at low conversion (< 10%), therefore there is probably not much inhomogeneity in the system from the start. At higher conversion (> 20%), a tail in the high molecular weight region develops and shifts towards increasing molecular weight with increasing conversion. This indicates that the character of the system changes at higher conversions.

## ***Chapter Four Results and Discussion***

---

Factors that can cause the system to change character are Ostwald ripening and particle coalescence or coagulation. These processes both affect the particle size distribution and could cause a small change in the RAFT agent concentration inside the particles by changing the monomer concentration or the total amount of monomer or polymer in the particles through the reaction history. It is known that transport processes between the droplets through the water phase can take place in miniemulsion systems and therefore cannot be dismissed (i.e. one-to-one copies of droplets are rarely observed). Monomer transportation is a factor to consider in the miniemulsion systems in this study. This will cause some particles to have different RAFT agent concentration and therefore different particles will have different targeted molecular weights. This could also be one of the reasons for the broadening of the molecular weight distributions and the high polydispersity values obtained so early in the reactions. Furthermore, monomer transportation processes result in broad particle size distributions, which result in different particles having different growth rates (this further complicates the miniemulsion system). Besides molecular diffusion of the dispersed phase, particle coagulation or coalescence is also likely to occur in the system, resulting in a small change in RAFT agent concentration and variation in particle size, as seen in the TEM analysis. Particle coagulation will also result in a loss of small particles and give more large particles in the final product.

In conventional emulsion polymerization and miniemulsion polymerization, two kinetic systems exist: zero-one and non-zero-one. Zero-one kinetics has been reported to model styrene emulsion systems to certain conversions.<sup>26</sup> These two systems can be applied to the miniemulsion system in this study.<sup>27</sup> Transition between a zero-one system and a non-zero-one system has been observed in particles in which the average particle radius varied.<sup>28</sup> The presence of small particles and large particles in the miniemulsion systems in this study should, therefore, be examined. The rates of volume growth of particles (rate of particle volume growth =  $\bar{n} k_p[M]$ ), of different radii were calculated using values shown in Appendix B, and using the appropriate equations in Chapter 2, (Section 2.3) for a simple zero-one system. It was calculated that for the larger particles (radius 60 nm) the rate of volume growth is twice as fast (rate calculated to be  $1600 \text{ s}^{-1}$ ) as the rate of

## Chapter Four Results and Discussion

volume growth in the smaller particles (radius 30 nm, rate of growth calculated to be 800 s<sup>-1</sup>). Therefore, the larger particles deplete monomer faster, and  $\overline{M}_n$  grows twice as fast in these particles as in the small particles. The RAFT agent concentration will also be lower in the larger particles. Furthermore, in the larger particles, the concentration of the polymer may become high (this depends on the monomer transport) and chains will become longer with many chain entanglements. The rate of termination (rate of termination =  $\langle k_t \rangle [P^*]^2$ , where  $[P^*]$  is the propagating radical concentration)<sup>21</sup> in the larger particles is much lower than in the smaller particles (note that it is  $\langle k_t \rangle$  that drops rapidly) and the average number of radicals per particle will become high at higher conversion ( $\bar{n} > 0.5$ ). As for the smaller particles, the chains are short, with little chain entanglement. The rate of termination is fast and  $\bar{n} < 0.5$ . Therefore, in the present system, it is proposed that the small particles follow the zero-one kinetic model and the larger particles, the non-zero-one model. Evidence of the system changing from zero-one (at low conversion) to non-zero-one (high conversion) is provided by the deviation from linearity in the kinetic data, see Figure 4.9, which indicates an increase  $\bar{n}$  or  $N_c$ .

### 4.5.2 Dynamic Light Scattering (DLS)

DLS results for reactions 4, 5 and 6 are tabulated in Table 4.7.

Table 4.7: DLS results for the poly(*n*-butyl methacrylate)-*b*-poly(styrene) diblock copolymers in RAFT-mediated miniemulsion, at 75 °C, initiated by AIBN.

Reaction	Z Average diameter (nm) Before Polymerization	Z Average diameter (nm) After Polymerization	PDI Before Polymerization	PDI After Polymerization
4	78	88	0.157	0.061
5	91	81	0.161	0.094
6	108	81	0.184	0.123

The final particle sizes of the latices were well within the particle range of miniemulsions. DLS showed a monomodal particle size distribution for all the reactions. Narrow PDI values ( $< 0.1$ ) were obtained for reactions 4 and 5 while reaction 6 showed the highest PDI value. The particle size after polymerization for reaction 4 was larger than before polymerization; this is possibly indicative of particle coagulation or possibly

## Chapter Four Results and Discussion

a batch of particles of high swollen radii growing faster. The particles of larger radii dominate in DLS. This result appears to be consistent with the TEM image in Figure 4.13.

### 4.5.3 Transmission Electron Microscopy (TEM)

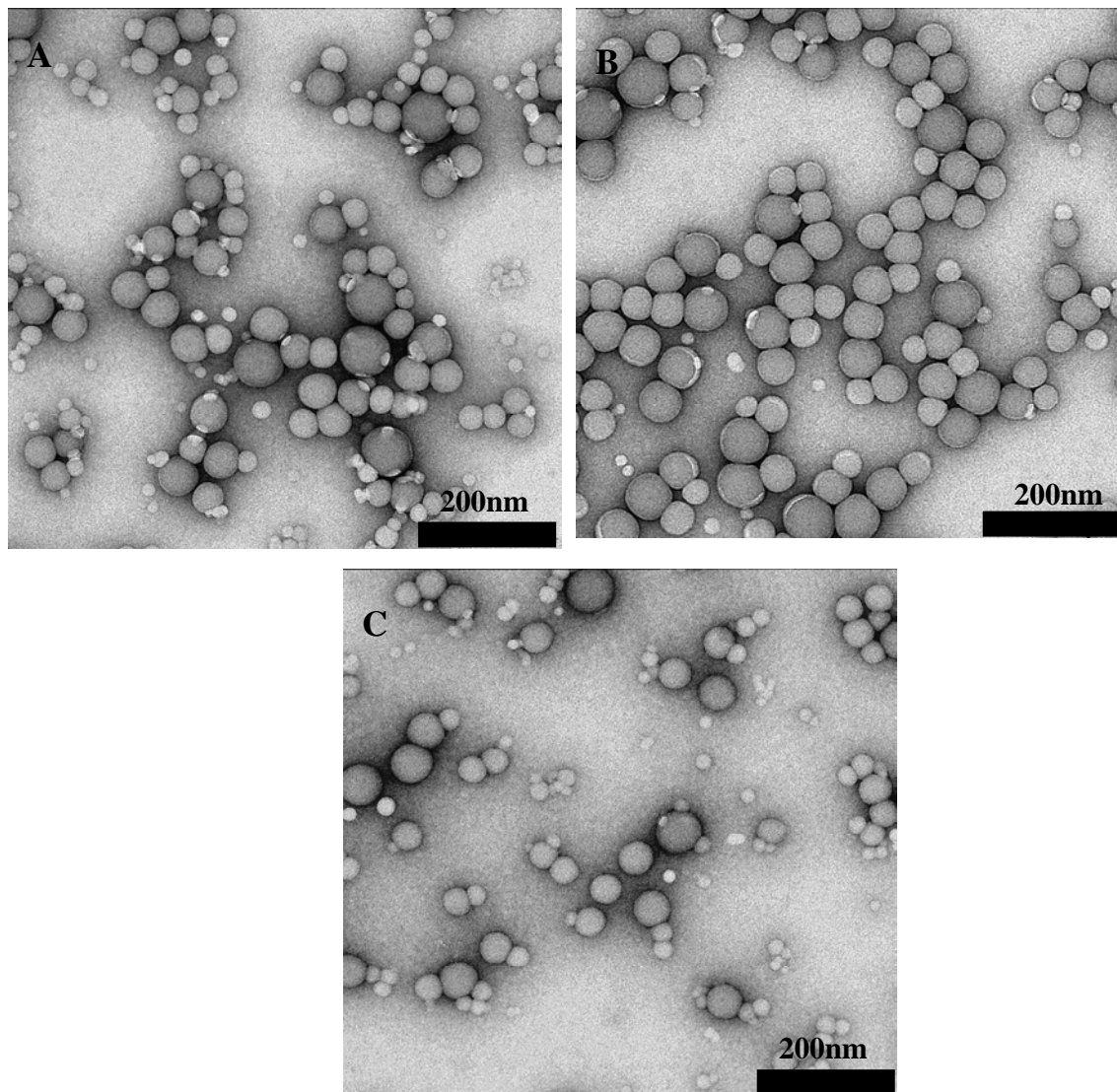


Figure 4.13: TEM images of poly(*n*-butyl methacrylate)-*b*-poly(styrene) latices prepared by RAFT-mediated miniemulsion polymerization at 75 °C for 2 hours, initiated by AIBN. (A) Reaction 4, [AIBN]/[RAFT agent] = 1:2 (B) Reaction 5, [AIBN]/[RAFT agent] = 1:10 (C) Reaction 6, [AIBN]/[RAFT agent] = 1:20.

TEM micrographs of the products of all three reactions are shown in Figure 4.13. The TEM images (A), (B) and (C) were very similar in that a broad distribution of particle



## ***Chapter Four Results and Discussion***

---

sizes was seen, with some particles having apparent acorn-like morphologies. The large particles ranged from 70 – 80 nm and the small particles from 30 – 50 nm. In the TEM images of the products of the three reactions in which different initiator concentrations were used, no trend is seen, which is consistent with other factors such as the quality of the initial dispersion or the particle size distribution in these systems, which are important factors to consider.

The TEM images were further examined by statistically analyzing the TEM particle size data. From the TEM images, the particle diameter of all the particles were measured using Digital Imaging Solutions software package for the TEM images both before polymerization (directly after sonication) and after polymerization. From the particle size statistics obtained, a graph of the particle diameter versus fraction was plotted (see Figure C1, Appendix C). From the graph apparent evidence of secondary particle formation and particle coalescence is illustrated. A shift in the two overlaying curves is seen. For the TEM sample before polymerization, a broad particle size distribution is seen, and the majority of the particles lie within the 30 – 70 nm range. For the TEM sample taken after polymerization, a slightly narrower particle size distribution is seen. The “tail” in the curve that is seen after polymerization, in the particle diameter range 20 – 30 nm, suggests that only a few secondary particles formed. This is consistent with the semilogarithmic plots, Figure 4.9, which could suggest secondary particle formation (increasing  $N_c$ ) at high conversion, although the SEC chromatograms showed no obvious secondary uncontrolled distribution. It is possible that there is an underlying uncontrolled distribution underneath the broad molecular weight distribution, which may then be difficult to detect. From the graph, many of the small particles seem to have disappeared (which could indicate that some droplets were unstable) and more larger particles are present after polymerization. This indicates that particle coalescence occurred in the system. Larger particles coalesce more easily than smaller particles, resulting in more larger particles. The results obtained from the graph suggest that secondary particles and particle coagulation result in a broad particle size distribution. Due to the initial broad particle size distribution or the broad particle size distribution that develops during the reaction different particles will have different targeted molecular weights, provided that monomer migration is occurring. This results in broad molecular weight distributions and

## ***Chapter Four Results and Discussion***

---

high polydispersity values. The broadening in the molecular weight distributions was evident in the SEC results obtained.

### **4.5.4 Conclusions**

In all three RAFT reactions, poly(*n*-butyl methacrylate)-*b*-poly(styrene) block copolymers were successfully synthesized. All three systems showed controlled and living behavior despite the high polydispersity values ( $> 2$ ) and broad molecular weight distributions obtained. It was expected that by varying the AIBN/RAFT agent concentration ratio that there would be an improvement in terms of the molecular weight distributions and polydispersity values. Results indicated, however, that the high polydispersity obtained was not related to the initiator concentration. Furthermore, the reason for the broadening of the molecular weight distribution and the steep increase in the polydispersity values was not only associated with radical-radical termination reactions, as repeatedly reported in the literature.<sup>2,4,29</sup> A thorough investigation of the kinetic results, SEC results and TEM results obtained suggest that monomer transportation and coagulation processes are also important factors to consider in the miniemulsion system. These processes affect both the concentration of RAFT agent inside the particles and the particle size distribution which explains the observed broadening of the molecular weight distributions in the systems in this study. Furthermore, in the system a transition in the two kinetic systems in the different particles of varying radii can also explain the observed broadening of the molecular weight distributions and high polydispersity values in the system. The possibility of secondary particle formation occurring in the system emerged from the kinetic data and TEM images, but this was not supported nor dismissed by the SEC results obtained.

### **4.6 Oil-soluble versus water-soluble initiators in RAFT-mediated miniemulsion systems**

In miniemulsion polymerization, oil-soluble and water-soluble initiators can be used.<sup>1</sup> The location where initiator fragmentation occurs depends on the type of initiator used. This will influence the radical concentration in the different phases of the miniemulsion system. The type of initiator therefore has an effect on the nucleation mechanism.

## Chapter Four Results and Discussion

---

The chemical structures of the two different initiators used in this study are seen in Figure 4.14.

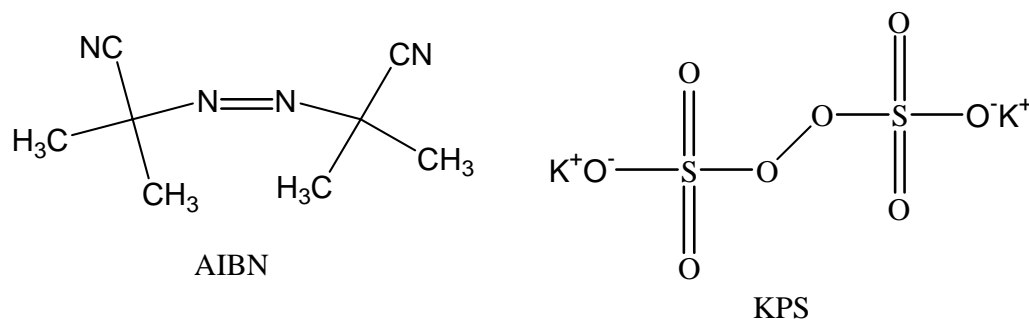


Figure 4.14: Chemical structures of the oil-soluble initiator, AIBN (2,2'-azobis(isobutyronitrile)) and the water-soluble initiator KPS (potassium peroxydisulfate).

The oil-soluble initiator AIBN was originally chosen for the use in this study to attempt to reduce the possibility of unfavorable nucleation mechanisms (mentioned in Chapter 2) from occurring. In addition other researchers have pointed out that organic phase initiation also suppresses secondary particle formation and the possibility of transport of the RAFT agent into new particles.<sup>4</sup>

The effect of a water-soluble initiator, KPS, on the RAFT-mediated miniemulsion system was also investigated. The use of a water-soluble initiator differs from the use of an oil-soluble initiator in that the initiator is dissolved in the aqueous phase and the polymerization is initiated from this phase via an entry process.<sup>22,30</sup>

### 4.6.1 Chain extension of initial poly(*n*-butyl methacrylate) block with styrene using water-soluble KPS initiator

The effect of the water-soluble initiator was evaluated by synthesizing poly(*n*-butyl methacrylate)-*b*-poly(styrene) under the same reaction conditions used in Section 4.5, reaction 5. It must be noted that for reaction 7, the initial PBMA block that was used came from batch 3 of the bulk polymerization ( $\overline{M}_n = 39\,400 \text{ gmol}^{-1}$ , PDI 1.19). In reaction 5, where AIBN initiator was used, the initial PBMA block came from batch 2 ( $\overline{M}_n = 39\,300 \text{ gmol}^{-1}$ , PDI 1.18). A polymerization using an initiator/RAFT agent

## Chapter Four Results and Discussion

concentration ratio of 1:10 (as in reaction 5) was carried out in order to minimize the probability of side reactions and termination. Details of the reaction formulation can be seen in Table 3.2, Chapter 3.

### 4.6.2 Results

Table 4.8 summarizes the final results obtained for the AB diblock copolymer.

Table 4.8: Characteristics of the polymer formed in the final latices obtained for the chain extension reactions in RAFT-mediated miniemulsion polymerization at 75 °C for 2 hours initiated by KPS.

Reaction	Monomer	Polymeric RAFT agent	KPS/Polymeric-RAFT agent (mol ratio)	Conversion (%)	$\bar{M}_{n,theo}$ gmol <sup>-1</sup>	$\bar{M}_{n,SEC}$ gmol <sup>-1</sup>	PDI
7	Sty	Batch 3	1:10	87	216000	260000	2.5

$\bar{M}_{n,theo}$  was calculated using equation 4.1 and the  $\bar{M}_n$  value obtained from SEC is based on PSt standards.

In Figure 4.15, high conversion (87%) was obtained within two hours. At this point the reaction was stopped due to the high viscosity of the reaction mixture. There appeared to be no induction period.

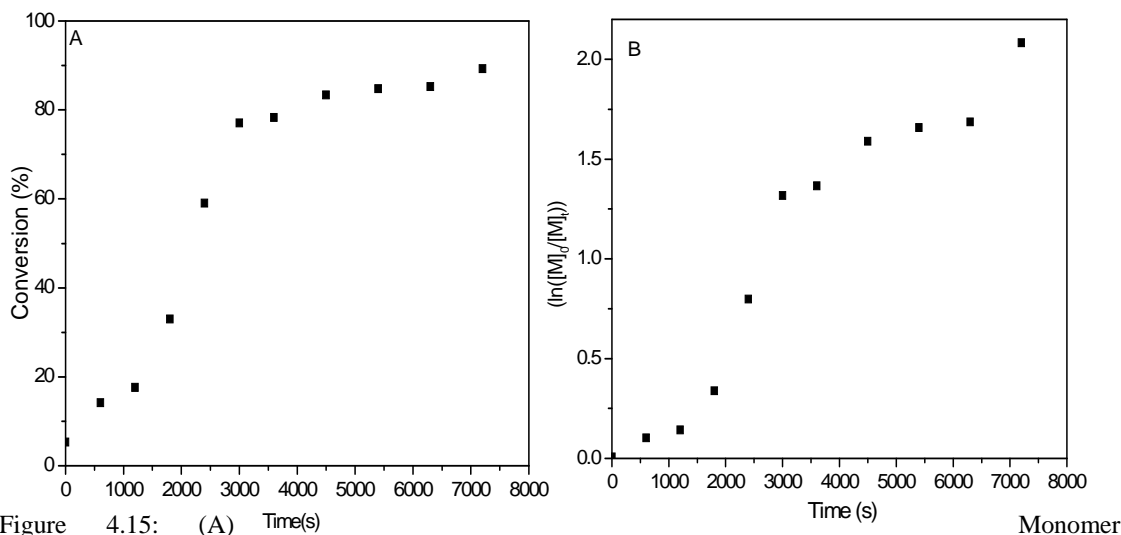


Figure 4.15: (A) Conversion (%) versus reaction time for the synthesis of poly(*n*-butyl methacrylate)-*b*-poly(styrene) in miniemulsion polymerization at 75 °C for 2 hours, initiated by KPS. (B) Semilogarithmic plot of monomer conversion versus reaction time for the synthesis of poly(*n*-butyl methacrylate)-*b*-poly(styrene) in miniemulsion polymerization at 75 °C for 2 hours, initiated by KPS.

## ***Chapter Four Results and Discussion***

---

Figure 4.15 (B) shows a steep acceleration in the polymerization rate from about 1200 – 1800 s and after 3000 s, a decrease in the rate of polymerization is seen which was not seen in previous reactions in section 4.5. The increase in the polymerization rate could be indicative of  $\bar{n}$  and/or  $N_c$  increasing as seen previously in section 4.5 (a change from zero-one system towards pseudo bulk, or secondary particle formation). The curve did not display a linear relationship. At such high conversion, the chains within the particles are long and entangled and move slowly. As monomer is consumed, the rate of termination decreases and  $\bar{n}$  increases. This can lead to an increase in the rate of polymerization, resulting in the Trommsdorff effect.<sup>27</sup>

Figure 4.16 shows a linear increase in  $\bar{M}_n$  with conversion. The predicted  $\bar{M}_n$  values and the SEC  $\bar{M}_n$  values agree quite well at low fractional conversion, indicating that the miniemulsion was well controlled. As the reaction progresses and higher fractional conversion is reached (> 80%), a deviation in the SEC  $\bar{M}_n$  from the predicted  $\bar{M}_n$  values is seen. The SEC  $\bar{M}_n$  values become increasingly larger than the predicted  $\bar{M}_n$  values. This suggests that some chains have polymerized conventionally (possibly secondary particles) however the kinetic data showed that the rate is decreasing at these high conversions which could suggest other factors such as coagulation could possibly explain the deviation in the SEC  $\bar{M}_n$  values. The polydispersity increased throughout the polymerization, as seen in the AIBN-initiated systems, leveling off at 2.5.

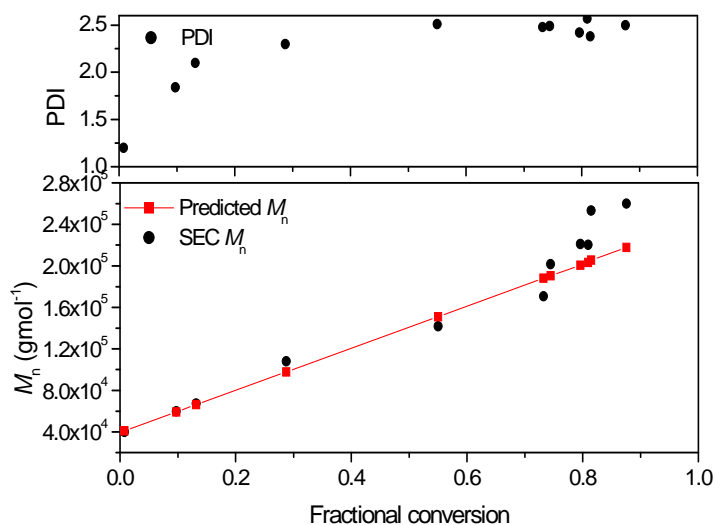


Figure 4.16: Evolution of  $\bar{M}_n$  and PDI for poly(*n*-butyl methacrylate)-*b*-poly(styrene) diblock copolymer in RAFT-mediated miniemulsion polymerization, at 75 °C for 2 hours, initiated by KPS.

The SEC chromatogram shown in Figure 4.17, indicates the living behavior of the system by the shift of the molecular weight distribution with increasing conversion.

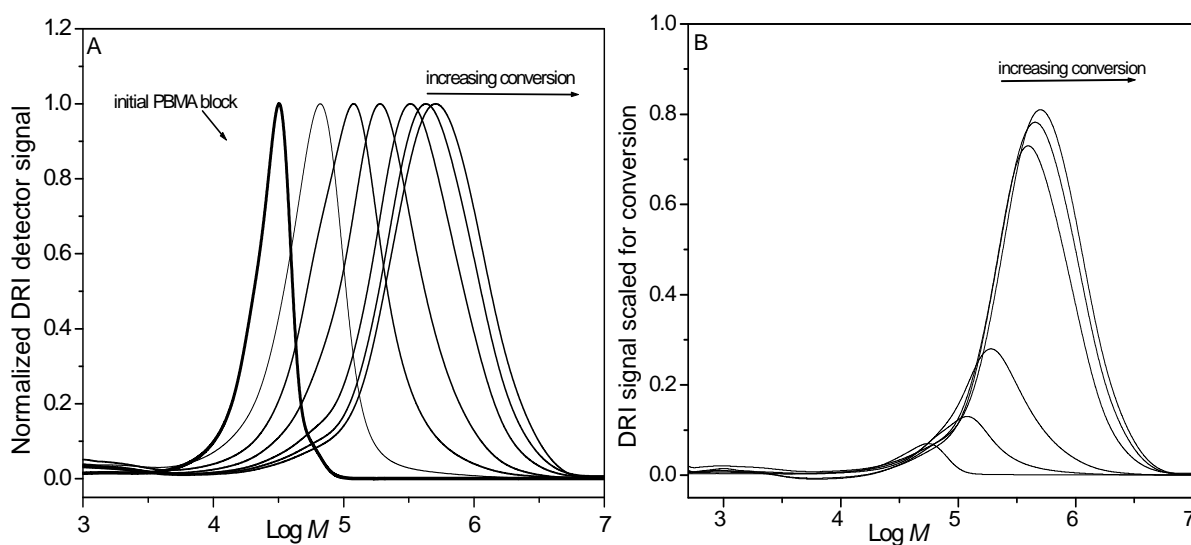


Figure 4.17: (A) Normalized SEC chromatogram for poly(*n*-butyl methacrylate)-*b*-poly(styrene) in RAFT-mediated miniemulsion, at 75 °C, initiated by KPS.

(B) DRI signal scaled for conversion for poly(*n*-butyl methacrylate)-*b*-poly(styrene) in RAFT-mediated miniemulsion, at 75 °C, initiated by KPS.

## ***Chapter Four Results and Discussion***

---

In the KPS-initiated system one finds not such a detectable low molecular weight tail (due to short PSt chains) as in the AIBN-initiated system. The Maxwell-Morrison model for radical entry could explain why it is unlikely for styrene homopolymer to form in this system.<sup>30</sup> According to this model, aqueous phase radicals must propagate to a length at which they become surface-active. This critical degree of polymerization is denoted as  $z$ . For styrene with a persulfate initiator, the value for  $z$  is 2 – 3.<sup>31</sup> The surface-active species enter the particles where they could encounter a RAFT agent. The intermediate radical fragments to give Z-X ( $z$ -mer) and PBMA radicals. The PBMA radicals are mediated to from a diblock. The Z-X species can be reactivated by PSt radical ends, at which point it is speculated that the  $z$ -mer might re-exit or other fates can occur.<sup>31</sup> In the SEC chromatogram, tailing in the high molecular weight distribution was already seen at conversions greater than 10% (clearly seen in Figure 4.17 (B)). Possible reasons for the observed broadening were discussed in Section 4.5 and are applicable to this system.

Research carried out by Butté *et al.*<sup>2</sup> on the synthesis of methyl methacrylate-styrene block copolymers in miniemulsion initiated by KPS, using an oligomeric RAFT agent, showed broadening in the high molecular weight region. This was proposed to be related to homogeneous nucleation. Similar results were observed by de Brouwer *et al.*<sup>4</sup> Chern and Liou<sup>32</sup> studied the effect of the type of initiator on the extent of homogeneous nucleation using AIBN (oil-soluble initiator), and KPS (water-soluble initiator) in miniemulsion polymerization. Results showed that AIBN promotes nucleation in the droplets while homogeneous nucleation predominates in the KPS system. Secondary particles are formed when the  $z$ -mers continue to propagate in the aqueous phase and forming  $j$ -mers. This can lead to homogeneous nucleation, resulting in secondary particles, which has an effect on both the molecular weight distribution and the polydispersity of the system. This could be an additional factor that contributed to the broadening, high polydispersity and possibly loss in control (at high conversion) observed in this system. This is supported by the TEM results shown in Figure 4.18, however SEC results showed no sign of a secondary uncontrolled distribution. A way that might prove secondary particle formation would be to statistically analyze the TEM data as in Section 4.5. However, due to a lack of statistical data, this could not be carried out

## ***Chapter Four Results and Discussion***

---

accurately and definite conclusions could not be drawn from the available data. As this is not the main objective of the study, proving secondary particle formation in the KPS-initiated system (as in Section 4.5) can be recommended as future work.

### **4.6.3 Dynamic Light Scattering (DLS)**

DLS results for reaction 7 are summarized in Table 4.9. The DLS experiments after polymerization showed a monomodal, relatively narrow particle size distribution and a low PDI value of 0.075.

Table 4.9: DLS results for the poly(*n*-butyl methacrylate)-*b*-poly(styrene) diblock copolymer in RAFT-mediated miniemulsion, at 75 °C, initiated by KPS.

<b>Reaction</b>	<b>Z Average diameter (nm) Before Polymerization</b>	<b>Z Average diameter (nm) After Polymerization</b>	<b>PDI Before Polymerization</b>	<b>PDI After Polymerization</b>
7	122	88	0.305	0.075

### **4.6.4 Transmission Electron Microscopy (TEM)**

The TEM micrograph in Figure 4.18 shows the presence of particles with different particle diameters and that small particles (20 – 30 nm) dominate. Larger particles in the size range of 70 – 85 nm were also present.



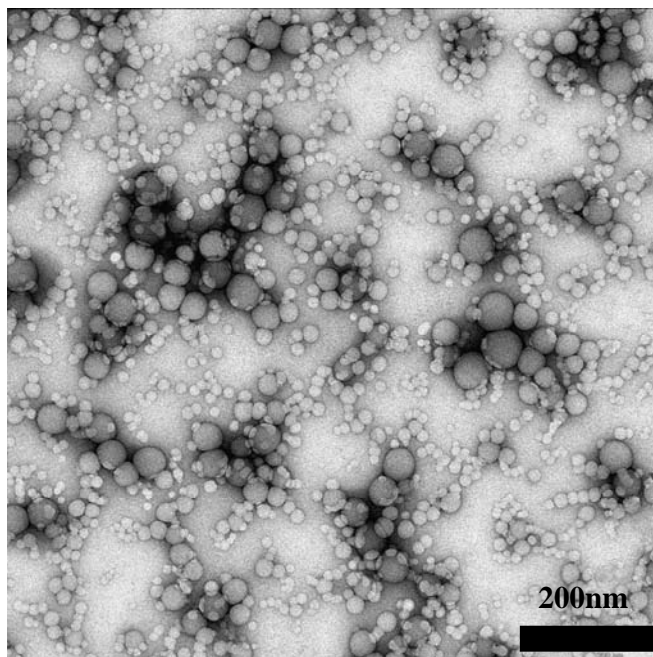


Figure 4.18: TEM image of poly(*n*-butyl methacrylate)-*b*-poly(styrene) latex prepared by RAFT-mediated miniemulsion polymerization, initiated by KPS.

The TEM micrograph shows overlapping of the particles, which is probably related to the concentration of the latex sample analyzed. A broad particle size distribution is seen in the TEM image. The TEM results obtained correspond to the DLS results for the large particles, since the small particles are difficult to observe in the DLS when large particles are present. A large population of the small particles appears to be secondary particles, possibly due to secondary nucleation mechanisms occurring, leading to a new distribution of particles. However, in the SEC chromatograms there is no evidence of a secondary uncontrolled distribution. The large number of small particles seen is consistent with secondary nucleation, which would further explain the increasing polymerization rate seen in Figure 4.15. However, in Figure 4.16, loss in control was seen at high conversion, which could suggest late secondary nucleation but this was not suggested by the rate data in Figure 4.15.

#### **4.6.5 Conclusions**

The chain extension process of the initial PBMA block with styrene in miniemulsion was successfully carried out. The system showed living behavior despite the high

## ***Chapter Four Results and Discussion***

---

polydispersity values. Loss in control at higher conversion was seen by the deviation in the predicted  $\overline{M}_n$  and SEC  $\overline{M}_n$  values. Kinetic data suggested that either  $\overline{n}$  and/or  $N_c$  increased throughout the reaction. This is consistent with the system changing from zero-one to non-zero-one behavior at higher conversions. Furthermore, an increase in  $N_c$  could be indicative of secondary particle formation occurring. The SEC chromatogram showed broad molecular weight distributions with a tail that shifted with increasing conversion, as seen in previous AIBN-initiated systems. The possible reasons for this occurring were discussed in detail in Section 4.4.4. They are also applicable to the KPS-initiated system. In addition, for the KPS-initiated miniemulsion, the initiator fragmentation occurs in the aqueous phase, therefore the concentration of the aqueous phase radicals is high. This results in a predominance of homogeneous nucleation over droplet nucleation (homogeneous nucleation is more probable in the KPS-initiated system than in the AIBN-initiated system), which would further result in secondary particle formation and an increase in  $N_c$ , causing high polydispersity values and broadening of the molecular weight distributions.

### **4.6.6 Overall conclusions**

In Section 4.5 and Section 4.6 the behavior of the RAFT-mediated miniemulsion systems was more thoroughly researched. The effect of the initiator/RAFT agent concentration ratio, including the effect of the type of initiator on the system, was investigated.

Living/controlled behavior was observed in all of the RAFT-mediated miniemulsion systems for the high molecular weight diblock copolymers synthesized. However the following common behavioral pattern was evident:

- I. Increase in the rate of polymerization at high conversion
- II. Steep increase in the polydispersity during polymerization and high polydispersity values
- III. Significant broadening in the molecular weight distributions

Based on the results obtained, inhomogeneity, monomer transport and particle coalescence are suggested to be one of the reasons for the observed behavior in these

mini-emulsion systems. Furthermore, the kinetic data suggests that a transition in kinetic behavior (zero-one to non-zero-one) is occurring in the system during the polymerization. At low conversion, the system follows zero-one kinetics and at higher conversion non-zero-one kinetics. The small particles are expected to obey zero-one kinetics and larger particles, non-zero-one kinetics. The kinetic data also indicated the possibility of an increase in the particle number, indicative of secondary particle formation, which is apparent in the TEM images and proven by the statistical data obtained from the TEM images for the AIBN-initiated systems. The above-mentioned is proposed to be the dominant reason for the observed behavior described in points I, II, and III (page 114) in the systems studied.

### **4.7 Chain extension of initial poly(*n*-butyl methacrylate) block of lower molecular weight with styrene in mini-emulsion**

From the results obtained in Section 4.5 and 4.6, one of the factors that should be considered and associated with the RAFT-mediated mini-emulsion systems is the broad particle distribution of the initial dispersion.

In an attempt to improve the particle size distribution and the quality of the initial dispersion, a lower molecular weight initial block was used. A lower molecular weight initial PBMA block has shorter chains, less chain entanglement and lower viscosity as opposed to a higher molecular weight block (longer chains, more chain entanglements, higher viscosity). Therefore, after the sonication process, the particle size distribution of the initial dispersion might be expected to be more monodisperse (less energy required to break up the particles that contain shorter chains than in previous cases). Therefore, the effect of changing the molecular weight of the system on the molecular weight distributions and the polydispersity was investigated.

The same experimental conditions were used as for the mini-emulsion polymerizations carried out in Section 4.5. In this case, the starting PBMA block had a molecular weight of 23 000 g mol<sup>-1</sup> as opposed to 39 000 g mol<sup>-1</sup>, and a lower molecular weight of 1×10<sup>5</sup>

## Chapter Four Results and Discussion

$\text{gmol}^{-1}$  as opposed to  $2 \times 10^5 \text{ gmol}^{-1}$  was targeted in the miniemulsion step. The reaction formulation is given in Chapter 3, Table 3.2.

### 4.7.1 Results

Results obtained for reaction 7 are summarized in Table 4.10.

Table 4.10: Characteristics of the polymer formed in the final latices obtained for the chain extension reactions in RAFT-mediated miniemulsion polymerization at  $75^\circ\text{C}$  for 3 hours, initiated by AIBN.

Reaction	Monomer	Polymeric RAFT agent	Conversion (%)	$\bar{M}_{n,theo}^*$ $\text{gmol}^{-1}$	$\bar{M}_{n,SEC}^*$ $\text{gmol}^{-1}$	PDI
8	Sty	Batch 5	94	97000	78100	1.35

\*  $\bar{M}_{n,theo}$  was calculated using equation 4.1 and the  $\bar{M}_n$  value obtained from SEC is based on PSt standards.

High conversion (94%) was obtained after 3 hours. At this point the reaction was immediately stopped due to the high viscosity of the reaction mixture. This observation was seen in previous reactions described in Sections 4.5 and 4.6. This is considered to be unusual and is a common problem or occurrence in these systems.

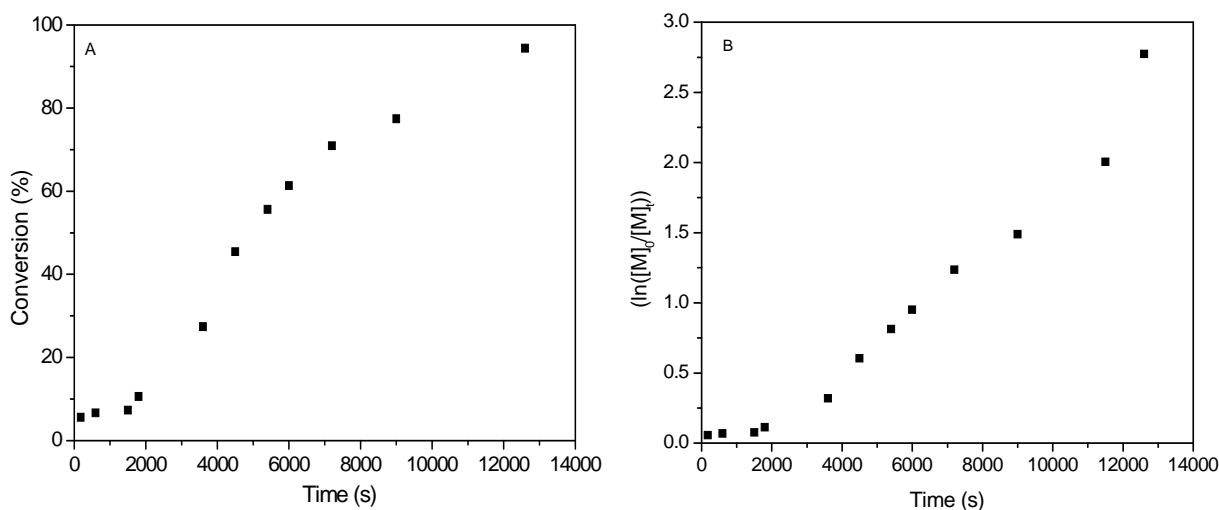


Figure 4.19: (A) Monomer conversion versus reaction time for the synthesis of poly(*n*-butyl methacrylate)-*b*-poly(styrene) in RAFT-mediated miniemulsion polymerization at  $75^\circ\text{C}$  for 3 hours, initiated by AIBN. (B) Semilogarithmic plot of monomer conversion versus reaction time for the synthesis of poly(*n*-butyl methacrylate)-*b*-poly(styrene) in RAFT-mediated miniemulsion polymerization at  $75^\circ\text{C}$  for 3 hours, initiated by AIBN.

## Chapter Four Results and Discussion

As before, an induction period was seen in the early stages of the polymerization followed by an increase in the reaction rate. A roughly linear increase in  $\ln([M]_0/[M]_t)$  was seen up to 60% conversion (indicating that  $\bar{n}$  and  $N_c$  are constant). At higher conversion, deviation from linearity and an increase in polymerization rate was seen, which is indicative of either  $\bar{n}$  and/or  $N_c$  increasing. This behavior was seen in previously described systems in Section 4.5 and 4.6. The sharp increase in the rate of polymerization as monomer conversion increases could indicate the Trommsdorff effect occurring at higher conversion and also a breakdown of zero-one behavior.

The living characteristics of the system are clearly seen in Figure 4.20 by the linear increase in  $\bar{M}_n$  with increasing conversion.

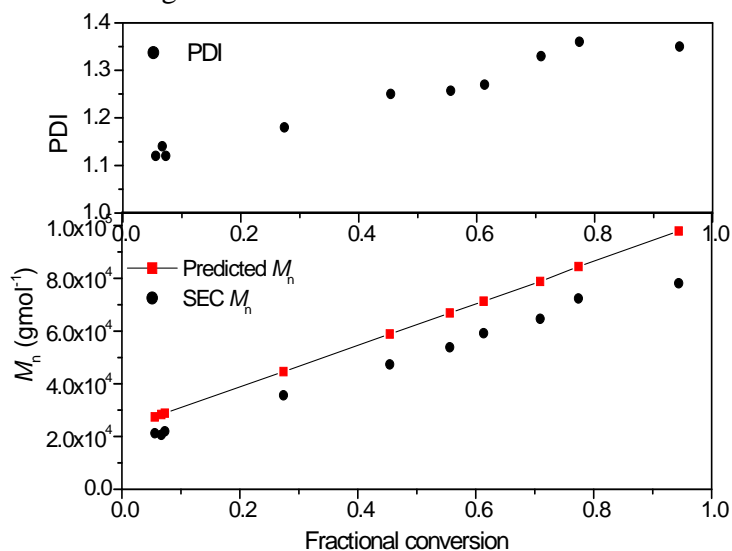


Figure 4.20: Evolution of  $\bar{M}_n$  and PDI for poly(*n*-butyl methacrylate)-*b*-poly(styrene) in RAFT-mediated miniemulsion polymerization at 75 °C for 3 hours, initiated by AIBN using PBMA-RAFT agent batch 5.

From the predicted  $\bar{M}_n$  versus SEC  $\bar{M}_n$  graph, Figure 4.20, one finds that the SEC  $\bar{M}_n$  values were slightly lower than those of the predicted  $\bar{M}_n$  values. The PDI started at 1.12 (initial block) and increased, reaching a final PDI value of 1.35. The polydispersity values were well below the benchmark of 1.5 for controlled/living polymerization. This indicated that good control was achieved in the synthesis of the diblock copolymer. In the

## Chapter Four Results and Discussion

systems where a higher molecular weight starting PBMA block was used (Section 4.5 and Section 4.6), the PDI values increased significantly in the early and middle stages of the polymerization, then stabilizing at PDI values between 2 and 2.5. This is in sharp contrast to the results obtained in the system where a lower initial block molecular weight and a lower targeted molecular weight diblock copolymer.

Figure 4.21 illustrates the SEC results obtained for the chain extension reaction using a lower molecular weight starting PBMA block. The initial PBMA block is indicated by a bold line.

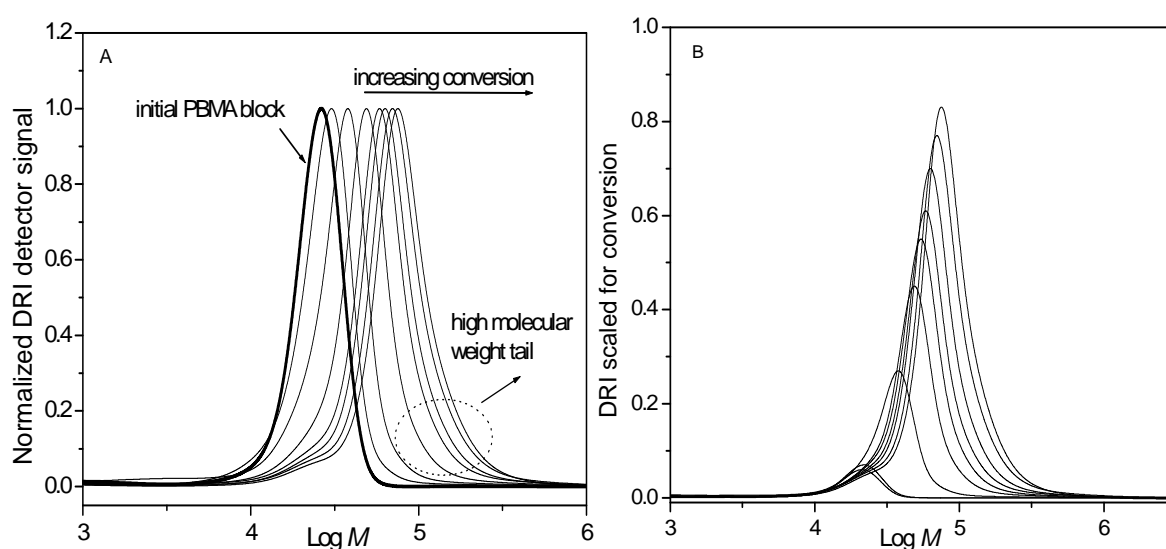


Figure 4.21: (A) Normalized SEC chromatograms for the chain extension of the initial PBMA block with styrene in RAFT-mediated miniemulsion polymerization at 75 °C initiated by AIBN, using PBMA-RAFT agent batch 5. (B) DRI signal scaled for conversion for poly(*n*-butyl methacrylate)-*b*-poly(styrene) in RAFT-mediated miniemulsion, at 75 °C, initiated by AIBN.

A shift towards increasing molecular weight with increasing conversion indicated the transformation of the initial PBMA block into a poly(*n*-butyl methacrylate)-*b*-poly(styrene) diblock copolymer. It was also evident that not all of the chains from the initial block underwent chain extension, as the initial PBMA block contains some terminated (inactive) chains. The low molecular weight tail was also attributed to PSt homopolymer originating from initiator-derived chains which should disappear as conversion increases, as observed. The molecular weight distributions were narrow with a

## ***Chapter Four Results and Discussion***

---

slight high molecular weight tail appearing in the high molecular weight region (indicated by the circle on the chromatograms). Slight broadening occurred at conversions higher than 20% (seen in Figure 4.21 (B)). It is at this point where the polydispersity values increased before stabilizing at about 1.35. However, in comparison to the system where a higher initial molecular weight PBMA block was used, the broadening observed (which was the dominant reason for the high polydispersity values obtained) in this case was not as prominent. A definite improvement is evident in the system. The fact that the final molecular weight of the diblock copolymer in this system was lower than that of previously described system could also be a possible reason for the improved results.

Figure 4.21 (B) illustrated the living nature of the system by the steady increase in the molecular weight as a function of conversion. In comparison to the RAFT miniemulsion system in Section 4.5 Figure 4.12, the presence of a tail in the high molecular weight distribution is not as prominent in the system where the initial block of lower molecular weight was used.

The RI-UV overlay of the final latex sample is displayed in Figure 4.22. In order to make a valid UV-RI comparison the UV 320 nm signal was modified as before (described in section 4.3). The UV-RI overlay indicated that most of the chains contained the thiocarbonyl-thio active end group. A low molecular weight tail as a result of inactive chains was evident. As expected, there was no UV 320 nm absorbance in the low molecular weight tail. These chains do not possess the dithioester moiety; they are dead chains that formed during the bulk polymerization step and were unable to be reinitiated in the miniemulsion step (as seen before). The low molecular weight chains could also contain PSt chains (initiator-derived chains). The strong UV 320 nm absorbance in the high molecular weight region could be due to baseline problems but is more likely due to the molecular weight being high and each styrene unit also giving some signal. The UV 254 nm signal closely matches the main distribution, indicating that styrene is incorporated in the final diblock copolymer.

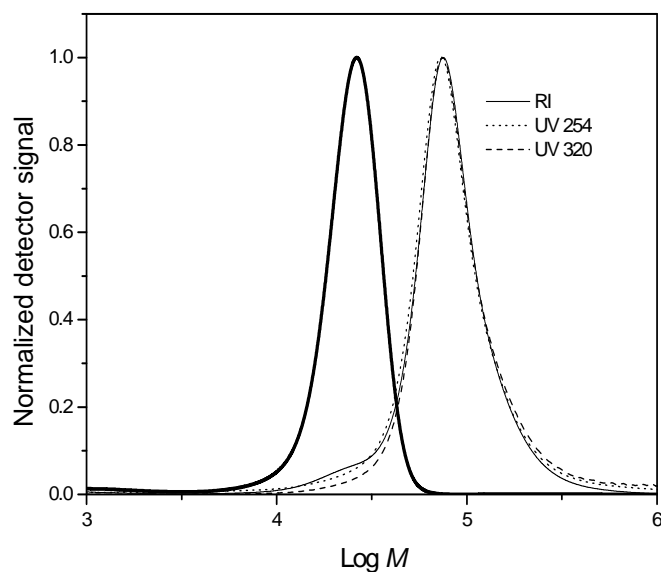


Figure 4.22: UV and RI overlay of the chain extension of initial poly(*n*-butyl methacrylate) block with styrene in miniemulsion at 75 °C initiated by AIBN using PBMA-RAFT agent batch 5. The RI detector signal for the initial PBMA block is also included (bold line).

#### 4.7.2 Dynamic Light Scattering (DLS)

DLS results are tabulated in Table 4.11.

Table 4.11: DLS results for the poly(*n*-butyl methacrylate)-*b*-poly(styrene) diblock copolymer in RAFT-mediated miniemulsion polymerization at 75 °C for 3 hours, initiated by AIBN.

<b>Reaction</b>	<b>Z Average diameter(nm) Before Polymerization</b>	<b>Z Average diameter(nm) After Polymerization</b>	<b>PDI Before Polymerization</b>	<b>PDI After Polymerization</b>
8	91	81	0.123	0.136

The DLS distribution graphs for both before and after polymerization are illustrated in Figure 4.23. The apparent shift in the distribution graph after polymerization towards smaller particle size is seen in the distribution graph and could indicate new particle formation which is consistent with the TEM images in Figure 4.24. There also appears to be a loss of some larger particles.



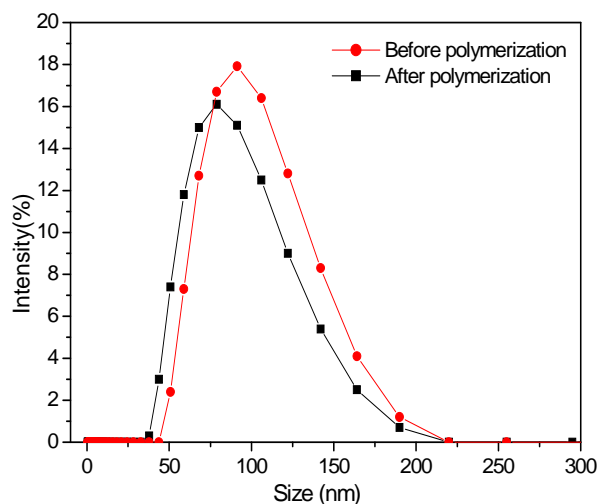


Figure 4.23: DLS size distribution graph for poly(*n*-butyl methacrylate)-*b*-poly(styrene) diblock copolymer in RAFT-mediated miniemulsion polymerization at 75 °C for 3 hours, initiated by AIBN.

### 4.7.3 Transmission Electron Microscopy (TEM)

The TEM micrographs of poly(*n*-butyl methacrylate)-*b*-poly(styrene) synthesized from PBMA end-capped with the RAFT agent functionality are shown in Figure 4.24. The TEM image (A), before polymerization (directly after sonication), presented the first block “cores”. The particle sizes ranged from 30 – 50 nm. In the TEM image (B), taken after polymerization, a non-uniform particle size distribution is seen. A few large particles, 50 – 60 nm in size, and slightly smaller particles, 25 – 30 nm, are seen. The overlapping of particles, resulting in varying particle size distributions, was seen in the TEM image (B). The broad particle size distribution is also seen in these TEM images as seen in the TEM images in Section 4.5. The very small particles are probably secondary particles. The TEM image (B) for the final latex appeared to be similar to the images shown in Section 4.5 (for the AIBN-initiated systems) where these small particles were also seen in the TEM images and in addition, secondary particle formation proven by statistically analyzing the TEM data.

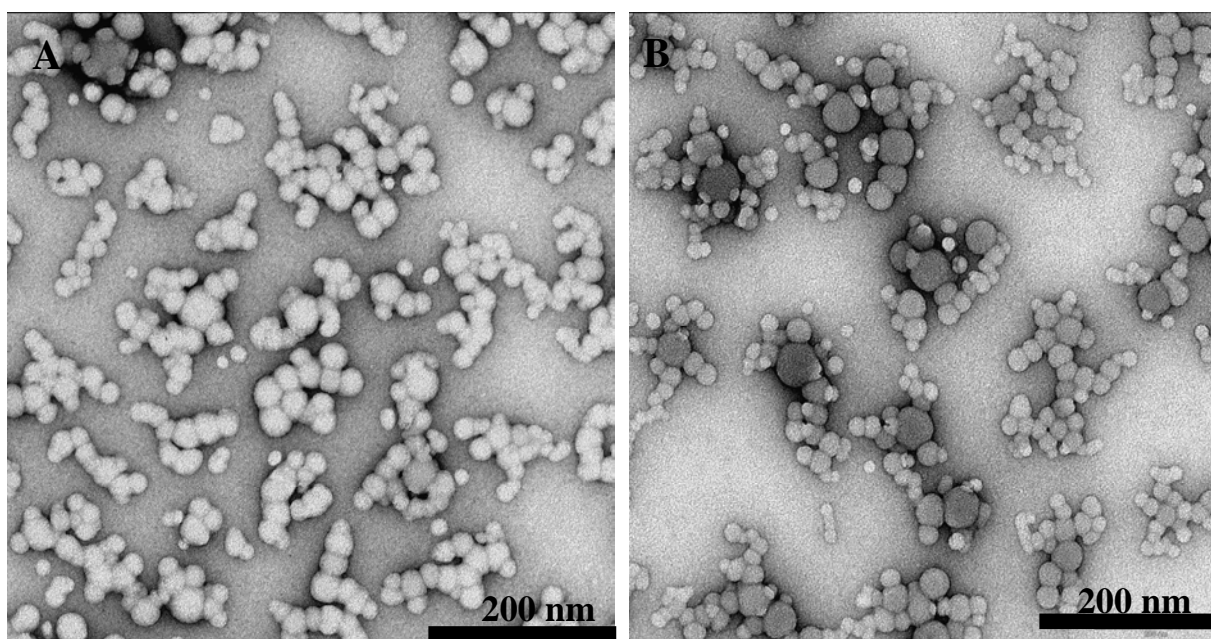


Figure 4.24: TEM images of poly(*n*-butyl methacrylate)-*b*-poly(styrene) latex prepared by RAFT-mediated miniemulsion polymerization at 75 °C for 3 hours, initiated by AIBN (A) before polymerization (B) after polymerization.

#### **4.7.4 Conclusions**

Diblock copolymers containing a lower molecular weight starting block (as to the diblock copolymers in sections 4.5 and 4.6) were successfully synthesized via the two-step process. The system showed living characteristics as indicated by the chain extension of the initial block synthesized in bulk into a diblock copolymer in miniemulsion.

The common behavioral pattern as seen in Section 4.5 and 4.6 was also evident in the system where the initial PBMA block of lower molecular weight was used, and a lower molecular weight diblock copolymer was synthesized. Kinetic results obtained still indicated an increase in the rate of polymerization at high conversion. PDI values steadily increased during the polymerization, but remained well below the benchmark of 1.5. The SEC chromatograms indicated the presence of a low molecular weight shoulder and slight broadening in the high molecular weight region. However, narrow molecular weight distribution and low polydispersity values were obtained ( $< 1.4$ ).

## ***Chapter Four Results and Discussion***

---

A possible reason for the improvement in the polydispersity and molecular weight distributions could be attributed to the lower starting PBMA block used in the miniemulsion system, although there may be other factors. Since the PBMA-RAFT agent chains are much shorter with less chain entanglements (compared to the PBMA-RAFT agents used in Section 4.5 and 4.6), the particles will be easier to break up during the sonication process. This could improve the particle size distribution and quality of the initial dispersion. This might be expected to result in less broadening in the molecular weight distribution, which will further improve the polydispersity of the system. Therefore, the initial dispersion and particle size distribution are important factors to consider in the system where lower molecular weight diblock copolymers were synthesized.

In addition, the diblock copolymer synthesized was of lower molecular weight compared to the diblocks synthesized in Section 4.5 and 4.6. This could indicate that the PDI is dependent on the targeted molecular weight. This has been reported in the literature.<sup>17</sup>

### **4.7.5 Overall conclusions**

The primary objective laid out in Chapter 1, section 1.4, on synthesizing diblock copolymers of high molecular weight via the two-step methodology illustrated in Chapter 3, Scheme 3.6, was achieved. Reactivation of the initial PBMA block with styrene in miniemulsion was successfully carried out. The majority of the chains were reinitiated in the chain extension step and a strong diblock component was seen in the SEC results obtained. Furthermore, all the RAFT-mediated miniemulsion polymerizations exhibited living/controlled characteristics.

In an attempt to synthesize diblock copolymers of narrow molecular weight via the two-step process, the RAFT-mediated miniemulsion systems were more thoroughly investigated. The thorough investigation in the miniemulsion systems lead to the establishment of possible reasons for the observed behavior in these systems. A detailed investigation of the kinetic results, SEC results and TEM results obtained for the AIBN-initiated systems and KPS-initiated system suggest that monomer transportation and

## ***Chapter Four Results and Discussion***

---

coagulation processes are important factors to consider in miniemulsion polymerization. An important observation made during the study was the broad particle size distribution seen before the polymerization and developing during the polymerization. This implies that Ostwald ripening and coagulation probably occur in these systems and can therefore not be neglected. Monomer transportation results in a broad particle size distribution which then further results in different particles having different growth rates. The different particle growth rates in addition to the complex radical movement already associated with the RAFT-mediated miniemulsion systems, further complicates the miniemulsion systems presented in this study.

A mathematical model based on a simple zero-one system was also established for the RAFT-mediated miniemulsion systems in this study. It is suggested that a transition in the two kinetic systems in the different particles of varying radii can also explain the observed broadening of the molecular weight distributions and high polydispersity values in these systems. At low conversion, the system follows zero-one kinetics and at higher conversion non-zero-one kinetics. The small particles are expected to obey zero-one kinetics and larger particles, non-zero-one kinetics.

The possibility of secondary particle formation occurring in all the miniemulsion systems emerged from the kinetic data where an increase in the particle number was observed. The presence of secondary particle formation was apparent in the TEM images for all the miniemulsion polymerizations carried out in the study. For the AIBN-initiated systems, secondary particle formation was proven by statistically analyzing the TEM data. No secondary uncontrolled distribution (indicative of secondary particle formation) was evident in the SEC chromatograms. Secondary particle formation was not supported nor dismissed by the SEC results obtained in this study.

In conclusion, from the results obtained in the study one is able to speculate the possible reasons for the observed behavior of the RAFT-mediated miniemulsion systems mentioned in the research project. However, these systems require further investigation in

## ***Chapter Four Results and Discussion***

---

order to establish a better understanding of the RAFT process and its application in heterogeneous aqueous media for the synthesis of AB diblock copolymers.

### **4.8 References**

- (1) Landfester, K. *Macromol. Rapid Commun.* **2001**, *22*, 897 - 936.
- (2) Butte, A.; Storti, G.; Morbidelli, M. *Macromolecules* **2001**, *34*, 5885 - 5896.
- (3) Vosloo, J. J.; De Wet-Roos, D.; Tonge, M. P.; Sanderson, R. D. *Macromolecules* **2002**, *35*, 4894 - 4902.
- (4) de Brouwer, H.; Tsavalas, J. G.; Schork, F. J.; Monteiro, M. J. *Macromolecules* **2000**, *33*, 9239 - 9246.
- (5) Lansalot, M.; Davis, T. P.; Heuts, J. P. A. *Macromolecules* **2002**, *35*, 7582 - 7591.
- (6) Muller, A. H. E.; Yan, D.; Litvinenko, G.; Zhuang, R.; Don, H. *Macromolecules* **1995**, *28*, 7335 - 7338.
- (7) Butte, A.; Storti, G.; Morbidelli, M. *Macromolecules* **2000**, *33*, 3485 - 3487.
- (8) Zhou, X.; Ni, P.; Yu, Z.; Zhang, F. *J. Polym. Sci. Part A: Polym. Chem.* **2007**, *45*, 471 - 484.
- (9) Huang, X.; Sudol, E. D.; Dimonie, V. L.; Anderson, C. D.; El-Aasser, M. S. *Macromolecules* **2006**, *39*, 6944 - 6950.
- (10) Landfester, K.; Bechthold, N.; Tiarks, F.; Antonietti, M. *Macromolecules* **1999**, *32*, 5222 - 5228.
- (11) Landfester, K.; Betchold, N.; Forster, S.; Antonietti, M. *Macromol. Rapid Commun.* **1999**, *20*, 81.
- (12) Blythe, P. J.; Sudol, E. D.; El-Aasser, M. S. *J. Polym. Sci. Part A: Polym Chem* **1997**, *35*, 807 - 811.
- (13) Matahwa, H.; McLeary, J. B.; Sanderson, R. D. *J. Polym. Sci. Part A: Polym Chem* **2006**, *44*, 427 - 442.
- (14) van Zyl, A.; Bosch, R. F. P.; McLeary, J. B.; Sanderson, R. D.; Klumperman, B. *Polymer* **2005**, *46*, 3607 - 3615.
- (15) McLeary, J. B.; Tonge, M. P.; De Wet-Roos, D.; Sanderson, R. D.; Klumperman, B. *J. Polym. Sci. Part A: Polym Chem* **2004**, *42*, 960 - 974.

## ***Chapter Four Results and Discussion***

---

- (16) Luo, Y.; Schork, F. J. *J. Polym. Sci. Part A: Polym. Chem.* **2002**, *40*, 3200 - 3211.
- (17) Yang, L.; Luo, Y.; Li, B. *J. Polym. Sci. Part A: Polym Chem* **2005**, *43*, 4972 - 4979.
- (18) Zhu, J.; Zhu, X.; Cheng, Z.; Liu, F.; Lu, J. *Polymer* **2002**, *43*, 7037 - 7042.
- (19) Buback, M.; Janssen, O.; Oswald, R.; Schmatz, S.; Vana, P. *Macromol. Symp.* **2007**, *248*, 158 - 167.
- (20) Moad, G.; Rizzardo, E.; Thang, S. H. *Aust. J. Chem.* **2005**, *58*, 379 - 410.
- (21) Lovell, P. A.; El-Aasser, M. S. In *Emulsion Polymerization and Emulsion Polymers*; El-Aasser, M. S.; Sudol, E. D., Eds.; Wiley & Sons: New York, 1997; pp 38 - 57.
- (22) Gilbert, R. G. In *Emulsion Polymerization: A Mechanistic Approach*; Ottewill, R. H.; Rowell, R. L., Eds.; Academic Press: London, 1995; pp 25 - 77.
- (23) Yang, L.; Luo, Y.; Li, B. *Polymer* **2006**, *47*, 751 - 762.
- (24) Favier, A.; Charreyre, M. *Macromol. Rapid Commun.* **2006**, *27*, 653 - 692.
- (25) Tsavalas, J. G.; Schork, F. J.; de Brouwer, H.; Monteiro, M. J. *Macromolecules* **2001**, *34*, 3938 - 3946.
- (26) Casey, B. S.; Morrison, B. R.; Maxwell, I. A.; Gilbert, R. G.; Napper, D. H. *J. Polym. Sci. Part A: Polym Chem* **1994**, *32*, 605 - 630.
- (27) Gilbert, R. G. In *Emulsion Polymerization A Mechanistic Approach*; Ottewill, R. H.; Rowell, R. L., Eds.; Academic Press: London, 1995; pp 143 - 207.
- (28) Prescott, S. W.; Ballard, M. J.; Gilbert, R. G. *J. Polym. Sci. Part A: Polym Chem* **2005**, *43*, 1076 - 1089.
- (29) Bowes, A.; McLeary, J. B.; Sanderson, R. D. *J. Polym. Sci. Part A: Polym. Chem.* **2007**, *45*, 588 - 604.
- (30) Maxwell, I. A.; Morrison, B. R.; Napper, D. H.; Gilbert, R. G. *Macromolecules* **1991**, *24*, 1629 - 1640.
- (31) Prescott, S. W.; Ballard, M. J.; Rizzardo, E.; Gilbert, R. G. *Macromolecules* **2005**, *38*, 4901 - 4912.
- (32) Chern, C.; Liou, Y. *J. Polym. Sci. Part A: Polym. Chem.* **1999**, *37*, 2537 - 2550.

## *Chapter Five*

### *Conclusion and recommendations*

The main conclusions drawn from results presented in the earlier chapters are given. A short discussion of recommendations for future research is also presented.

The primary objective of this study was the use of RAFT-mediated miniemulsion for the synthesis of well-defined high molecular weight AB diblock copolymers of *n*-butyl methacrylate and styrene in heterogeneous media via a two-step process. The first step involved the synthesis of the starting block, also referred to as a polymeric RAFT agent, in bulk. The majority of the chains contained the thiocarbonyl-thio moiety on the chain ends after the first step, which made these chains potentially active for chain extension in the second step. In the second step the first block acted as a hydrophobic polymeric RAFT agent that was then chain extended with the second monomer in miniemulsion. During the course of the study the effects of certain variables on the miniemulsion system were investigated. The conclusions follow.

### **5.1 Conclusions**

- 1) The monofunctional RAFT agent, CIDB, was an effective RAFT agent for controlling the molecular weight of the bulk polymerization of *n*-butyl methacrylate. The polymeric RAFT agent (initial PBMA blocks) with molecular weights ranging from 20 000 – 40 000 gmol<sup>-1</sup> and low PDI values (< 1.2) were successfully synthesized. At the end of the reaction, most chains contained the RAFT agent functionality (confirmed by UV-RI analysis), and could further be used in the second miniemulsion chain extension step, with styrene monomer.
- 2) The products of preliminary experiments involving the chain extension of PBMA and PSt starting blocks with the same monomer in the second miniemulsion step exhibited living characteristics. Most chains were reactivated upon further addition of fresh monomer and initiator. The hydrophobic polymeric RAFT agent proved to be a good candidate for controlling the miniemulsion polymerization.
- 3) Preliminary experiments for the chain extension of PBMA starting block with styrene in miniemulsion was successfully carried out. Stable latices of poly(*n*-butyl methacrylate)-*b*-poly(styrene) were synthesized. High conversions (> 80%) were obtained. The distinct features of CFRP were seen in the miniemulsion system.



Polydispersity values did not decrease with increasing conversion (as is expected in an ideal CFRP environment) instead they increased throughout the polymerization. High polydispersity values ( $> 2$ ) were obtained but despite this the system exhibited controlled and living characteristics. Dynamic light scattering data showed that particle sizes for the miniemulsion polymerizations were well within the range of 50 – 500 nm. TEM analysis confirmed the results obtained from light scattering and provided visual evidence of the particle morphology and secondary particle formation.

4a) The PBMA-*b*-PSt diblock copolymer miniemulsion system was investigated more thoroughly in Section 4.5. The effect of changing the initiator/RAFT agent concentration ratios on the RAFT-mediated miniemulsion system was investigated. All of the miniemulsion systems exhibited control and living features despite the high polydispersity values ( $> 2$ ). When changing the initiator/RAFT agent concentration ratios, not much improvement in terms of the polydispersity values and broad molecular weight distributions for the different systems were observed. This indicated that the initiator concentration has no significant effect on the molecular weight distribution and the steep increase in the polydispersity of the systems recorded in this study. Possible reasons for the observed broadening in the molecular weight distributions and high polydispersity values were discussed in detail in Section 4.4.4 and Section 4.5.

4b) The effect of using a water-soluble initiator KPS, in the RAFT-mediated miniemulsion system was also investigated. Its use did not result in much improvement, although somewhat higher polydispersity values ( $> 2.5$ ) compared to those arising from the AIBN-initiated systems that were studied (Section 4.5) were obtained. A similar behavioral pattern as was observed in the AIBN-initiated system was seen. Since the polymeric RAFT agent (initial block) is highly hydrophobic, no control over the molecular weight was expected in the particles (if they exist although they were deduced from TEM spectra) formed by homogeneous nucleation.

4c) Based on the results obtained from the diblock copolymers of *n*-butyl methacrylate and styrene of high molecular weight, poly(*n*-butyl methacrylate)-*b*-poly(styrene) diblock copolymers of lower molecular weight were synthesized.

Living radical polymerization characteristics were achieved in the system. High conversion (> 90%) was obtained. Polydispersity values increased during the polymerization, although they remained well below the benchmark of 1.5 for controlled living systems. SEC chromatograms showed narrow molecular weight distributions. The results indicated that the particle size distribution and the quality of the initial dispersion are probably important factors to consider, not only in the miniemulsion system presented in this study but also in similar RAFT-mediated miniemulsion systems reported in the literature. In addition, it is possible that the PDI of the diblock copolymer miniemulsion system is dependent on the molecular weight of the final polymer.

### **5.2 Recommendations for future work**

RAFT-mediated polymerization in aqueous media still remains a challenge to many polymer scientists. The complex kinetics and mechanisms involved are not yet fully understood and require further attention.

In this study, the research goals were achieved, but much research still needs to be carried out in order to optimize the RAFT-mediated miniemulsion system for the synthesis of AB diblock and ABA triblock copolymers.

An optimum system would imply that a minimum amount of secondary particle formation is present, the RAFT agent remains inside the particles and radical exit is minimized. A better understanding of the mechanism and quantification of side reactions is needed in order to optimize reaction conditions. In successfully managing to achieve this, the desired product of specific properties can be synthesized and could be of commercial value in the near future.

Focusing on the system used in this study, the following aspects require further research:

- Since these RAFT-mediated miniemulsion systems are sensitive to reaction formulations, one can carry out a mechanistic investigation into the behavior of the system in the presence of individual variables in an attempt to optimize the system. The impact that the different variables, such as different surfactants (ionic surfactants versus non-ionic surfactants), the initiator, monomer and hydrophobe can have on this type of system should be investigated. Possible ways to improve the particle size distribution and the quality of the initial dispersion warrant investigation.
  
- By statistically analyzing TEM data, secondary particle formation can be proven. This could be a novel method which can prove secondary particle formation in the KPS-initiated system.
  
- The use of a difunctional RAFT agent to synthesize ABA triblock copolymers via this two-step approach can also be investigated. To date, the driving force behind the synthesis of ABA triblock copolymers is due to the unique morphology that these polymers can adopt. A remarkable range of materials with designer architectures can be synthesized using these RAFT agents for the synthesis of ABA triblock copolymers.
  
- Using the methodology used in this study for the synthesis of diblock copolymers, diblock copolymers starting with any block that can have a RAFT agent attached and is insoluble, and chain extending it in miniemulsion, can be synthesized. An example would be starting with a PDMS macro-RAFT agent and chain extending with a second monomer, for example styrene, in miniemulsion. The PDMS macro-RAFT agent will form the starting block. This could offer a new way of synthesizing PDMS diblock copolymers in emulsion systems (a novel process).
  
- Rheological properties and thermomechanical properties of the AB diblock copolymers synthesized in this study can also be analyzed. A systematic study to find optimal properties should also be studied.

## ***Chapter Five Conclusion and recommendations***

---

In conclusion, controlled radical polymerization via the RAFT technique has attracted considerable interest as a method for the synthesis of block copolymers. In addition, the application of this technique in heterogeneous systems provides economic advantage over homogeneous systems. The synthesis of well-defined polymeric materials via the methodology presented in this thesis has great potential in paving the way for the preparation of new classes of materials.

**Appendix A 2-cyanoisoprop-2-yl dithiobenzoate (CIDB)**

---

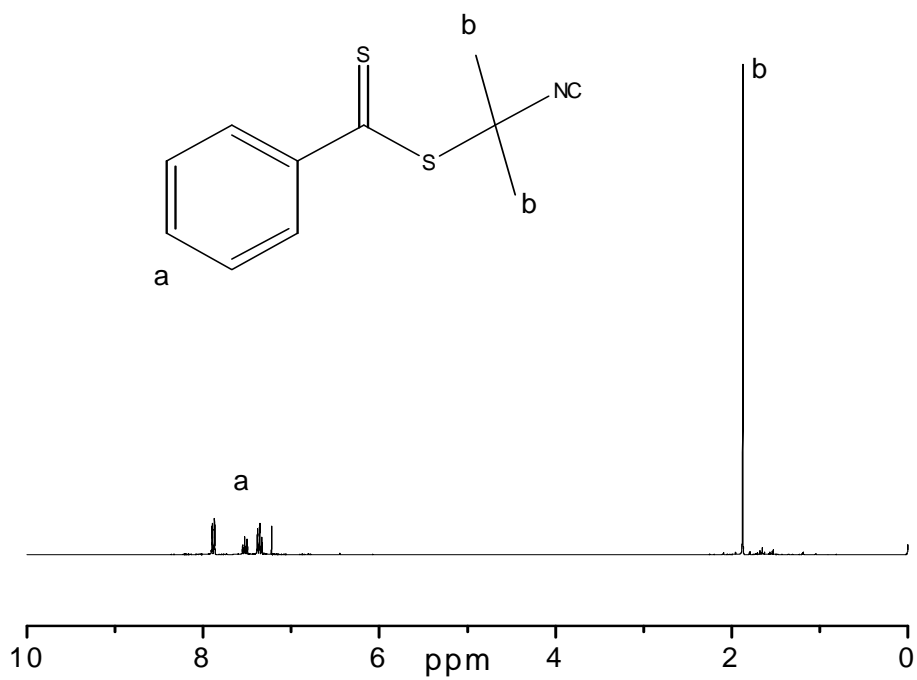


**Figure A1:**  $^1\text{H}$  NMR spectrum of 2-cyanoisoprop-2-yl dithiobenzoate in  $\text{CDCl}_3$

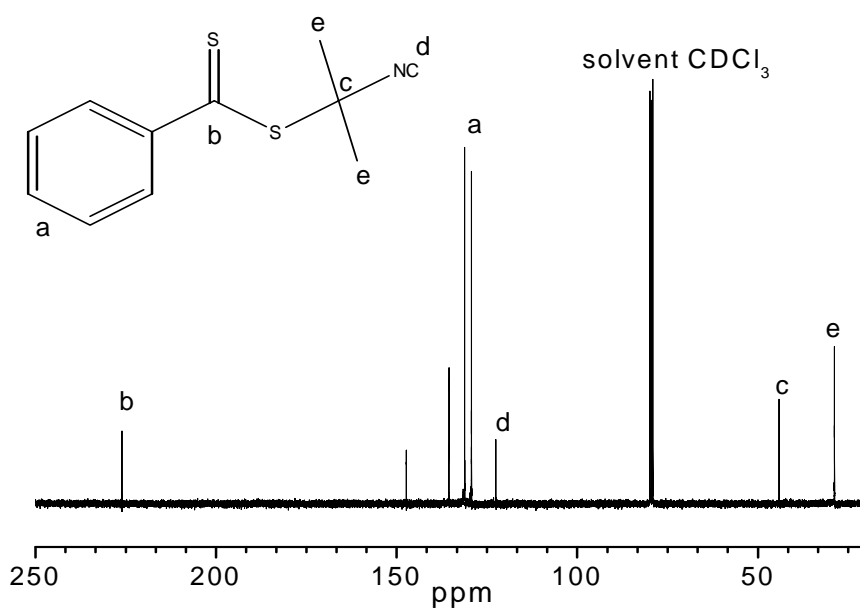


**Figure A2:**  $^{13}\text{C}$  NMR spectrum of 2-cyanoisoprop-2-yl dithiobenzoate in  $\text{CDCl}_3$

## Appendix A 2-cyanoisoprop-2-yl dithiobenzoate (CIDB)

### NB 02, RAFT-CZOB

NB\_PdSci\_060821\_2 8 (0.151) Cn (Top,4, Ht); Sm (Mn, 3x0.80); Sb (1,40.00); Cm (8-3:4)

1: Scan ES+  
2.94e7

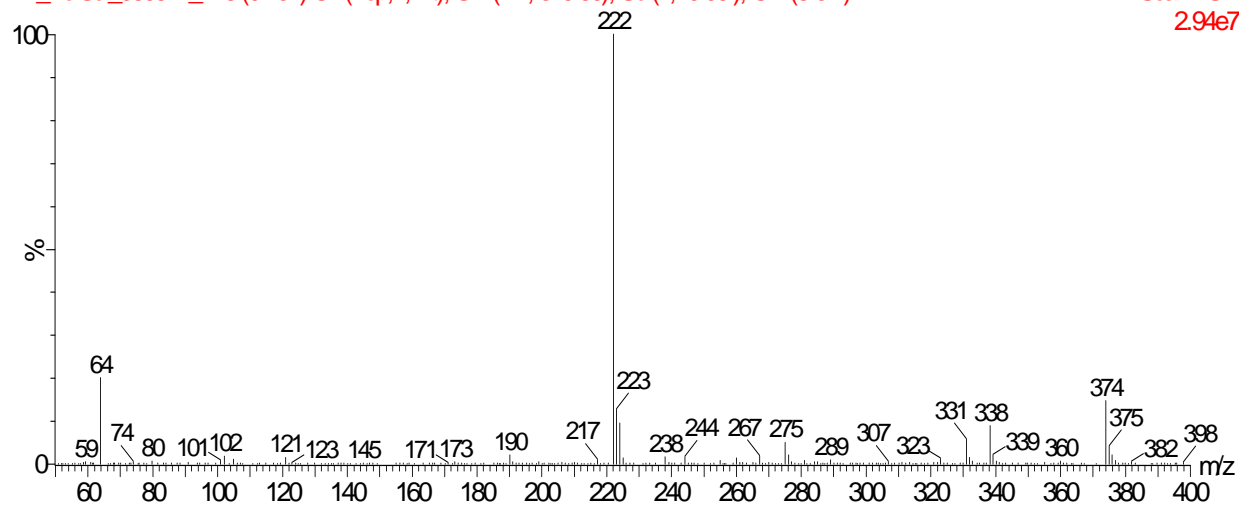


Figure A3: ESMS spectrum of 2-cyano isoprop-2-yl dithiobenzoate

## Appendix B Mathematical model for the miniemulsion system

The mathematical model used in this study is based on a simple zero-one system.

Particle radius ( $r_s$ ) nm	$\rho^{*a}$ $s^{-1}$	$k^{*b}$ $s^{-1}$ for a set $N_c$	$nbar^{*c}$
30	0.015	$5 \times 10^{-2}$	0.19
45	0.015	$2.56 \times 10^{-2}$	0.27
60	0.015	$1.52 \times 10^{-2}$	0.33

<sup>a</sup> Entry rate coefficient,  $\rho$ , was calculated using equation 2.10.

<sup>b</sup> Exit rate coefficient was calculated using equation 2.11 and equation 2.13.

<sup>c</sup> Average number of radicals per particle was calculated using equation 2.9.

$$n_s^- = \text{Error!} \quad (2.9)$$

$$\rho \approx \text{Error!} \quad (2.10)$$

$$k = 2k_{tr}C_p \text{ Error!} \quad (2.11)$$

$$k_{dM} = \text{Error!} = \text{Error!} \quad (2.13)$$

The following values were used in the equations:

$N_c$	$10^{17} \text{ dm}^{-3}$ (typical value for the miniemulsion system in this study)
$N_A$	$6.023 \times 10^{23} \text{ mol}^{-1}$
$k_d$	$4.45 \times 10^{-5} \text{ s}^{-1}$
$k_{t, \text{aq}}$	$1.75 \times 10^9 \text{ M}^{-1} \text{ s}^{-1}$
$k_{p, \text{aq}}$	$2260 \text{ M}^{-1} \text{ s}^{-1}$
$z$	2
$C_W$	$4.3 \times 10^{-3} \text{ M}$
$C_P$	$5.5 \text{ M}$
$D_W$	$1.5 \times 10^{-5} \text{ M}^2 \text{ s}^{-1}$
$k_p$ at 75 °C	$565 \text{ L} \cdot \text{mol}^{-1} \text{ s}^{-1}$
$k_{tr}$ at 75 °C	$0.038 \text{ M}^{-1} \text{ s}^{-1}$
$k_{p1}$	$2260 \text{ M}^{-1} \text{ s}^{-1}$

- (1) Gilbert, R. G. In *Emulsion Polymerization A Mechanistic Approach*; Ottewill, R. H.; Rowell, R. L., Eds.; Academic Press: London, 1995; pp 143 - 207.
- (2) Brandrup, J.; Immergut, E. H.; Grulke, E. A. In *Polymer Handbook*, Fourth ed.; Brandrup, J., Ed.; Wiley & Sons, 1998; Vol. 1, pp 13 - 95.
- (3) Vosloo, J. J.; De Wet-Roos, D.; Tonge, M. P.; Sanderson, R. D. *Macromolecules* **2002**, *35*, 4894 - 4902.

## Appendix C Statistical analysis of TEM

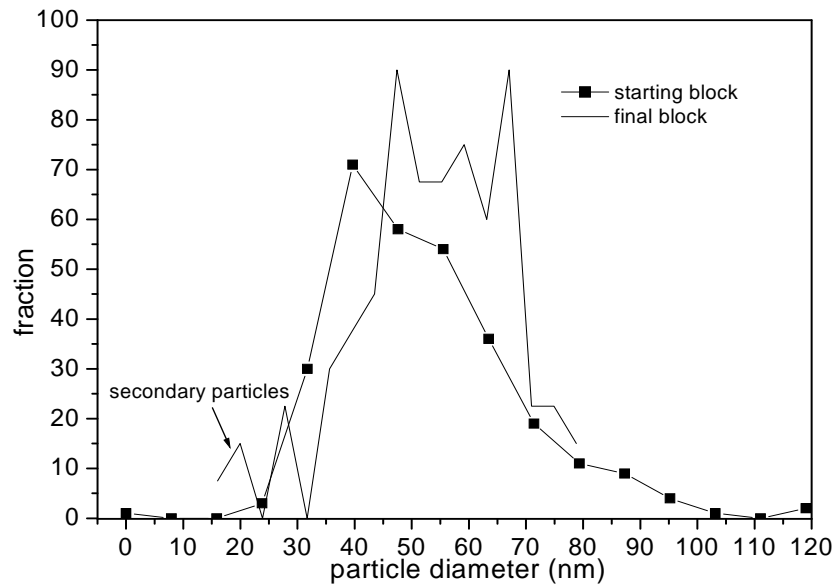


Figure C1: Particle diameter versus particle fraction for the RAFT-mediated miniemulsion polymerization initiated by AIBN.

Volume of a sphere:  $V = \pi d^3/6$ , where  $d$  is the particle diameter

$$V_{\text{initial}} = V_{\text{core}}$$

$$V_{\text{final}} = V_{\text{core}} + V_{\text{new}}$$

$$V_{\text{final}} = V_{\text{total}}$$

Assume constant density for initial and final polymers, then

$$V_{\text{final}} = V_{\text{core}} \times 10 \text{ (roughly at 100\% conversion)}$$

$$d_{\text{final}}^3 = 10 \times d_{\text{core}}^3$$

$$d_{\text{final}} = d_{\text{core}} \times 10^{1/3}$$

This corresponds to the mean diameter averages measured:

$$d_{\text{core}} = 24 \text{ nm} \quad d_{\text{final}} = 52 \text{ nm}$$